

# NANoREG

Grant Agreement Number 310584

## Deliverable D 2.10

Protocol(s) for size-distribution analysis of primary NM particles in air, powders, and liquids

Due date of deliverable: 2016/05/31 (*approved postponement*)

Actual submission date: 2016/05/25

Author(s) and company:	Jan Mast, Pieter-Jan De Temmerman (CODA-CERVA)
Work package/task:	WP2 / Task 2.2a
Document status:	draft / <u>final</u>
Confidentiality:	confidential / restricted / <u>public</u>
Key words:	

### DOCUMENT HISTORY

Version	Date	Reason of change
1	2016/05/11	First draft v.01 (CODA-CERVA)
2	2016/05/25	First draft v.02 with remarks D2.10 partners
3	2016/11/03	Change of dissemination level to public Hyperlinks for SOPs included in approved version
4	2017/02/21	Project Office harmonised lay-out





This work is licensed under the Creative Commons Attribution-NonCommercial-ShareAlike 4.0 International License.

To view a copy of this license, visit <http://creativecommons.org/licenses/by-nc-sa/4.0/> or send a letter to Creative Commons, PO Box 1866, Mountain View, CA 94042, USA.

**Lead beneficiary for this deliverable: Jan Mast, CODA-CERVA, Partner number 26**

Owner(s) of this document	
Owner of the content	CODA
Co-Owner 1	LTH
Co-Owner 2	INL
Co-Owner 3	NMBU
Co-Owner 4	NRCWE
Co-Owner 5	VN
Co-Owner 6	IIT
Co-Owner 7	INMETRO
Co-Owner 8	KRISS

## Table of Content

<b>1</b>	<b>DESCRIPTION OF TASK .....</b>	<b>6</b>
<b>2</b>	<b>DESCRIPTION OF WORK &amp; MAIN ACHIEVEMENTS .....</b>	<b>6</b>
2.1	SUMMARY .....	6
2.2	BACKGROUND OF THE TASK .....	6
2.3	DESCRIPTION OF THE WORK CARRIED OUT .....	8
2.3.1	Development of an approach for TEM-based size and shape analysis .....	8
2.3.2	Examined MNM: .....	8
2.3.2.1	Colloidal NM .....	8
2.3.2.2	Aggregated, fractal-like representative test materials, selected from the NANOREG core materials .....	9
2.3.3	Intra-laboratory and inter-laboratory validation and method comparison .....	9
2.3.4	Size characterisation with on-line technique of spherical or near-spherical airborne nanoparticles generated from colloidal suspension .....	11
2.3.5	Context of the peer-reviewed, NANOREG approved publications resulting from D2.10 .....	11
<b>3</b>	<b>DEVELOPMENT AND IMPLEMENTATION OF SOPS FOR TEM SIZE AND SHAPE ANALYSIS OF THE PRIMARY PARTICLES OF NANOMATERIALS.....</b>	<b>13</b>
3.1	MODIFIED “FINAL PROTOCOL FOR PRODUCING SUITABLE MANUFACTURED NANOMATERIAL EXPOSURE MEDIA”  .....	13
3.1.1	Background information .....	13
3.1.2	Principle and scope .....	14
3.1.3	Instructions .....	14
3.1.4	Applications .....	14
3.2	“PREPARATION OF EM-SPECIMENS CONTAINING A REPRESENTATIVE SAMPLE OF THE PARTICLES IN DISPERSION”  .....	14
3.2.1	Background information .....	14
3.2.2	Principle and scope .....	15
3.2.3	Instructions .....	15
3.2.4	Applications .....	16
3.3	“TRANSMISSION ELECTRON MICROSCOPIC IMAGING OF NANOMATERIALS”  .....	16
3.3.1	Background information .....	16
3.3.2	Principle and scope .....	17
3.3.3	Instructions .....	17
3.3.4	Applications .....	17
3.4	GUIDELINES FOR QUALITATIVE CHARACTERIZATION OF NANOMATERIALS IN DISPERSION IN A REGULATORY FRAMEWORK  .....	18
3.4.1	Background information .....	18
3.4.2	Principle and scope .....	18

3.4.3	Guidelines to describe the physical properties of a nanomaterial in dispersion based on EM micrographs.....	19
3.4.3.1	Description of possible visible impurities.....	19
3.4.3.2	Description of the aggregation/agglomeration state .....	19
3.4.3.3	Characterisation of the aggregates/agglomerates .....	19
3.4.3.4	Characterisation of the primary particles .....	19
3.4.3.5	Evaluation whether a quantitative TEM-analysis is feasible.....	20
3.4.4	Applications .....	21
3.5	“ELECTRON MICROSCOPIC IMAGE ANALYSIS OF COLLOIDAL NANOMATERIALS” ① .....	22
3.5.1	Background information .....	22
3.5.2	Principle and scope .....	23
3.5.3	Instructions .....	23
3.5.4	Application .....	23
3.6	“ELECTRON MICROSCOPIC IMAGE ANALYSIS OF PRIMARY PARTICLES IN AGGREGATED NANOMATERIALS” ① .....	24
3.6.1	Background information .....	24
3.6.2	Principle and scope .....	24
3.6.3	Instructions .....	25
3.6.4	Applications .....	25
3.7	DATA ANALYSIS AND REPRESENTATION OF MEASUREMENT RESULTS ACCORDING TO RELEVANT ISO-NORMS .....	25
<b>4</b>	<b>VALIDATION OF SOPS FOR TEM SIZE AND SHAPE ANALYSIS OF THE PRIMARY PARTICLES OF NANOMATERIALS. ....</b>	<b>26</b>
4.1	INTRA-LABORATORY VALIDATION OF QUANTITATIVE TEM ANALYSIS OF COLLOIDAL NANOMATERIALS.....	26
4.1.1	General.....	26
4.1.2	Accuracy of TEM measurements of colloidal nanomaterials .....	26
4.1.3	Precision of TEM measurements of colloidal nanomaterials.....	26
4.1.3.1	Calculation of measurement uncertainties.....	26
4.1.3.2	Calibration .....	27
4.1.3.3	Trueness .....	28
4.1.3.4	Combined and expanded measurement uncertainty .....	29
4.1.3.5	Measurement uncertainties of the minimal size in one dimension.....	29
4.1.3.6	Measurement uncertainties of the shape measurement .....	31
4.1.4	Application of the SOPs to resolve different subpopulations of MNM in a multimodal mixtureT.....	31
4.1.5	Comparison of EM measurements with the results of complementary techniques PTA, DLS, SEM and SP-ICP-MS.....	32
4.2	INTRA-LABORATORY VALIDATION OF QUANTITATIVE TEM ANALYSIS OF AGGREGATED/AGGLOMERATED NANOMATERIALS.....	37
4.3	BETWEEN-LABORATORY VALIDATION (ILC) OF THE METHOD DEVELOPED FOR QUANTITATIVE TEM ANALYSIS .....	39
4.3.1	Aim of the ILC study in D2.10 .....	39
4.3.2	Instructions for quantitative TEM analysis.....	39
4.3.3	Design of the ILC study in D2.10 .....	39
4.3.4	Competence of the participants .....	40

4.3.5	Inter-laboratory validation of the SOPs for near-monomodal, near-mondisperse, colloidal MNM with focus on the application of the EC definition of MNM .....	40
4.3.6	Inter-laboratory validation of the SOPs for near-monomodal, near-mondisperse, colloidal MNM with focus on the shape characteristics .....	43
4.3.7	Inter-laboratory validation of the SOPs for fractal-like, aggregated MNM with focus on the application of the EC definition of MNM .....	43
<b>5</b>	<b>SIZE CHARACTERISATION WITH ON-LINE TECHNIQUE OF SPHERICAL OR NEAR-SPHERICAL AIRBORNE NANOPARTICLES GENERATED FORM COLLOIDAL SUSPENSION .....</b>	<b>49</b>
5.1	COMPARISON OF DIFFERENT ON-LINE AEROSOL INSTRUMENT FOR AIRBORNE NANO PARTICLES. (FROM LEVIN ET AL [26]) .....	49
5.2	DETERMINATION OF THE PRIMARY PARTICLE SIZE AND SURFACE AREA FOR AIRBORNE AGGREGATES USING ON-LINE AEROSOL MEASUREMENT TECHNIQUE. (FROM SVENSSON ET AL [27]) .....	49
<b>6</b>	<b>EVALUATION AND CONCLUSIONS.....</b>	<b>53</b>
<b>7</b>	<b>DATA MANAGEMENT .....</b>	<b>54</b>
<b>8</b>	<b>DEVIATIONS FROM THE WORK PLAN.....</b>	<b>54</b>
<b>9</b>	<b>REFERENCES / SELECTED SOURCES OF INFORMATION (OPTIONAL) .....</b>	<b>55</b>
<b>10</b>	<b>LIST OF ABBREVIATIONS (OPTIONAL).....</b>	<b>61</b>
<b>11</b>	<b>ATTACHMENTS .....</b>	<b>62</b>

# 1 Description of task

The aim of D2.10 is to establish standard operating procedures for the quantitative size and shape analysis of manufactured nanomaterials. Examined methods include transmission electron microscopy, nanoparticle tracking analysis and single particle ICP-MS.

The developed methodologies will be validated on reference and representative nanomaterials for application for regulatory use.

## 2 Description of work & main achievements

### 2.1 Summary

This deliverable presents the final standard operation procedures (SOPs) developed for the quantitative size and shape analysis of manufactured nanomaterials using TEM.

It focusses on the implementation of the EC definition of nanomaterials. The deliverable is a result of work produced in Task 2.2a, which was to develop SOPs for quantification of number-based size-distribution

The SOPs comprise:

- A protocol for sample preparation of EM samples bringing the nanomaterial in dispersion, which is a modification of “The generic NANOGENOTOX batch dispersion protocol for in vitro studies”
- A protocol for specimen preparation bringing a representative fraction of the material on an EM-grid.
- A protocol for TEM imaging recording representative and selected EM images.
- Guidelines for qualitative characterization of nanomaterials in dispersion in a regulatory framework based on representative and selected EM-micrographs
- A protocol for image analysis of colloidal nanomaterials which includes detection, classification and measurement of primary particles.
- A protocol for image analysis of aggregated, fractal-like nanomaterials which includes detection, classification and measurement of primary particles in aggregates.

Data analysis and representation of measurement results is performed according to relevant ISO-norms. All protocols are performance tested and validated using intra- and inter-laboratory validation approaches.

The EM-based results were related to and interpreted with the results obtained with alternative methods. These include ensemble techniques based on light scattering, such as dynamic light scattering (DLS), particle tracking analysis (PTA) and single particle inductively coupled plasma-mass spectrometry (SP-ICP-MS) [1].

Near-spherical airborne primary nanoparticles were generated from colloidal suspensions for five aerosols of gold-aggregates with CMD in the range of 28 to 78 nm . Measurement procedures for on-line characterisation of spherical or near-spherical airborne nanoparticles were developed and measurement uncertainties were determined. This on-line technique is based on Scanning Mobility Particle Sizer with a global uncertainty budget. The approach used a combination of a differential mobility analyser (DMA), an aerosol particle mass analyzer (APM) and diffusion limited cluster aggregation theory (later called DMA-APM-DLCA). For comparison, a TEM based primary particle analysis was also performed. Measurements with SMPS (instrument with the best diameter resolution) and other on-line techniques like DMS 500, (ELPI), FMPS were compared.

### 2.2 Background of the task

TEM analyses can play an important role in the implementation of the newly established regulatory framework of the European Commission (EC) regulating the use of nanomaterials in consumer products [2-8].

TEM is one of the few techniques that can identify nanoparticles according to the current definitions. If particles can be brought on an electron microscopy (EM) grid and if their distribution is homogeneous and representative for the sample, the combination of transmission electron microscopy (TEM)

imaging with image analysis is one of the few methods that allow obtaining number-based distributions of the particle size and shape, describing the sample quantitatively [9-11]. EM further is a well suited technique because of its resolution covering the size range from 1 nm to 100 nm specified in various definitions of NM [12], and its ability to visualize colloidal nanomaterials as well as primary particles in aggregates in two dimensions.

Disadvantages of EM analysis of nanomaterials include the bias from suboptimal sampling and sample preparation, the estimation of properties of 3D objects from 2D projections, the interpretation of the size of primary particles in aggregates or agglomerates, the relatively high number of particles required for measurement, and the need to develop algorithms for automated image analysis for each separate type of nanomaterial. In many cases, technical solutions that can overcome these disadvantages are available or under development, e.g. more advanced EM techniques such as electron tomography and cryo-EM can be used to obtain information about the 3rd dimension of the particles and to avoid artefacts [13-17].

A review discussing the different steps required for the physical characterization of nanomaterials in dispersion by transmission electron microscopy in a regulatory framework is given by Mast *et al.* [18].

The implementation of the EC-definition of a nanomaterial [4] across various regulatory fields requires a detailed detection and characterization of manufactured nanomaterials by appropriate, validated testing methods [19, 20]. In this deliverable, SOPs for quantitative TEM analysis in the context of the EC definition are proposed and applied and validated on a series of nanomaterials, by intra-laboratory and inter-laboratory validation based on the estimation of the measurement uncertainties and by interpretation of the obtained results with alternative methods. These include ensemble techniques based on light scattering, such as dynamic light scattering (DLS) and particle tracking analysis (PTA), and single particle inductively coupled plasma-mass spectrometry (SP-ICP-MS) [1].

## 2.3 Description of the work carried out

### 2.3.1 Development of an approach for TEM-based size and shape analysis

In this deliverable a TEM based approach is developed and validated to measure the size and shape of MNM. A strong focus lies on the implementation of the EC-definition of a nanomaterial [4] across various regulatory fields.

Typically, a complete TEM analysis to measure the size and shape of the particles of a MNM definition includes following steps:

- i. Sample preparation bringing the nanomaterial in dispersion,
- ii. Specimen preparation bringing a representative fraction of the material on an EM-grid,
- iii. TEM imaging recording representative and selected EM images,
- iv. Descriptive TEM performing a descriptive, qualitative analysis,
- v. Image analysis performing a quantitative analysis which includes detection, classification and measurement of primary particles,
- vi. Data analysis and representation of the measurement results.

To implement these steps in practice, the following combination of guidelines and SOPs is developed and applied:

- i. Modified “Final protocol for producing suitable manufactured nanomaterial exposure media” [21] (3.1)
- ii. “Preparation of EM-specimens containing a representative sample of the particles in dispersion” (3.2)
- iii. “Transmission electron microscopic imaging of nanomaterials” (3.3)
- iv. Guidelines for qualitative characterization of nanomaterials in dispersion in a regulatory framework (3.4)
- v. For colloidal nanomaterials: “Electron microscopic image analysis of colloidal nanomaterials”(3.5)  
For aggregates materials: “Electron microscopic image analysis of primary particles in aggregated nanomaterials”(3.6)
- vii. Data analysis and representation of measurement results according to relevant ISO-norms (3.7)

To precisely and accurately measure the size and shape of (nano)materials in the context of the EC definition [22] using TEM, it is efficient to modify the generic dispersion protocol (3.1). For the examined materials and conditions, a minor modification omitting the pre-wetting step with ethanol and the treatment with 0.05% w/v BSA-kept the particles in a highly dispersed state, allowed representative transfer to an EM-grid, and it improved the separation of the particles from the background based on mass-density contrast and the identification of the primary particles in aggregates.

### 2.3.2 Examined MNM:

#### 2.3.2.1 Colloidal NM

- A selection of the (certified) reference materials and representative near-spherical test materials, with varying amplitude contrast and ranging from 10 to 200 nm in size: ERM-FD304 (nanosilica), ERM-FD100 (nanosilica), RM8012 (colloidal gold NIST), RM8013 (colloidal gold NIST), RM8011 (colloidal gold NIST), NM-300K (nanosilver) and tailor-made spherical and monodisperse SiO<sub>2</sub>NPs@IIT and AgNPs@IIT.
- Non-spherical colloidal NM with a rod-shaped morphology (Au nanorods)
- Tailor made mixtures composed of NM populations of spherical amorphous silica nanoparticles of different sizes and concentration (provided by IIT from HiQNano, <http://www.hiq-nano.com>). They will be tested using the initial proposed SOPs. Following a hypothesis driven research approach, a mixture of different sizes (e.g., nominal 25, 50 and 115 nm) will be produced to test the reliability of the previous mentioned SOPs.



#### **2.3.2.2 Aggregated, fractal-like representative test materials, selected from the NANoREG core materials**

- Powdered, fractal-like aggregated NM: synthetic amorphous silica (JRCNM02000)
- Powdered, fractal-like aggregated NM: titanium dioxide (JRCNM01000 and JRCNM01003)
- Powdered, fractal-like aggregated NM: cerium oxide (JRCNM02102)

#### **2.3.3 Intra-laboratory and inter-laboratory validation and method comparison**

This methodology is validated on a series of nanomaterials for application for regulatory use, focusing on the EC recommended definition of nanomaterials. This validation includes intra-laboratory and inter-laboratory validation based on the estimation of the measurement uncertainties. Further, the obtained measurements are related with the results of alternative or complementary methods. These include ensemble techniques based on light scattering, such as dynamic light scattering (DLS) and particle tracking analysis (PTA), and single particle inductively coupled plasma-mass spectrometry (SP-ICP-MS) [1].

In CODA-CERVA, the SOPs were intra-laboratory validated for a series of 8 near-spherical, near-monomodal colloidal materials ranging from 10 to 200 nm in diameter, on three colloidal rod-like MNM, and on 4 fractal-like aggregated MNM. These validation dossiers consider the homogeneity and stability of the test samples, they specify the working range and the selectivity and precision of the methods as well as the calibration uncertainty. For (certified) reference materials trueness uncertainty is determined. Uncertainties are determined in a top-down validation study and combined in an expanded measurement uncertainty. Figure 1 illustrates the design of the top-down validation study.

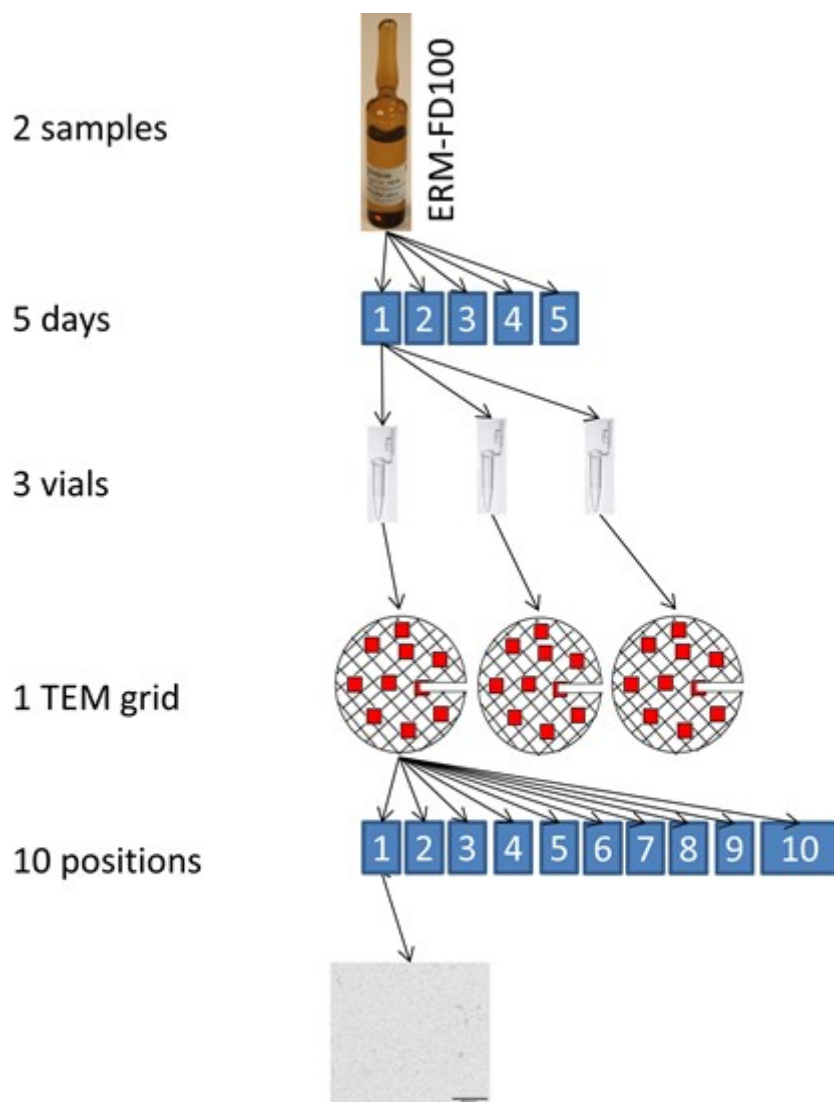


**Figure 1 Schematic overview of the top-down validation study design**

The SOPs are further validated in inter-laboratory comparisons (ILC), to which in total 9 partners contributed (**Error! Reference source not found.**). The definitive version of the SOPs are distributed, implemented and validated by investigating 2 near-spherical and 4 agglomerated and aggregated materials. A graphical representation of these inter-laboratory validation studies (ILC) is provided in Figure 2 indicating the material types, the materials, the tested particles and the measurands.

In total 9 partners contributed to the ILC. For the colloidal MNM all partners provided datasets (**Error! Reference source not found.**) such that a reliable evaluation can be made. Only few laboratories provided experimental data for the fractal-like materials. To draw definitive conclusions further experimental work is advisable. Although the SOPs were conceived to be platform-independent. To efficiently introduce the methods in each partner's laboratory and to minimize the inter-laboratory variance, specific guidelines were provided taken in account the specific microscope and software configurations. Despite this guidance and support, it appeared not easy for the participants of the ILC to select the imaging conditions and the settings and measurands in their software. A major compilation was that quantitative EM analyses had to be introduced in the laboratories of several partners, and/or that partners were dependent on the infrastructure of other laboratories. Continued efforts for standardization remain important.

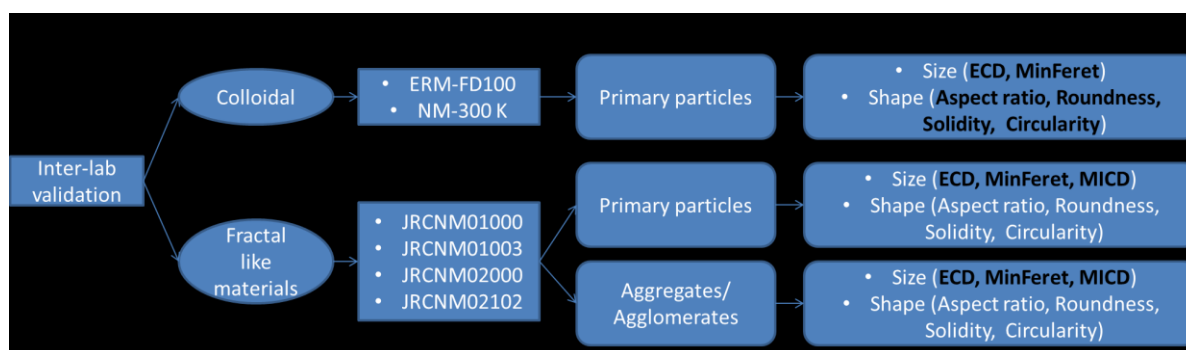


**Figure 2 Graphical table of content of the between-laboratory validation (ILC) indicating the material types, materials and particles tested and measurands measured. The result of measurands presented in this report are indicated in black. The result of measurands indicated in white are available for further analysis.**

The participating laboratories accurately and precisely measured the size of the near-monodisperse near-spherical synthetic amorphous silica certified reference materials (ERM-FD100), demonstrating their technical competence.

Application of the SOPs in the labs participating further allowed to precisely measure the minimal external size and the shape of the primary particles of a metallic, colloidal, near-spherical, near-monodisperse representative test material NM-300K), and resulted in a second ILC in a precise median Feret min measurements, and of the primary particles of aggregated and agglomerated synthetic amorphous silica JRCNM02000, titanium dioxide JRCNM01000 and JRCNM01003 and cerium oxide JRCNM02102. For comparison, the aggregate properties were measured also.

Results of TEM analysis were related to the results obtained using complementary techniques including SEM, SP-ICP-MS, DLS and PTA.

#### 2.3.4 Size characterisation with on-line technique of spherical or near-spherical airborne nanoparticles generated from colloidal suspension

Near-spherical airborne primary nanoparticles were generated from colloidal suspensions. Five aerosols of gold-aggregates with CMD in the range of 28 to 78 nm were examined with regards to primary particle size and specific surface area (SSA). Measurement procedures for spherical or near-spherical airborne nanoparticles characterization were developed for on-line techniques. The size of the particles was characterised with the on-line technique based on Scanning Mobility Particle Sizer with a global uncertainty budget. The approach used a combination of a differential mobility analyzer (DMA), an aerosol particle mass analyzer (APM) and diffusion limited cluster aggregation theory (later called DMA-APM-DLCA). For comparison, a TEM based primary particle analysis was also performed. Measurements with SMPS (instrument with the best diameter resolution) and other on-line techniques like DMS 500, (ELPI), FMPS were compared. Three different types of nanoparticle sizing instruments (Fast Mobility Particle Sizer (FMPS), Electrical Low Pressure Impactor (ELPI) and Scanning Mobility Particle Sizer (SMPS)) and one only measuring number concentration Condensation Particle Counter (CPC) were compared in terms of size distributions and number concentration. The particle size range studied was 50 to 800 nm. The comparison was done using spherical oil droplets for 39 different sizes, with geometric mean diameter (GMD) ranging from 50 to 820 nm.

#### 2.3.5 Context of the peer-reviewed, NANoREG approved publications resulting from D2.10

The results of D2.10 were published in several peer-reviewed, NANoREG approved publications. Their context is given below.

In the publication of Mast et al. [18] detailed background information regarding the Physical characterization of nanomaterials in dispersion by transmission electron microscopy in a regulatory framework is reviewed. It is shown that TEM is one of the few techniques that can identify nanoparticles according to the current definitions of nanomaterials. The different steps required to analyse dispersed nanomaterials by TEM are described in detail and related to existing literature.

Methodologies to obtain homogeneous and stable dispersions of colloidal nanomaterials and powders are presented. The preparation of TEM specimens to obtain a representative distribution of particles on the grid is discussed. The application of TEM imaging methods, electron diffraction and analytical TEM to obtain complementary information on the size, morphology, crystallographic structure, electronic structure and composition of nanomaterials is reviewed. In a qualitative TEM analysis the key properties of the physical form of the nanomaterial under which it is exposed to in vitro and in vivo test systems are described based on TEM micrographs. Subsequently, a quantitative analysis which includes detection, classification and measurement of primary particle properties and validation of the measurement results can be performed. The possibility to extract 3D information by fractal analysis of electron micrographs of aggregated nanomaterials with a fractal-like structure is explored.

In the publication of De Temmerman et al. [23] detailed background information is given regarding the calculation of measurement uncertainties of size, shape, and surface measurements using transmission electron microscopy of near-monodisperse, near-spherical nanoparticles. The different steps required to determine the measurement uncertainties of dispersed nanomaterials by TEM are described in detail and related to existing literature. In this publication Transmission electron microscopy (TEM) is combined with a systematic selection procedure for unbiased random image collection, semi-automatic image analysis and data processing and validated for size, shape and surface topology measurements of silica nanoparticles. This method relies on a high level of automation of calibration, image acquisition, image analysis and data analysis and gives robust results for the modal ECD. The largest contribution to the expanded uncertainty stems from the uncertainty associated to the trueness of the TEM method.

In the publication De Temmerman et al. [24] detailed background information is given regarding the semi-automatic size measurement of primary particles in aggregated nanomaterials by transmission electron microscopy. The different steps required to measure the size of primary particles in aggregated nanomaterials by TEM are described in detail and related to existing literature. In this publication transmission electron microscopic imaging and semi-automatic image analysis are combined for detecting and measuring the primary particles of aggregated nanomaterials (NMs). A high level of automation allows efficiently measuring the diameter of the maximal inscribed circle ( $D_p$ ), a measure for the minimal primary particle size in one dimension. This maximal diameter of the inscribed circle is shown to be commutable with Feret min measurements. The method to determine the fractal properties and the volume specific surface area of fractal-like aggregates is refined supporting on the  $D_p$  and the overlap coefficient measurements for each individual primary particle.

In the publication De Temmerman et al. [25] detailed background information is given regarding the size measurement uncertainties of near-monodisperse, near-spherical nanoparticles using transmission electron microscopy and particle tracking analysis. The different steps required assess the precision and accuracy of the TEM and PTA methods are described in detail and related to existing literature. By obtaining a high level of automation, PTA proves to give precise and non-biased results for the modal hydrodynamic diameter in size range between 30 and 200 nm, and TEM proves to give precise and non-biased results for the mean area-equivalent circular diameter in the size range between 8 and 200 nm of the investigated near-monomodal near-spherical materials.

In the publication of Levin et al. [26] detailed background information is given regarding the limitations in the Use of Unipolar Charging for Electrical Mobility Sizing Instruments: A Study of the Fast Mobility Particle Sizer. The Limitations in the Use of Unipolar Charging for Electrical Mobility Sizing Instruments are described in detail and related to existing literature. The study concludes that particle distributions with a true GMD above 200 nm cannot be measured reliably with the FMPS.

In the publication of Svensson et al. [27] detailed background information is given regarding the characteristics of airborne gold aggregates generated by spark discharge and high temperature evaporation furnace: Mass–mobility relationship and surface area. The characteristics of gold aggregates from three generators (one commercial and one custom built spark discharge generator and one high-temperature furnace) have been characterized. The aggregate surface areas were determined using five approaches – based on aggregation theory and/or measured aggregate properties. The characterization included mass-mobility relationships, effective densities (assessed by an Aerosol Particles Mass analyzer), primary particle analysis (based on Transmission Electron Microscopy), as well as total mass and number concentration outputs. The aggregate effective densities differed considerably between generators.

### 3 Development and implementation of SOPs for TEM size and shape analysis of the primary particles of nanomaterials

To measure the size and shape of a MNM using TEM, the following combination of guidelines and SOPs is developed and applied:

- i. Modified “Final protocol for producing suitable manufactured nanomaterial exposure media” [21] (3.1)
- ii. “Preparation of EM-specimens containing a representative sample of the particles in dispersion” (3.2)
- iii. “Transmission electron microscopic imaging of nanomaterials” (3.3)
- iv. Guidelines for qualitative characterization of nanomaterials in dispersion in a regulatory framework (3.4)
- v. For colloidal nanomaterials: “Electron microscopic image analysis of colloidal nanomaterials”(3.5)  
For aggregates materials: “Electron microscopic image analysis of primary particles in aggregated nanomaterials”(3.6)
- viii. Data analysis and representation of measurement results according to relevant ISO-norms (3.7)

For each of these SOPs, specific background information, the principle and scope, application instructions and applications in the context of this project are presented below.

#### 3.1 Modified “Final protocol for producing suitable manufactured nanomaterial exposure media” [U](#)

##### 3.1.1 Background information

To be able to interpret the results of *in vivo* and *in vitro* tests, a physico-chemical characterisation of the nanomaterial samples in the stock dispersion and in the administration medium prior to and during administration is considered indispensable [28-30]. These guidelines consider quantitative and qualitative TEM analyses instrumental to determine the properties of as-produced, nanoparticle powders and nanoparticles in dispersion. It is required that the examined dispersions are stable enough such that a representative specimen can be prepared. To achieve an EM-specimen fit for quantitative analysis, a homogeneous distribution of particles on an EM-grid is required. Nanomaterials that are already dispersed in liquid, as well as powdered nanomaterials may need to undergo specific treatments, such as dispersion, dilution and drying [20]. The “Final protocol for producing suitable manufactured nanomaterial exposure media” is modified to prepare samples suitable for preparation of EM specimens for quantitative EM analysis in the context of the EC definition of NM.

For colloidal solutions, sample preparation does not tend to introduce a significant bias in the size measurement of the particles [31]: the solutions are stable and their particles do not sediment permanently when kept in bottles under ordinary laboratory conditions. For colloidal gold and silica reference materials, NIST [32-34] and IRMM [35, 36] instruct to gently invert the sample vial several times to assure homogeneity and re-suspension of any settled particles. Other producers like Thermo Scientific suggest to prepare their 3000 series Nanosphere size standards with a vortex mixer [37].

In case of powdered nanomaterials, finely dispersed and stable dispersions are more difficult to prepare [38]. Specific protocols proposed by Guiot and Spalla [38], De Temmerman et al. [11] and Bihari et al. [39] systematically analyse the importance of sonication, the selection of dispersion medium, and the addition of stabilization agents to determine an optimized nanoparticle dispersion method specific for each type of nanomaterial. These protocols aim to prepare samples in their most disperse state, facilitating characterization of these materials. For toxicity testing in a regulatory framework, a generic dispersion protocol is suggested to disperse particles eliminating some of the variation associated with different material-specific dispersion protocols [40-42]. These protocols combine pre-wetting of the material with electro-steric stabilization resulting in comparable, stabilized dispersions of various types of (powdered) nanomaterials. A compromise needs to be found between

obtaining the material in its most disperse form and the applicability of the protocols on different types of nanomaterials. Furthermore, it has to be considered that dispersion of particles may lead to partial dissolution of particles or to swelling [20]. The generic Nanogenotox [40], Prospect [41] and NIST [42, 43] protocols are tested on a variety of nanomaterials to optimise the protocol for dispersing a range of nanomaterials using stabilizing components such as serum and bovine serum albumin that are compatible with the medium and performance of the test. These protocols focus on bringing the material in a stable dispersion in water or buffer. The advantage is that the dispersion of various types of nanomaterials are prepared in the same way, reducing sample preparation bias when comparing test results of these nanomaterials. However, dispersing materials in complex media such as buffers, cell or bacteria culture media and biological fluids, can induce strong agglomeration and reduce the stability of the material. Verleysen et al. [10] and Guiot and Spalla [38] showed that among others the pH of the dispersion medium can be modified to improve the stability of dispersions of titanium oxide nanomaterials. Alternatively, surfactant stabilized preparations such as oligonucleotides and polyethylene glycols are proposed to stabilize materials under higher salt concentrations [44]. In the context of measuring the size and shape of (nano)materials according to the EC definition [22] using TEM a minimal modification of the original Nanogenotox dispersion protocol was envisaged.

### 3.1.2 Principle and scope

The original SOP “Final protocol for producing suitable manufactured nanomaterial exposure media” was developed as a generic approach for the preparation of batch dispersions for *in vitro* and *in vivo* toxicity testing in the NANOGENOTOX project [21]. The method aims to produce a highly dispersed state of any MN by ethanol (EtOH) pre-wetting to handle hydrophobic materials followed by dispersion in sterile-filtered 0.05% w/v BSA-water at a fixed concentration of 2.56 mg/ml using probe sonication. The protocol may not produce the smallest possible particle size in the dispersion, but is a generically applicable procedure that ensures reasonable dispersion of the test materials selected for the NANOGENOTOX project, with the aim to use or characterize the dispersion immediately after its production [21].

To precisely and accurately measure the size and shape of (nano)materials in the context of the EC definition [22] using TEM, it is efficient to modify the generic dispersion protocol. For the examined materials and conditions, a minor modification omitting the pre-wetting step with EtOH and the treatment with 0.05% w/v BSA-kept the particles in a highly dispersed state, allowed representative transfer to an EM-grid, and it improved the separation of the particles from the background based on mass-density contrast and the identification of the primary particles in aggregates.

### 3.1.3 Instructions

The modified version of the “Final protocol for producing suitable manufactured nanomaterial exposure media” [22] brings the powdered, fractal like materials in a stable dispersion. Modifications are limited and include the omission of the pre-wetting step with EtOH and the dispersion in sterile-filtered water instead of dispersion in presence of sterile-filtered 0.05% w/v BSA.

### 3.1.4 Applications

In WP2 of the NANoREG project, this modified SOP was shown efficient for the preparation of dispersions of titanium dioxide JRCNM01000 and JRCNM01003, synthetic amorphous silica JRCNM02000 and cerium oxide JRCNM02102 for the preparation of EM specimens (3.2) in the context of measuring the size and shape properties of (nano)materials using TEM.

For other (nano-)materials and conditions, alternative modifications can be required.

## 3.2 “Preparation of EM-specimens containing a representative sample of the particles in dispersion” [U](#)

### 3.2.1 Background information

As opposed to ‘on-line’ sizing methods like PTA and DLS, the specimen preparation for conventional TEM analysis requires recovering particles from the dispersion, coating them on an appropriate support and drying them [20]. Recovering nanoparticles from suspension is generally done by floating the grid on a droplet of suspension (grid on drop) [10, 11] or placing a droplet of suspension on the grid (drop on grid) [32-34], followed by washing the grid and passively drying at room temperature.



Using these approaches, a representative and homogeneous distribution of the particles on the grid can be obtained relatively easily and cheaply for many materials.

Alternatively, ultracentrifugation allows to quantitatively recover nanoparticles from the liquid medium [45]. This has the advantage that the nanoparticles are actively concentrated and quantitatively centrifuged on the TEM grid. However, the amount of salts and debris that attach to the grid, and concomitant background, increases proportionally with the concentration of the particles. Dilution of the sample avoids such increased background but can influence the properties of agglomerates.

The above-described preparation methods profit from the use of a stable film on the EM-grids. This stability can be assured by using TEM grids with a small mesh size (e.g. 400 mesh) combining a Formvar or Pioloform film with the depositing of carbon to reinforce the surface. To assure adhesion of a representative fraction of the particles to the grid, it is essential that the charge of the particles is compatible with the charge of the grid surface. The carbon layer is, for example, hydrophobic, reducing the recovery of charged particles from suspension [46]. Rendering the grids hydrophilic by pre-treatment of the grids with BSA, bacitracin, Alcian blue or glow discharge allows adapting the charge of the grids to the charge of the particles and generally increases the recovery of particles [46]. Alcian blue pretreatment of the EM-grids results in positively charged grids while glow discharging is mostly applied to charge grids negatively. After glow discharging, positive charges can be introduced by performing an additional treatment with bivalent ions like  $\text{Ca}^{2+}$  and  $\text{Mg}^{2+}$ . Alternatively, functionalized “smart” hydrophobic, hydrophilic, positively and negatively charged grids are commercially available [47]. It has to be considered that the background can be reduced by avoiding multiple layers on the TEM grids (formvar/pioloform, carbon, Alcian blue, etc.). Another possibility is high vacuum baking, which has the extra benefit of reducing carbon contamination during acquisition.

Most samples for TEM must be “supported” by a thin electron transparent film, to hold the particles in place. Certain specific particles, such as carbon nanotubes, are “self- supporting” and have a length that can span the holes in holey grids. For these types of nanomaterials, using holey grids can be beneficial because there is no background from the film on the images. Disadvantages of using holey grids are that only a small amount of particles remains attached to the grid, that the specimen drift might be higher and that the interaction of particles with the borders of the holes in the film selects subpopulations of nanoparticles [48].

### 3.2.2 Principle and scope

The proposed method for preparation of EM specimens brings particles in dispersion in contact with an EM-grid and allows them to interact with the grid surface. When excess fluid is drained off and grids are air-dried, a fraction of the particles remains attached to the grid by different types of interactions (electrostatic, apolar, van der Waals).

This procedure aims to prepare a TEM specimen from dispersed particles. The concentrations of particles, and the type and charge of the grid are chosen such that the fraction of nanoparticles attached to the grids optimally represents the dispersed particles, and that the particles of interest can be detected individually. Transfer of the particles to the grid is not complete such that absolute counts cannot be realized.

The SOP is useful for particles that can be metallic, metal oxides or other. The particles can be monodisperse or polydisperse, aggregated or not. The medium can be polar (water, phosphate buffered saline,...) or apolar (hexane, acetone,...).

The prepared EM specimens are useful for descriptive TEM analyses or quantitative TEM analyses. To be suitable for quantitative TEM analysis, the particles should be evenly distributed over the grids, while the fraction of the attached NPs represents the dispersed particles optimally.

### 3.2.3 Instructions

The SOP “Preparation of EM-specimens containing a representative sample of the particles in dispersion” is applied to prepare an EM specimen by coating particles in a stable dispersion to an EM grid.

### 3.2.4 Applications

In WP2 of the NANoREG project, this SOP was shown efficient for the preparation of EM specimens from colloidal samples and from dispersions of powdered, fractal-like, aggregated nanomaterials.

EM specimens prepared from colloidal samples include the silica, near-spherical, monomodal, certified reference materials ERM-FD100, ERM-FD102 and ERM-FD304, a multimodal mixture of near-spherical, silica materials of nominal diameters of 25, 50 and 115 nm, the colloidal silver representative test material NM-300K, polystyrene latex beads P and H, colloidal gold spherical NIST reference materials RM8011, RM8012 and RM8013 and three colloidal gold rod shaped nanomaterials with nominal diameters ranging from 12-22 nm and nominal lengths ranging from 54-68 nm.

These colloidal samples were applied as-received (without filtration, centrifugation or sonication prior to analysis), or after dilution. In case dilution is required, ultrapure water (resistivity of 18.2 M $\Omega$ .cm at 25 °C), which has undergone an additional filtration process with 0.1  $\mu$ m filter pore size is recommended. Aliquots shall be taken from the recipient by using a pipette and disposable plastic tips avoiding to touch the edges of the recipient. Each aliquot should be taken using one new plastic tip.

Examined dispersions of powdered, fractal-like, aggregated nanomaterials include titanium dioxide JRCNM01000 and JRCNM01003, synthetic amorphous silica JRCNM02000 and cerium oxide JRCNM02102.

## 3.3 “Transmission electron microscopic imaging of nanomaterials” [U](#)

### 3.3.1 Background information

When a representative EM-specimen of particles in dispersion can be prepared, different TEM imaging techniques can be applied and combined with image analysis to obtain information on the size, morphology, crystallographic structure and composition of the nanomaterial. Detailed information about TEM imaging and analysis can be found in textbooks, for example by M. De Graef [49] and by D. B. Williams and C. B. Carter [50].

To characterize nanomaterials and to implement the EC nanomaterial definition on a larger scale, conventional bright field TEM has the advantage over other, more advanced imaging modes that it is cheap, widely available and easy to use. In the bright field imaging mode, contrast originates from the absorption and scattering of electrons in the specimen, due to the thickness and composition of the material so that one can refer to it as 'mass-thickness contrast'. In addition, in crystalline materials, the crystallite orientation introduces diffraction contrast.

EM imaging tends to be different for descriptive and quantitative TEM analyses. To perform a descriptive, qualitative analysis, all relevant features of the nanomaterial, including size and shape of the particles, surface structure, crystallinity and distribution of particles on the grid are visualized. Representative images are typically recorded at high (approximately 400000x), medium (approximately 40000x) and low magnifications (approximately 1000x) to illustrate several particle properties and to provide an overview of the specimen. To perform a quantitative analysis, multiple images of different regions on the grid are usually recorded at one magnification only. To assure unbiased random image collection a systematic micrograph selection procedure can be used. De Temmerman et al. [11] avoid for example subjectivity in the selection of particles by the microscopist, by recording micrographs randomly and systematically, at positions pre-defined by the microscope stage and evenly distributed over the entire grid area. When the field of view is obscured, e.g. by a grid bar or an artifact, the stage can be moved sideways to the nearest suitable field of view. The selected magnification has to allow measuring particle features with high enough accuracy and measuring enough particles to obtain sufficient precision and to limit the time needed for analysis. Therefore, a medium magnification is usually selected, depending on the size of the primary particles of the nanomaterial.

A disadvantage of characterizing nanomaterials by TEM can be that a statistically relevant number of particles cannot be analysed in a time and labor efficient manner. Because generally applied guidelines are still missing, particle numbers vary from a few particles to several thousand in reports characterizing nanomaterials. An objective approach to estimate of the number of particles required



for the estimation of a quantitative parameter with a certain confidence level, was proposed by De Temmerman et al. [9, 51]. Expression of the measurement uncertainties of the size as a function of the number of measured particles demonstrated that no more than 200 particles have to be measured to obtain a relative laboratory uncertainty of 5% for sizing colloidal silica reference nanomaterials [51]. This number is in agreement with the calculations proposed by Matsuda and Gotoh [52], but requires adjustment for nanomaterials with a more polydisperse size distribution.

The pixel size and the field of view determine the useful range, which is defined by the lower and upper size of the detection limit. Applying the criterion of Merkus [53] for the lower particle size detection limit, large systematic size deviations can be avoided if the smallest particle area is at least hundred pixels. The field of view restricts the upper size detection limit to one tenth of the image size [54].

### 3.3.2 Principle and scope

The proposed method for TEM imaging of nanomaterials aims to record a set of calibrated transmission electron micrographs showing particles that are representative for the NM on the EM grid starting from EM specimens containing particles that optimally represent the particles in the original sample, and that contain particles of interest that can be detected individually. The TEM specimen preparation can be performed based on the grid-on-drop or drop-on-grid methods described in 3.2, or on other specimen preparation methods including cryo-EM, aerosol sampling and on grid ultracentrifugation centrifugation.

To assure unbiased random image collection the systematic micrograph selection procedure of De Temmerman et al. [11] is applied. The magnification of the micrographs and the number of particles (micrographs) are determined such that the images are suitable for subsequent descriptive and quantitative image analyses. The pixel size and the associated magnification is determined based on the criterion of Merkus [53]. The upper size detection limit is limited to one tenth of the image size supporting on ISO 13322-1, 2014 [54]. The number of particles required to estimate a quantitative parameter with a certain confidence level is determined based on the method proposed by De Temmerman et al. [9, 51].

### 3.3.3 Instructions

The SOP “Transmission electron microscopic imaging of nanomaterials” is applied to obtain representative EM micrographs of nanomaterials coated on TEM grids suitable for quantitative TEM analysis.

To assure a maximum traceability of information, storage of micrographs in a dedicated database with their administrative and sample preparation information as well as the information related to their imaging conditions is recommended [29]. Both commercial [55, 56] and freely accessible software solutions [57-59] that integrate the database in the image analysis software are available. Modifications of the imaging and database software are applied in CODA-CERVA to transfer the micrographs and their associated microscope data efficiently into the database while simultaneously calibrating the images [11].

### 3.3.4 Applications

In WP2 of the NANoREG project, this SOP was shown efficient to make micrographs of colloidal samples and of dispersion of powdered, fractal-like, aggregated nanomaterials suitable for quantitative analyses.

Examined colloidal samples include the silica, near-spherical, monomodal, certified reference materials ERM-FD100, ERM-FD102 and ERM-FD304, a multimodal mixture of near-spherical, silica materials of nominal diameters of 25, 50 and 115 nm, the colloidal silver representative test material NM-300K, polystyrene latex beads P and H, colloidal gold spherical NIST reference materials RM8011, RM8012 and RM8013 and three colloidal gold rod shaped nanomaterials with nominal diameters ranging from 12-22 nm and nominal lengths ranging from 54-68 nm.

Examined dispersions of powdered, fractal-like, aggregated nanomaterials include titanium dioxide JRCNM01000 and JRCNM01003, synthetic amorphous silica JRCNM02000 and cerium oxide JRCNM02102.

### 3.4 Guidelines for qualitative characterization of nanomaterials in dispersion in a regulatory framework [U](#)

#### 3.4.1 Background information

An increasing number of publications demonstrate that the physico-chemical properties of a nanomaterial like its particle size and shape, can strongly influence its toxicological properties [60-62] and its dosimetric fate in the entire organism, including the organ of uptake, circulation and secondary organs of accumulation [29]. Overviews of the physico-chemical properties of a nanomaterial require to assess its safety and toxicological potential are given in [28, 29, 63, 64].

The characterization of nanomaterials, describing and measuring these properties is not a trivial task. Among others because nanomaterials often show distributions of sizes and shapes making this measurement challenging, especially in dispersion [60, 61, 65-69].

A descriptive or qualitative TEM analysis allows describing key properties of the physical form of a nanomaterial under which it is exposed to *in vitro* and *in vivo* test systems based on TEM micrographs. It is further instrumental to judge the relevance and suitability of a quantitative TEM analysis and to avoid/evaluate possible measurement artefacts or bias in *in vitro* and *in vivo* systems [64]. A qualitative analysis contains representative images that give an overview of the sample and show all typical features. In addition, selected micrographs can highlight abnormal or rare features, such as impurities, large agglomerates, crystal defects, etc.

Even though there is a general need for harmonization of the methodologies used for the characterization of nanomaterials, currently, no formal guidelines for the unambiguous and detailed description of a nanomaterial are available. Description of following parameters is considered important. The primary particle size tends to be a relatively robust parameter as compared to the aggregate/agglomerate size, since it is less influenced by environmental conditions (pH, solvent, sonication, presence of proteins etc) [54, 70]. It is correlated with nano-specific properties such as the volume specific surface area (VSSA) ([9, 38] and [71]). Broad application of sizing methods in particle characterization shows that particle size is often an important factor, but is not sufficient to allow particle phenomena such as powder flow, mixing, abrasion or biological response to be understood. Particle shape and morphology play an important role in particle systems as well [70, 71].

Particle morphology represents the extension of a simple shape description to more complex descriptions including characteristics such as porosity, roughness and texture [70]. Various glossaries of terms giving descriptions, in words, of particle shape and morphology already exist [72-78]. These descriptions may be useful for the classification and identification of particles but, at the moment, there is insufficient consensus on the definition of particle shape and morphology in the quantitative terms necessary for them to be implemented in software routines. A future revision of this part of ISO 9276 may cover this [70]. ISO/TS 27687 defines specific nanoparticles based on their shape, such as nanofibers and nanoplatelets [79]. In addition to particle size, shape and morphology, the crystallographic phase, texture, and crystallographic defects can be examined and reported.

An important characteristic of materials consisting of a collection (or 'population') of particles is their polydispersity [20]. A monodisperse material consists only of particles of the same size and shape. A material consisting of particles is to a certain degree always polydisperse: it contains particles of various sizes and/or shapes. How the sizes and shapes of the individual particles vary is described by the particle size and shape distributions, which can be monomodal, bimodal, trimodal or polymodal.

#### 3.4.2 Principle and scope

A descriptive or qualitative EM analysis aims to provide a description of specific physical properties of a nanomaterial that determine, among others, its interaction with biological and environmental systems based on calibrated, bright-field TEM or SEM micrographs taken at low to intermediate magnification. It allows evaluating under which physical form the NM is exposed to *in vivo* and *in vitro* test systems, and whether a subsequent quantitative TEM analysis of the NM is feasible. The procedure is based on guidelines described in literature [70, 78-82]. In principle this method allows to describe the characteristics of any kind of nanoparticles.

A descriptive EM analysis includes (i) an estimate of the size (distribution) of the primary and aggregated/agglomerated particles; (ii) representative and calibrated micrographs; (iii) the

agglomeration- and aggregation status; (iv) the general morphology; (v) the surface topology; (vi) the structure (crystalline, amorphous, ...); (vii) and the presence of contaminants and aberrant particles. In addition, such qualitative analysis evaluates the relevance and suitability of a quantitative TEM analysis based on the amount of particles on the EM grid and the homogeneity of their distribution.

The proposed methodology complies with the EFSA Guidance document that foresees application of electron microscopy (TEM) such that the generated data is in line with the current Guidance document. It describes several key parameters important to assess the nanoparticle safety as specified in [28, 29, 63, 64].

### **3.4.3 Guidelines to describe the physical properties of a nanomaterial in dispersion based on EM micrographs**

A descriptive EM analysis of a nanomaterial in dispersion includes a description of possible visible impurities, a description of the aggregation/agglomeration state, the size and shape of the aggregates/agglomerates, a description of the polydispersity, size, shape, surface topology and crystal structure of primary particles and an evaluation whether a quantitative TEM-analysis is feasible.

#### **3.4.3.1 Description of possible visible impurities**

Examples of descriptions of observed impurities on the TEM grid are : the sample is pure, no impurities are found, occasionally an impurity is observed, nanoparticles are embedded in a matrix or connected to each other, the grid is covered with impurities, between the impurities the NP are visible, micrographs only contain impurities, no nanoparticles are observed

#### **3.4.3.2 Description of the aggregation/agglomeration state**

Possible descriptions of the aggregation status of the sample include: the particles are individual particles, the particles are agglomerated and agglomerates contain X to Y particles per agglomerate and on average x particles), the particles are aggregated and aggregates contain X to Y particles per agglomerate and on average x particles.

#### **3.4.3.3 Characterisation of the aggregates/agglomerates**

To characterize the aggregates/agglomerates

- The size of the aggregates/agglomerates is estimated (approximately XX nm, smaller than XX nm, ranging from XX nm to XX nm, or  $XX \pm XX$  nm for  $N = XX$ ).
- The shape of the aggregates/agglomerates is described according to López-de-Uralde [83]. Spheroidal, ellipsoidal, linear and branched/dendritic aggregates/agglomerates are distinguished (Figure 3).

#### **3.4.3.4 Characterisation of the primary particles**

To characterize the primary particles

- The polydispersity of the primary particles of the NM is indicated. Monomodal, bimodal, trimodal and polymodal distributions are distinguished.
- The size of the primary particles is estimated (approximately XX nm, smaller than XX nm, ranging from XX nm to XX nm, or  $XX \pm XX$  nm for  $N = XX$ ).
- The crystal structure of the primary particles is described based on the presence (diffraction contrast) or absence (amorphous). This can be illustrated based on the TEM electron diffractogram.
- The shape and surface topology of the primary particles is described according to Barrett [77] (Figure 4) and Krumbein and Sloss [78] Figure 5.
- The 3D structure of the primary particles is described. Spherical, rod-shaped, tubular, pyramidal, cubic, orthorhombic, polyhedral, star shaped 3 D morphologies are distinguished.

### 3.4.3.5 Evaluation whether a quantitative TEM-analysis is feasible

A quantitative TEM analysis is feasible if:

- The EM specimen is representative for the sample
- The particles are evenly distributed over the grid
- The particles can be distinguished from the background and matrix

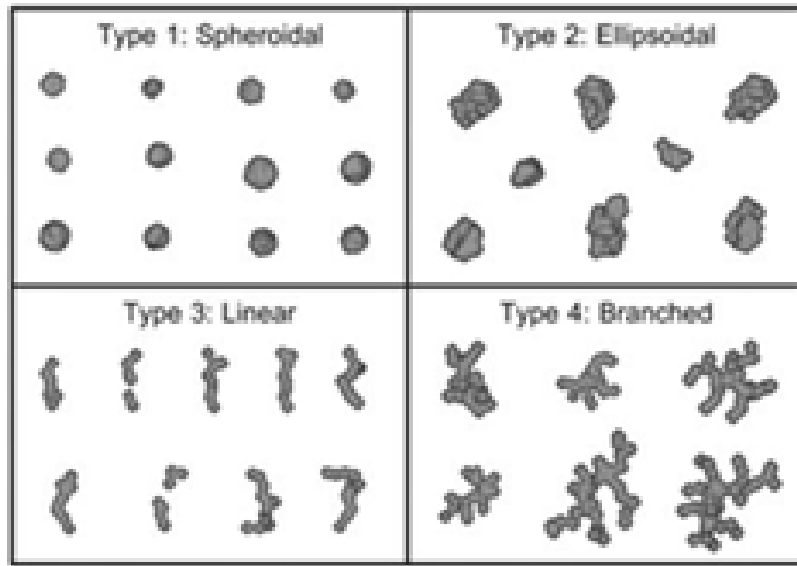


Figure 3 Description of the size, shape and surface topology of primary particles [83]

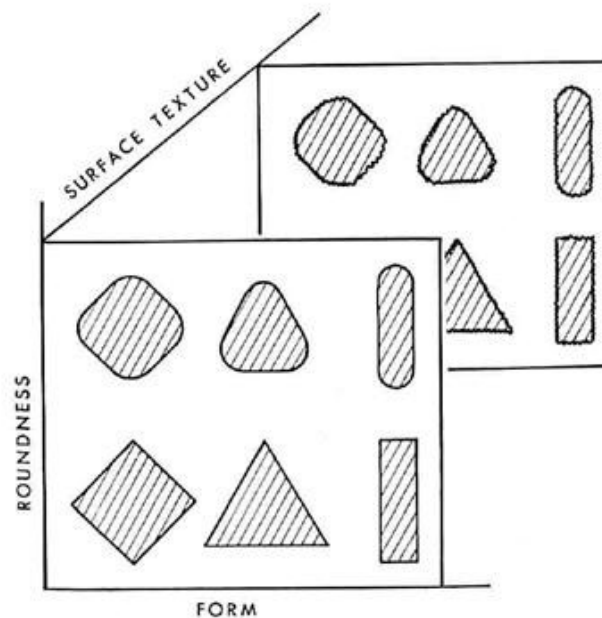


Figure 4 Description of the different structures of primary particles and aggregates/agglomerates [77]



















		Shape factor						
		Value	0,00-0,17	0,17-0,33	0,33-0,50	0,50-0,66	0,66-0,83	0,83-1,00
Sphericity	0,66-1,00							High Sphericity
	0,33-0,66							Medium Sphericity
	0,00-0,33							Low Sphericity
		Very Angular	Angular	Sub-Angular	Sub-Rounded	Rounded	Well Rounded	

Figure 5 Description of the surface topology of primary particles and aggregates/agglomerates [78]

#### 3.4.4 Applications

In WP2 of the NANoREG project, guidelines described in 3.4 are applied to describe the EM specimens of colloidal samples and of dispersion of powdered, fractal-like, aggregated nanomaterials suitable for quantitative analyses.

Examined colloidal samples include the silica, near-spherical, monomodal, certified reference materials ERM-FD100, ERM-FD102 and ERM-FD304, a multimodal mixture of near-spherical, silica materials of nominal diameters of 25, 50 and 115 nm, the colloidal silver representative test material NM-300K, polystyrene latex beads P and H, colloidal gold spherical NIST reference materials RM8011, RM8012 and RM8013 and three colloidal gold rod shaped nanomaterials with nominal diameters ranging from 12-22 nm and nominal lengths ranging from 54-68 nm.

Examined dispersions of powdered, fractal-like, aggregated nanomaterials include titanium dioxide JRCNM01000 and JRCNM01003, synthetic amorphous silica JRCNM02000 and cerium oxide JRCNM02102.

In addition, the guidelines were applied for a large variety of dispersions of nanomaterials Including synthetic amorphous silica [84, 85], ZnO [86], titania [87, 88], the silver representative test material NM-300K [89], silver nanoparticles from decoration of pastry [90].

To efficiently implement the guidelines in 3.4 on a large number of samples in CODA-CERVA, a step-by-step approach based on the FormTool, a free add-on for MS Word [91] is applied to report the qualitative EM analyses uniformly and efficiently. This user-friendly and powerful document assembly software creates an 'intelligent' MS-Word template that simplifies repetitive tasks increasing throughput speed of qualitative analyses and reducing errors. The tool allows tabulating the information required in 3.4.3 in a structured manner. Choices are suggested in drop-lists to assure uniformity in responses. From the table, a continuous text is generated. The FormTool add-on has been systematically applied to judge the quality of dispersion protocols developed for all priority materials in the nanodefine project: BaSO<sub>4</sub> fine grade, BaSO<sub>4</sub> ultrafine grade, CaCO<sub>3</sub>, pigment yellow 380, pigment yellow 386, carbon nanotubes, kaolin, methacrylate, nano steel, titanium oxide and zeolite.



### 3.5 “Electron microscopic image analysis of colloidal nanomaterials”

#### 3.5.1 *Background information*

To our knowledge, no generally accepted and validated procedure is available for electron microscopic image analysis of nanomaterials. [29]. General approaches of quantitative image analysis methodology are proposed by NIST [80]. More specific imaging and image analysis guidelines are given in ISO publications [54, 70, 78, 92]. Data analysis and representation can be done in combination with the methods described in ISO publications [54, 70, 92, 93]. Basic principles are (i) the traceability of information, imaging and results, (ii) detection, measurement, classification and representation of results on a per-particle level (number-based), (iii) (for practicality) automation of repetitive tasks.

For simple models, like colloidal materials, particles can relatively easily be detected using grey scale thresholding: they are relatively abundant and have a homogeneous size, density, shape and surface topology [32-34, 51, 94, 95].

A major advantage of such grey scale thresholding is that all nanoparticles in a micrograph can be detected simultaneously, allowing a statistically relevant number of measurements avoiding the tedious repetitive task of manual measurement. This reduces operator-induced bias. Since this method contains no steps that are specific for a certain material, it can readily be adapted to detect aggregates and agglomerates of a variety of nanomaterials [84, 86, 96], provided that they can be coated quantitatively to the EM-grid and distinguished from the background. For most metal oxides and for metallic nanomaterials, the latter poses no problem.

When the background signal of the micrographs is not homogeneous and cannot be corrected sufficiently [97, 98], grey scale thresholding can be difficult. Particle detection approaches based on magic wand [99], Hough transform [100] and template matching [101] can be useful alternatives to manual detection.

For automatically detected particles, multiple and arithmetically complex parameters, such as described in [10, 11, 70], can be measured simultaneously on high numbers of particles. Access to multiple parameters such as the aspect ratio, the mean diameter and the convexity allows selecting the parameter in function of a specific material or purpose. Verleysen [10] and De Temmerman [11] illustrate this in the scope of definition, characterization of colloidal, aggregated and agglomerated nanomaterials. Principle-component analysis and cross correlation analyses allow grouping measurands in independent classes. Representation of the number-based distribution of one representative measurand of each class allows a detailed, quantitative characterization of a nanomaterial. For agglomerated/ aggregated synthetic amorphous silica and TiO<sub>2</sub>, three independent groups of measurands are observed: size, shape and surface topology. This grouping is in line with the guidelines in [3, 29, 102, 103] that parameters of these classes are essential for the characterization and identification of a nanomaterial, e.g. in the context of the risk assessment of the application of nanomaterials in the food and feed chain. The findings of [104] corroborate this, showing that the size, physical form and morphology parameters determine the access of nanomaterials to human cells and cell organelles. In this context, the properties of individual particles measured in two dimensions can be more meaningful. Subpopulations that cannot be distinguished based on one parameter can be distinguished based on combinations of parameters for size, shape and surface.

Access to multiple parameters also allows post-analysis classification of the detected particles, avoiding the distortions in the shape and size of the detected particles introduced by a separator filter based approach as suggested by [105] and [106]. Information of the size, shape and surface topology can be used to classify particles as single primary particles or aggregates/agglomerates, and erroneously detected particles like crystallized salts, precipitated proteins and holes in the grid. Automation of this classification can include a learning step where a preliminary manual classification is used as reference and input in linear discriminant analysis or cluster analysis [51]. Alternatively, for particles with a homogeneous size, shape and surface topology template matching can be used to detect specific particles of interest [101]. A manual classification deleting artifacts from the images and excluding them from the dataset tends to be time consuming and the results may vary between operators.

The data collected for each characteristic parameter can be presented by its conventional descriptive statistics such as mean, median and percentiles [80, 92]. ISO 9276-1 [93] and ISO 9276-3 [107]

provide guidelines for representation of results of particle size analysis. Representation as a number-based distribution by binning the data over a selected range and fitting a (log) normal distribution allows a more precise estimation of the mode. Weighing the number of non-empty bins to the number of measurements in the largest bin followed by lognormal is suggested to balance the uncertainty of the measurement of the mode (bin width) and the number of particles supporting this measurement (bin height) for non-normal distributions. It is an alternative for the Freedman-Diaconis rule, Scott's rule and the Sturges rule, designed for normal distributed data [108-110].

### 3.5.2 Principle and scope

This procedure aims to analyse the 2D properties of the particles on EM micrographs. To be suitable for quantitative characterisation, the images should have a homogeneous background and the particles should be clearly distinguishable from the background.

This method allows characterising NM on EM-micrographs using image analysis software.

- The NM can be metallic consisting for example of Ag or Au, an oxide including  $\text{SiO}_2$ ,  $\text{TiO}_2$ ,  $\text{Fe}_2\text{O}_3$ ,  $\text{Fe}_3\text{O}_4$ , and other.
- The NM can be monodisperse or polydisperse.
- Freeware and/or commercial image analysis softwares can be applied.

### 3.5.3 Instructions

The SOP "Electron microscopic image analysis of colloidal nanomaterials" is applied to analyze micrographs of colloidal samples quantitatively.

### 3.5.4 Application

In WP2 of the NANoREG project, this SOP was shown efficient to examined colloidal samples include the silica, near-spherical, monomodal, certified reference materials ERM-FD100, ERM-FD102 and ERM-FD304, a multimodal mixture of near-spherical, silica materials of nominal diameters of 25, 50 and 115 nm, the colloidal silver representative test material NM-300K, polystyrene latex beads P and H, colloidal gold spherical NIST reference materials RM8011, RM8012 and RM8013 and three colloidal gold rod shaped nanomaterials with nominal diameters ranging from 12-22 nm and nominal lengths ranging from 54-68 nm.

### 3.6 “Electron microscopic image analysis of primary particles in aggregated nanomaterials”

#### 3.6.1 Background information

The European Commission recently published its Recommendation on a common definition of the term ‘nanomaterial’ for regulatory purposes. A nanomaterial as defined in this recommendation should consist for 50 % or more of particles having a size between 1 nm-100 nm [22]. To fulfill the requirements of this definition, the nanoparticle characterization method has to be able to determine the median value of the number-based particle size distribution [20]. Consequently, particle size distributions weighted according to the surface area, volume, and light-scattering intensity per size group have to be mathematically converted to the number-based size distributions required in the definition. This conversion is based on various assumptions, and becomes increasingly prone to error, difficult or impossible if the mass fraction of nanoscale particles is not sufficiently large. For more complex distributions and aggregated NMs, these “ensemble methods” are prone to error [20]. Transmission electron microscopy coupled to image analysis has the advantage that it is a counting method with a sub-nm resolution and can visualize and measure primary particles (PPs) in more complex aggregated and agglomerated powdered NMs [20]. The characterization of PPs in aggregated/agglomerated nanomaterials is successfully applied for  $\text{Al}_2\text{O}_3$  [111], carbon [30],  $\text{Fe}_3\text{O}_4$  [111],  $\text{Fe}_2\text{O}_3$  [111], synthetic amorphous silica [30, 84],  $\text{TiO}_2$  [30, 111],  $\text{ZrO}_2$  [111] and  $\text{ZnO}$  [86] NM. However, the traditional technique to measure the size of the PPs inside aggregates and agglomerates relies on tedious manual measurements with extensive operator intervention and interpretation of the EM micrographs [30, 111]. Automatic image analysis is in practice needed to obtain a sufficient number of particles to reconstruct a reliable particle size distribution [20]. Automation of the detection of PPs in aggregated and agglomerated NMs is achieved by Grishin [112] and Park [113] using the Hough transform based detection and the ultimate erosion points based detection, respectively. However, these automated methods do not allow measuring the median minimal PP size in one dimension of the NM as specified in [22].

In this SOP, an approach is proposed that estimates the median minimal PP size of aggregated NMs and its number-based distribution in the context of the EC-definition.

#### 3.6.2 Principle and scope

This procedure aims to analyse the 2D properties of the primary particles on EM micrographs. The image analysis program detects aggregated particles on an EM micrograph based on their grey value, which reflects the mass-density contrast of the material. Aggregates that are distinguishable from the background are detected and semi-automatically measured. Multiple measurands are measured simultaneously on individual aggregates. The primary particles in the aggregates are detected based on watershed segmentation and their minimal size and overlap coefficient are measured based on an Euclidean distance map.

A typical particle analysis consists of following steps:

- Image preparation
- Setting and adjusting the threshold value
- Defining the detection area
- Setting the detection parameters
- Detection of the primary particles in aggregated NM
- Selection of the primary particle parameters
- Defining the classification schemes
- Classification of the particles according the selected parameters
- Exporting of results in excel spreadsheets and storage of the (annotated) images in the NM database



### 3.6.3 Instructions

The SOP “Electron microscopic image analysis of primary particles in aggregated nanomaterials” is applied to measure the primary particle size of aggregated fractal like nanomaterials coated on TEM grids.

### 3.6.4 Applications

In WP2 of NANoREG project, the proof of principle of the methodology is developed using the model of the powdered, aggregated TiO<sub>2</sub> representative test nanomaterial NM-100 with a mean primary particle diameter near the 100 nm limit. This method is further evaluated on SAS, carbon black and other TiO<sub>2</sub> NM[24].

Since this methodology estimates the primary particles size, their overlap coefficient and the size of the aggregates, it also allowed to refine the method for fractal analysis of Brasil et al. [114]. The fractal properties of the aggregates and the volume specific surface area (VSSA) can be estimated supporting on the diameter of the maximal inscribed circle and overlap coefficient measurements for each individual PP.

The SOP was applied and validated in NANoREG for the measurement of primary particles of Titanium dioxide JRCNM01000 and JRCNM01003, Synthetic amorphous silica JRCNM02000 and Ceriumoxide JRCNM02102.

## 3.7 Data analysis and representation of measurement results according to relevant ISO-norms

The measurement results are calculated and represented according to available ISO-norms. The results of particle size analysis are represented according ISO 9276-2:2014 and ISO 9276-5:2005, the particle shape and morphology are described and quantitatively represented according to ISO 9276-6:2008, an experimental curve to a reference model is adjusted to the data as in ISO 9276-3:2008, particles are classified according to ISO 9276-4:2001.

Guidelines to objectively selecting the best measurand for omitting the agglomerated particles based on linear discriminant analysis approach are represented in [115]. The characteristic parameters can be grouped into classes by examination of the correlation matrix. To characterize the NM in detail, at least one representative parameter is selected from each of the classes [87].

## 4 Validation of SOPs for TEM size and shape analysis of the primary particles of nanomaterials.

### 4.1 Intra-laboratory validation of quantitative TEM analysis of colloidal nanomaterials

#### 4.1.1 General

In the EM service of CODA-CERVA, the developed method for quantitative TEM analysis combining the SOPs for TEM specimen preparation, TEM imaging and TEM image analysis was validated for a series of colloidal nanomaterials ranging in size from approximately 10 nm to 200 nm, and varying in shape from near-spherical to rod-shaped.

Below, an overview of the key results for selected parameters is given focussing on the measurands applied to implement the EC definition of nanomaterials. A more elaborate description of the applied methodology, results and discussion is given in the peer-reviewed NANoREG publications for near-spherical, near-monomodal silica JRC certified reference materials [115], the representative test material NM-300K [90], NIST reference materials [25]. Formal validation files with detailed results are included in the quality control system of the EM service of CODA-CERVA.

#### 4.1.2 Accuracy of TEM measurements of colloidal nanomaterials

To assess the accuracy of the TEM measurements, the measured size is compared with the (certified) reference size values for a panel of colloidal, near-spherical nanomaterials, spanning a size range from 8.9 to 202 nm.

For each individual particle, 23 measurands are measured, but since only (certified) reference values of the ECD are available, only the accuracy of ECD measurements can be evaluated. Mean ECD values are compared for the colloidal gold reference materials RM8011, RM-8012 and RM-8013 from NIST (Gaithersburg, MD, USA) [32-34]. Modal ECD values are compared for the near-monodisperse, near-spherical, certified reference materials ERM-FD100, ERM-FD304 and ERM-FD102 for IRMM (JRC, Geel, Belgium). Since, to our knowledge, for materials in the size range of 100 to 200 nm, no reference materials are certified for size measurement by TEM, the mean ECD value of the colloidal polystyrene size calibration materials P1 and H1 (NanoSight, Wiltshire, United Kingdom) assessed by TEM was compared with their mean hydrodynamic diameter.

Table 1 shows that in CODA-CERVA these modal and median ECD measurements are accurately measured. The TEM measurements are not significantly different from the (certified) reference values since the 'true' value falls within the 95% confidence interval around the measured value as described in the application note of Linsinger [116].

#### 4.1.3 Precision of TEM measurements of colloidal nanomaterials

##### 4.1.3.1 Calculation of measurement uncertainties

The intra-laboratory precision (composed of repeatability and intermediate precision) of the quantitative TEM method is assessed by measurements performed on ERM-FD100 and ERM-FD304 similar to the test design described in [117]. Repeatability indicates the closeness between results of measurements, performed over a short period, using the same instrument and performed by the same operator. The relative repeatability uncertainty is calculated from the dataset using Equation 1. The mean sum of squares is calculated using one-way ANOVA (analysis of variance).

**Table 1 Comparison of measured ( $C_m$ ) and (certified) reference ECD ( $C_{crm}$ ) values, absolute 95% expanded uncertainty ( $U(x)$  in nm) and difference between measured and certified ECD ( $\Delta m$ ).**

	$C_m$	$C_{crm}$	$U(x)$	$\Delta m$
ERM-FD100	20.3 nm <sup>a</sup>	19.4 nm <sup>a</sup>	1.7 nm	0.86 nm
ERM-FD304	27.5 nm <sup>a</sup>	27.8 nm <sup>a</sup>	1.6 nm	1.56 nm
ERM-FD102_Small	18.6 nm <sup>a</sup>	18.2 nm <sup>a</sup>	0.5 nm	0.4 nm
ERM-FD102_Large	83.5 nm <sup>a</sup>	84.0 nm <sup>a</sup>	2.0 nm	0.5 nm
RM-8011	9.3 nm <sup>b</sup>	8.9 nm <sup>b</sup>	0.7 nm	0.4 nm
RM-8012	27.4 nm <sup>b</sup>	27.6 nm <sup>b</sup>	1.1 nm	0.2 nm
RM-8013	58.5 nm <sup>b</sup>	56 nm <sup>b</sup>	3.0 nm	2.5 nm
Latex beads P	99.7 nm <sup>b</sup>	105 nm <sup>c</sup>	3.6 nm	2.3 nm
Latex beads H	203.1 nm <sup>b</sup>	202 nm <sup>c</sup>	5.1 nm	1.1 nm

<sup>a</sup> Modal ECD

<sup>b</sup> Mean ECD

<sup>c</sup> Mean hydrodynamic diameter

$$\text{Equation 1} \quad u(r) = \frac{\sqrt{MS_{within}}}{C_m}$$

With  $u(r)$  the relative repeatability uncertainty,  $MS_{within}$  the mean of squares within the measurement days and  $C_m$  the mean measured value. The relative intermediate precision uncertainty (day-to-day variability) is determined with Equation 2:

$$\text{Equation 2} \quad u(ip) = \frac{\sqrt{\frac{MS_{between} - MS_{within}}{n_r}}}{C_m}$$

With  $u(ip)$  the relative intermediate precision uncertainty,  $MS_{between}$  the mean sum of squares between different days and  $n_r$  the number of measurement replicates per day.

The relative intra-laboratory precision uncertainty is then determined by combining the relative repeatability uncertainties and the relative intermediate precision (Equation 3).

$$\text{Equation 3} \quad u(lab) = \sqrt{u^2(r) + u^2(ip)}$$

The intra-laboratory precision uncertainty summarises the uncertainties related to the non-systematic variability in sample preparation, image acquisition, image analysis and data analysis.

#### 4.1.3.2 Calibration

The magnifications of 18500 times and 68000 times are calibrated using the cross-grating method and the image shift method based on a 2160 lines/mm optical diffraction-cross grating (Agar Scientific, Stansted, England). The calibration method is implemented following ASTM E766 [118] guidelines and by using the magnification calibration software which is integrated in the Tecnai user interface software (FEI, Eindhoven, The Netherlands) [118].

Since the uncertainty associated with the calibration procedure is added as a Type B uncertainty and is not covered by the intra-laboratory uncertainty, such improvements in the calibration procedure can be included in the method validation dossier without repeating the validation experiment [119]. Table 2 shows that the calibration uncertainty depends on the magnification calibration method and the magnification. The cross-grating calibration method (X-grating) used for magnifications up to 18500 times is less effective than the image shift calibration method (Im.shift) used for higher magnifications. Application of the latter method on the magnification of 18500 times is expected to lower the calibration uncertainty systematically with 0.9 %, but requires adaptation of the applied calibration

software (FEI, Eindhoven, The Netherlands). Currently we are investigating how we can make a more conservative estimation of the calibration uncertainty based on e.g. quality control charts.

**Table 2 Overview table of the calibration uncertainty and CCD to TEM ratio for different magnifications and methods.**

Method	Magnification	Count	Uncertainty $\pm$ sd <sup>a</sup> (%)	CCD to TEM Ratio $\pm$ sd <sup>a</sup>
X-grating	440	14	1.04 % $\pm$ 0.82 %	1.48 $\pm$ 0.09
X-grating	690	14	0.87 % $\pm$ 0.67 %	1.40 $\pm$ 0.1
X-grating	890	14	0.94 % $\pm$ 0.65 %	1.42 $\pm$ 0.04
X-grating	1200	17	0.89 % $\pm$ 0.45 %	1.43 $\pm$ 0.01
X-grating	1400	14	0.77 % $\pm$ 0.48 %	1.40 $\pm$ 0.01
X-grating	1900	14	0.72 % $\pm$ 0.46 %	1.41 $\pm$ 0.01
X-grating	2900	14	0.7 % $\pm$ 0.4 %	1.37 $\pm$ 0.02
X-grating	4800	14	0.72 % $\pm$ 0.39 %	1.39 $\pm$ 0.01
X-grating	6800	14	0.75 % $\pm$ 0.44 %	1.38 $\pm$ 0.01
X-grating	9300	14	0.78 % $\pm$ 0.49 %	1.40 $\pm$ 0.01
X-grating	11000	14	0.75 % $\pm$ 0.47 %	1.43 $\pm$ 0.01
X-grating	13000	14	0.88 % $\pm$ 0.45 %	1.41 $\pm$ 0.01
X-grating	18500	14	0.91 % $\pm$ 0.58 %	1.37 $\pm$ 0.01
X-grating	23000	10	0.81 % $\pm$ 0.71 %	1.35 $\pm$ 0.01
Im.shift	23000	4	0.26 % $\pm$ 0.32 %	1.37 $\pm$ 0.01
Im.shift	30000	14	0.08 % $\pm$ 0.06 %	1.34 $\pm$ 0.01
Im.shift	49000	14	0.09 % $\pm$ 0.06 %	1.38 $\pm$ 0.01
Im.shift	68000	14	0.14 % $\pm$ 0.14 %	1.39 $\pm$ 0.01
Im.shift	98000	14	0.21 % $\pm$ 0.25 %	1.39 $\pm$ 0.01
Im.shift	120000	13	0.35 % $\pm$ 0.27 %	1.36 $\pm$ 0.01
Im.shift	150000	13	0.46 % $\pm$ 0.38 %	1.43 $\pm$ 0.05
Im.shift	180000	11	0.64 % $\pm$ 0.43 %	1.40 $\pm$ 0.02

<sup>a</sup> Standard deviation

#### 4.1.3.3 Trueness

The results of a method are 'true' if the method is free of systematic and significant bias. Whether a method produces significantly biased results can be assessed by comparing the results with reference values, for example by measuring one or more suitable CRMs as described in ERM Application Note 1 [120]. When the combined uncertainty of the measurement results and the certified value is larger than the absolute difference between the certified and the measured value ( $\Delta_m$ ), then it can be concluded that the measured value is not significantly different from the certified value. If the opposite is the case, then the method results are significantly biased and a correction of the results is preferred. Instead one can also choose to include the measured bias in the measurement uncertainty, especially when the bias value is not very well known.

This trueness assessment is not free of uncertainty itself, so even if the assessment indicates that the results are without significant bias, an uncertainty associated with the assessment of the trueness of

the method must be taken into account. The trueness uncertainty,  $u(t)$ , can be calculated by combining the uncertainty of the measurements on the CRMs,  $u(m)$ , with the uncertainties of the certified values of the CRMs,  $u(CRM)$  following Equation 4.

$$\text{Equation 4} \quad u(t) = \sqrt{u^2(m) + \frac{\sum u^2(CRM)}{n_{CRM}^2}}$$

With  $\sum u^2(CRM)$  the sum of the squares of the relative uncertainties of the certified values of the CRMs and  $n_{CRM}$  the number of CRMs.

In validation studies, such as the study presented in this paper, the uncertainty  $u(m)$  of the results obtained on the CRMs is usually not a full measurement uncertainty, as it does not yet contain the  $u(t)$  contribution. Instead,  $u(m)$  contains repeatability and intermediate precision uncertainty contributions and can be estimated from Equation 5.

$$\text{Equation 5} \quad u(m) = \sqrt{\frac{u^2(r)}{n_t} + \frac{u^2(ip)}{n_d}}$$

With  $u(ip)$  the relative intermediate precision uncertainty,  $u(r)$  the relative repeatability uncertainty,  $n_d$  the number of test days and  $n_t$  the total number of measurement replicates. Please note that the precision contributions to  $u(m)$  are different from those to  $u(lab)$  because the number of replicates and measuring days in the validation study is higher than during routine use of the method. Also, since two CRMs are tested, the measurement uncertainty of the technique is calculated from the average of the relative repeatability and relative intermediate precision uncertainties of measurements of the two CRMs.

Formally, only for ECD the trueness uncertainties of TEM analyses can be estimated using the certified uncertainty of ERM-FD100 and the indicative uncertainty of ERM-FD304. Because other certified values are lacking, it is chosen to tentatively estimate the trueness uncertainties of the six other size measures also via the certified ECD value of ERM-FD100 and the indicative ECD value of ERM-FD304.

#### 4.1.3.4 Combined and expanded measurement uncertainty

The uncertainty contributions explained above are to be combined in the method's full uncertainty budget. The intra-laboratory precision uncertainty  $u(lab)$  is a type A uncertainty: it is derived from repeated testing and covers all sources of variation between analyses and the typical between-day variation. A type B uncertainty component (values taken from certificates, expert judgement, etc.) is the uncertainty of the certified values of the used CRMs,  $u(CRM)$  and the calibration uncertainty,  $u(cal)$ . The trueness uncertainty  $u(t)$  is a mix of A and B type uncertainties [119].

If one assumes that all the uncertainty contributions for the quantitative TEM method are covered by the intra-laboratory precision uncertainty and the uncertainties for trueness and calibration, then the combined measurement uncertainty can be estimated from (Equation 6):

$$\text{Equation 6} \quad u_c(x) = \sqrt{u^2(lab) + u^2(t) + u^2(cal)}$$

The uncertainties are combined using the normal root-sum-square manner, resulting in the combined measurement uncertainty  $u_c(x)$ . When assuming that the combined uncertainty is normally distributed and a confidence level of approximately 95% is required, and when the degrees of freedom of the individual uncertainty contributions permit, then the combined uncertainty can be multiplied by a coverage factor ( $k$ ) of 2 to obtain the expanded measurement uncertainty  $U(x)$  [119].

#### 4.1.3.5 Measurement uncertainties of the minimal size in one dimension.

Measurement uncertainties of 23 measurands are estimated for all examined materials. In [115] the combined uncertainty of the measurements is, for example, shown for ERM-FD100 and ERM-FD304.

In the context of the EC definition of a nanomaterial [22], the median minimal external dimension of the particles is applied to define nanomaterials. For colloidal materials, this can be approximated by the median maximal inscribed circle diameter (MICD) and the Feret min diameter. For irregularly

shaped particles, Feret min diameter estimation tends to give a biased result overestimating the minimal external dimension of particles [121]. In such cases, MICD can give a better approximation.

Figure 6 illustrates that the developed SOPs allow measuring the Feret min and MICD of the near-spherical nanomaterials ERM-FD100 and NM-300K with a similar high precision. Since not all particles are perfectly spherical (0) the Feret min values of the examined near-spherical particles are somewhat higher than the MICD values.

An advantage of the Feret min diameter is that its measurements can be verified by manual measurement more easily than MICD measurements. Because of the lack of certified reference materials, many automated image analysis methods are verified based on manual measurement. Hence, Feret min Diameter is often selected as the parameter of choice to implement the EC-definition. To be in line with existing literature data, below, the intra-laboratory measurement uncertainties of the Feret Min diameter are represented. The intra-laboratory precision uncertainty is combined with the calibration uncertainty to calculate the combined uncertainty.

Table 3 shows that in CODA-CERVA, the median Feret min Diameter is estimated precisely by TEM for the colloidal gold reference materials (RM8011, RM-8012 and RM-8013), colloidal gold nanorods, colloidal polystyrene size calibration materials (P1 and H1), colloidal silver nanomaterial (NM-300K), and for the near-monodisperse near-spherical synthetic amorphous silica certified reference materials (ERM-FD100, ERM-FD304 and ERM-FD102). The 68 % uncertainties lie between 1.1 % and 4.3 % depending on the material. For rod-like materials the uncertainties are larger than for near-spherical materials.

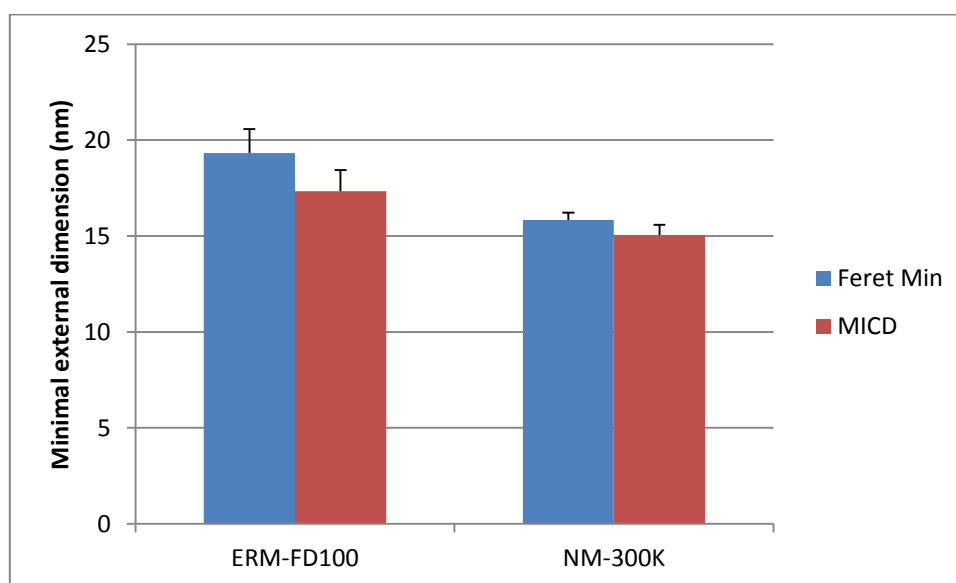


**Figure 6 Comparison of the minimal external dimension of ERM-FD100 and NM-300K particles estimated as Feret min diameter and as MICD. The bar represents the expanded intra-laboratory uncertainty (95%).**

Table 3 shows that in CODA-CERVA, the median Feret min Diameter is estimated precisely by transmission electron microscopy (TEM) for the colloidal gold reference materials (RM8011, RM-8012 and RM-8013), colloidal gold nanorods, colloidal polystyrene size calibration materials (P1 and H1), colloidal silver nanomaterial (NM-300K), and for the near-monodisperse near-spherical synthetic amorphous silica certified reference materials (ERM-FD100, ERM-FD304 and ERM-FD102). The 68 % uncertainties lie between 1.1 % and 4.3 % depending on the material. For rod-like materials the uncertainties are larger than for near-spherical materials.

**Table 3 Estimation of the intra-lab uncertainties of the size measurement using quantitative TEM of the median minimal size in one dimension, estimated as Feret min.**

Name	Median $\pm$ U(x)	u(r)	u(ip)	u(lab)	u(cal)	u <sub>c</sub> (x)
NM-300K	15.6 $\pm$ 0.6 nm	2.02 %	0.00 %	2.02 %	0.1 %	2.0 %
ERM-FD100	19.2 $\pm$ 1.0 nm	1.31 %	1.79 %	2.22 %	1.3 %	2.6 %
FD102_Small	18.8 $\pm$ 1.6 nm	3.70 %	1.5 %	4.0 %	1.3 %	2.9 %
FD102_Large	82.2 $\pm$ 1.4 nm	0.50 %	0.4 %	0.64 %	0.9 %	2.4 %
ERM-FD304	26.1 $\pm$ 1.0 nm	1.61 %	0.20 %	1.62 %	1.3 %	2.1 %
RM8012	26.7 $\pm$ 1.0 nm	1.80 %	0 %	1.8 %	0.9 %	2.0 %
RM8013	57.3 $\pm$ 2.6 nm	1.60 %	1.47 %	2.17 %	0.9 %	2.3 %
Rods 9-15 nm	14.3 $\pm$ 1.2 nm	3.55 %	0.00 %	3.55 %	1.07 %	4.29 %
Rods 12-18 nm	15.4 $\pm$ 1.3 nm	3.45 %	0.00 %	3.45 %	1.07 %	4.21 %
Rods 19-25 nm	25.1 $\pm$ 2.1 nm	2.02 %	1.16 %	2.33 %	1.07 %	3.34 %
Latex beads P	98.2 $\pm$ 3.2 nm	1.24 %	0.55 %	1.35 %	0.9 %	1.6 %
Latex beads H	199.9 $\pm$ 4.4 nm	0.67 %	0 %	0.67 %	0.9%	1.1 %

#### 4.1.3.6 Measurement uncertainties of the shape measurement

Measurement uncertainties of 23 measurands are estimated for all examined materials. These include 5 measurands estimating the shape and the surface structure. In [115] the combined uncertainty of these measurands is, for example, shown for ERM-FD100 and ERM-FD304.

The aspect ratio is most frequently used, among others, to classify particles as nanorods based on [122]. Table 4 shows that in CODA-CERVA the aspect ratio can be measured precisely. The 68% uncertainties lie between 1.1 % and 4.5 %. For near-spherical materials the uncertainties are lower than for materials that are rod-shaped.

**Table 4 Estimation of the intra-lab uncertainties of the measurement of the shape, estimated as aspect ratio, using quantitative TEM.**

Name	Median $\pm$ U(x)	u(r)	u(ip)	u <sub>c</sub> (x)
NM-300K	1.13 $\pm$ 0.02 nm	1.00 %	0.00 %	1.00 %
ERM-FD100	1.18 $\pm$ 0.03 nm	1.16 %	0.18 %	1.18 %
Rods 9-15 nm	2.51 $\pm$ 0.1 nm	2.01 %	0.11 %	2.02 %
Rods 12-18 nm	2.81 $\pm$ 0.3 nm	4.51 %	0.39 %	4.52 %
Rods 19-25 nm	3.43 $\pm$ 0.3 nm	4.06 %	0.00 %	4.06 %

#### 4.1.4 Application of the SOPs to resolve different subpopulations of MNM in a multimodal mixture

It is challenging to measure the size and shape properties of MNM that are polydisperse in size, particularly when the fraction of the smallest particles is small. As a proof-of-principle, it was demonstrated that the developed TEM-based SOPs allowed measuring the size and shape properties of the primary particles of a trimodal MNM where the fractions of the smaller particles are smaller than those of the larger particles. For this purpose, tailor-made MNM were produced by IIT (Italy). Table 5 and Figure 7 illustrate, for example, that similar ECD are measured for silica nanoparticles in a



monomodal preparation as in a mixture combining these three preparations. Similar results were obtained for other size and shape parameters (not shown).

**Table 5 Maximal inscribed circular diameter measurements of synthetic amorphous silica near-spherical particles showing the mode, median and mean size.**

Name	Mode	Median	Mean	N
Ag@IIT NPs	20.3 nm	20.4 nm	20.0 nm	39589
SiO <sub>2</sub> @IIT NPs 25 nm	25.2 nm	25.2 nm	27.2 nm	17953
SiO <sub>2</sub> @IIT NPs 50 nm	51.4 nm	51.6 nm	53.6 nm	5774
SiO <sub>2</sub> @IIT NPs 115 nm	119.4 nm	118.6 nm	118.4 nm	2712
SiO <sub>2</sub> @IIT Mix NPs 25-50-115 nm				
• 25 nm < 30 nm	23.6 nm	22.9 nm	22.6 nm	10
• 50 nm > 30 nm < 65 nm	51.4 nm	49.9 nm	48.8 nm	112
• 115 nm > 65 nm	112.3 nm	112.4 nm	111.6 nm	424

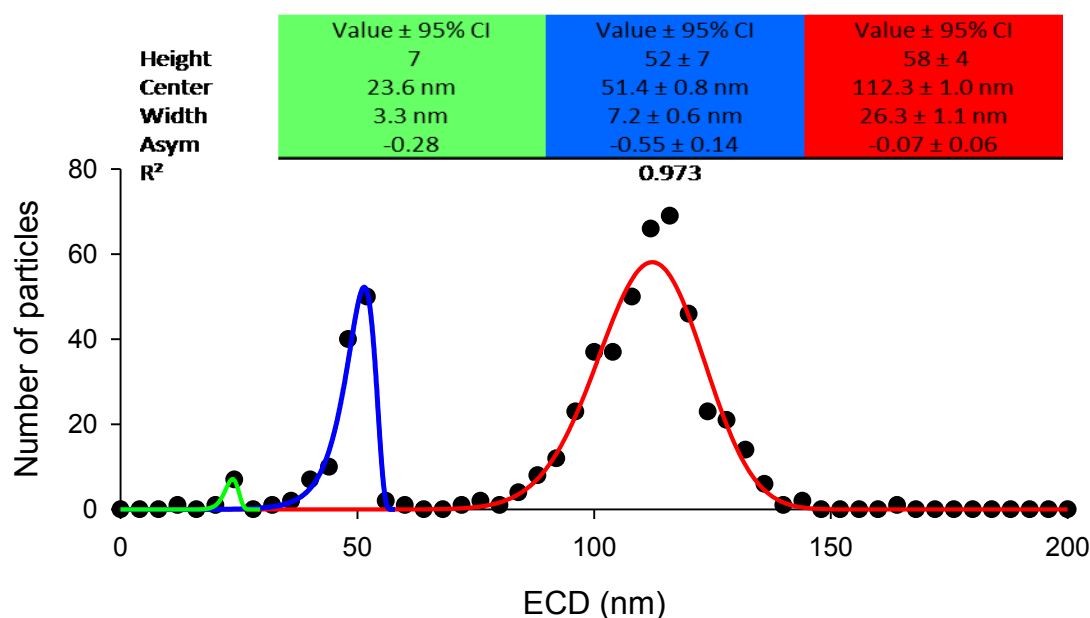


**Figure 7** Number based size distribution of SiO<sub>2</sub>@IIT Mix NPs sample 25-50-115 nm. The height, mode (center) and Half width at half max (HWHM) of the distributions describing the fitted curve are indicated close to the relevant peaks together with the 95% CI indicating how precisely these quantitative parameters are estimated by the model.

#### 4.1.5 Comparison of EM measurements with the results of complementary techniques PTA, DLS, SEM and SP-ICP-MS

TEM results were compared with results of other techniques like single particle induced coupled plasma mass spectrometry (SP-ICP-MS), dynamic light scattering (DLS) and particles tracking analysis (PTA).

An intra-laboratory validation of SEM was performed on ERM-FD100 by INMETRO using in house SOPs. A FEI Helios NanoLab 650 was used for imaging acquisition in conventional secondary electron mode (SE-TLD detector) and transmitted scanning mode (Bright Field TSEM detector).



**Table 6 Standard measurements uncertainties of modal and median ECD obtained for ERM-FD100 sample**

Measurand	ECD mode		ECD median	
	TLD	TSEM	TLD	TSEM
Mean measured value, $C_m$ (nm)	19.22	19.22	20.40	20.41
Standard deviation (nm)	2.71	2.66	2.02	1.43
Certified value (nm)	19.40	19.40	-	-
Relative measurement uncertainty $u_m$ (%)	5.72	6.21	4.69	3.18
Combined uncertainty $u_c$ of measurement, $u_m$ and certified, $u_{cert}$ (%)	6.67	7.16	5.69	4.90
Expanded uncertainty (k=2) $U_c(ERM)$ (nm)	2.56	2.64	2.32	1.72
Absolute difference between certified and measured value, $\Delta m$ (nm)	0.18	0.95	1.00	0.91
$U_c(ERM) - \Delta m^a$	2.38	1.69	1.32	0.82

<sup>a</sup> To evaluate the method performance,  $\Delta m$  is compared with  $U_c(x)$  values. If there is no significant difference between the measurement result and the certified value [120]

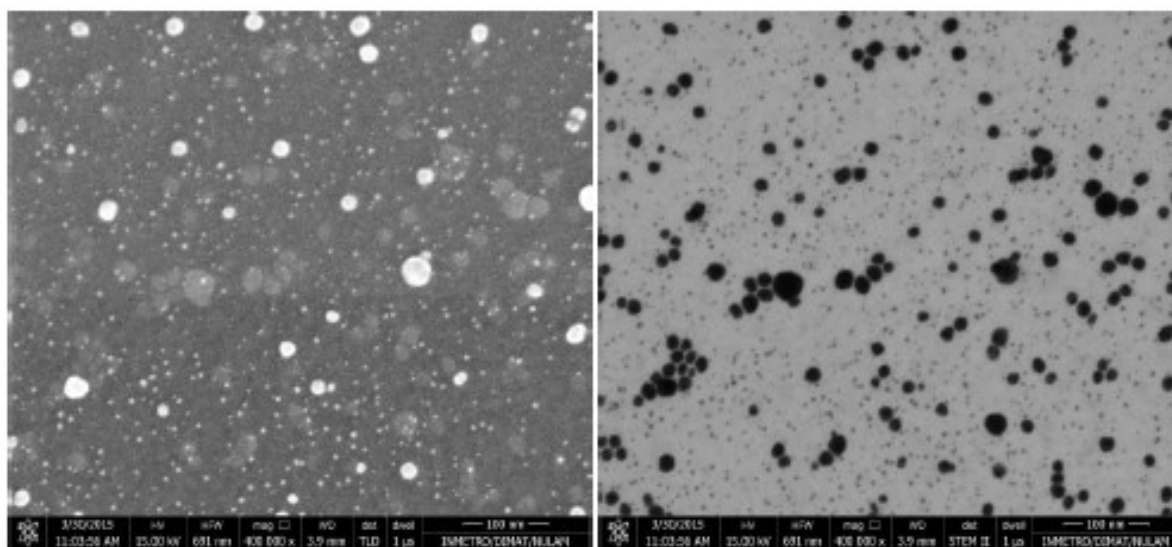


**Figure 8 SEM images of NM300K sample acquired by SE-TLD (left) and TSEM (right) detectors.**

The measured value by SEM is not significantly different from the certified value. The SEM results for ERM-FD100 are not significantly different from the TEM measurements and indicate that there is no significant method defined bias.

An intra laboratory validation of SP-ICP-MS was performed on NM-300K by CODA-CERVA using in house SOPs. The particle size measured by SP-ICP-MS relates the best with the ECD measured by TEM, assuming that the particles are spherical. The results of Table 7 and Table 8 illustrate that there is a method defined difference in medians of 3,4 nm and in means of 3,9 between the SP-ICP-MS measurements and the ECD TEM measurements reported in Table 7. The TEM size however falls within the 95% CI around the sizes measured by SP-ICP-MS indicating no significant method bias with the TEM measurements for a colloidal, metallic, near-spherical, near-monomodal nanomaterial like NM-300K. For other types of NM, this has to be evaluated on an ad hoc base.

**Table 7 Inter-laboratory comparison of the Mean median ECD measurements for NM-300K.**

Lab	Mean median ECD	Mean mean ECD
A	16.4 nm	16.7 nm
B	15.1 nm	15.3 nm
C	15.9 nm	16 nm
D	16.3 nm	16.6 nm

D*	15.9 nm	16.2 nm
E	14.7 nm	15 nm
F	16.4 nm	17.8 nm
G	15.9 nm	16.1 nm
H	15.6 nm	15.7 nm
Mean	15.8 nm	16.1 nm
Sd	0.6 nm	0.8 nm

**Table 8 Overview of selected validation parameters for NM-300K by SP-ICP-MS**

	Particle size			Particle number concentration	Particle mass concentration
	Median	Mean	Mode		
Mean value	19.2 nm	20.0 nm	18.6 nm	$2.0 \cdot 10^{18} \text{ kg}^{-1}$	97100 mg/kg
U	3.8 nm	4.2 nm	3.5 nm	$0.8 \cdot 10^{18} \text{ kg}^{-1}$	17500 mg/kg
LOD	12 nm	12 nm	12 nm	$8.0 \cdot 10^6 \text{ part/L}^{(b)}$	0.35 ng/L <sup>(b),(c)</sup>
LOQ	13 nm	13 nm	13 nm	-	-
Repeatability ( $s_r$ )	4.3%	4.8%	4.1%	11.3%	8.9%
Intermediate precision ( $s_{ip}$ )	9.3%	9.6%	8.7%	19.6%	8.9%
Apparent bias <sup>(d)</sup>	+17%	+21%	+16%	-	-
Relative recovery	-	-	-	78% / 86% <sup>(e)</sup>	99%
Measurement uncertainty (U; k = 2)	20%	21%	19%	42%	18%

<sup>(a)</sup> Reported values are the averages of the results obtained at both dilution levels; <sup>(b)</sup> In the diluted suspension; <sup>(c)</sup> The LOD for mass concentration depends on the particle size: 0.35 ng/L is the LOD for particles of 20 nm; <sup>(d)</sup> Apparent bias versus the equivalent circle diameter determined by TEM; <sup>(e)</sup> respectively taking into account 3.5% ionization or 3.5% ionization & 8.6% of particles < LOD.

The differences between the mean and median sizes measured by SP-ICP-MS and TEM can be explained by the fact that under the applied conditions (magnification, CCD camera, microscope configuration, the limit of quantification for TEM size analysis of NM-300K is lower than the limit of quantification by SP-ICP-MS (13 nm) and by the observation (by TEM) that the particles are not perfectly spherical. Because the detection limit of SP-ICP-MS for Ag is about 13 nm, only a part of the distribution was measured (Figure 9) and size measurements of NM-300K by SP-ICP-MS are therefore larger than the ECD measurements by TEM.

An intra-laboratory validation of PTA was performed on colloidal gold reference materials (RM-8012 and RM-8013), on polystyrene latex beads (P and H), on colloidal silver representative test material (NM-300K) on colloidal gold nanorods with sizes between 9 and 25 nm and on a fractal like representative test material NM-100 by CODA-CERVA using in house SOPs. The results of Table 9 illustrate that for near-spherical, near- monodisperse, colloidal materials (RM8012, RM8013, P, H and NM-300K), the PTA results seem to be close to the TEM results reported in Table 3. The TEM size falls within the 95% CI around the sizes measured by PTA indicating that there is no significant method bias with the TEM measurements. For rod-like and fractal-like materials PTA measures the hydrodynamic diameter. This measurand cannot be directly compared to the dimension of the particles measured by TEM.

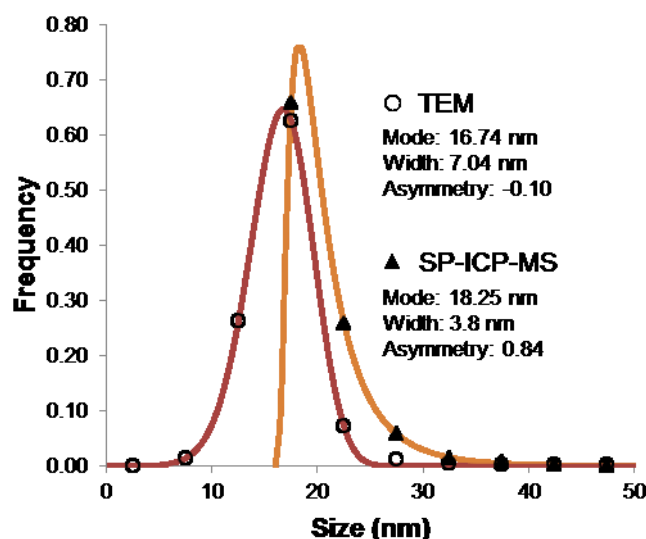


Figure 9 Comparison of TEM particle size measurement (Feret min) and SP-ICP-MS particle size measurement (volume equivalent spherical diameter) for NM-300K (Adapted from [90]).

Table 9 Overview table of the hydrodynamic diameter measured by PTA showing mean modal values and 95% expanded uncertainties.

	Hydrodynamic diameter $\pm U(x)$
RM8012	30.3 nm $\pm$ 15%
RM8013	53.7 nm $\pm$ 7%
Latex beads P	104.6 nm $\pm$ 9%
Latex beads H	199.6 nm $\pm$ 8%
NM-300K	36.8 nm $\pm$ 47 %
Rods 9-15 nm	51.8 nm $\pm$ 30%
Rods 12-18 nm	55.1 nm $\pm$ 18%
Rods 19-25 nm	36.9 nm $\pm$ 47%

INMETRO characterized tested ERM-FD100 and NM-300K by DLS and NRCWE characterized NM-300K using their in house SOPs. The results in Table 10 show that size measurements of ERM-FD100 is not significantly different from the certified Intensity-weighted harmonic mean diameter (19.0 nm  $\pm$  0.6 nm). The DLS results for ERM-FD100 are not significantly different from the TEM measurements and indicate that there is no significant method defined bias. For these near-spherical, near-monomodal, colloidal particles, the hydrodynamic diameter measurements by DLS overestimate the particle size of NM-300K by about 20 nm (Table 10 and Table 11). The values measured by INMETRO and NRCWE, as the values measured in CODA-CERVA (not shown) correspond well with the values given in the characterization report of NM-300K and with the PTA results [123].

Table 10 Results average of ERM-FD100 and NM-300K analysed by INMETRO by DLS

Parameter	FD 100 S0070	NM300K Ag S07424	NM300K Ag S07425	NM300K Ag S07426
Concentration w/w %	1	0.787	0.844	0.611
Z-Average (nm)	18.83	34.73	31.44	36.03

Standard Deviation	0.18	2.87	1.50	2.78
PDI	0.096	0.533	0.495	0.548
Standard Deviation	0.004	0.085	0.047	0.060
Zeta Potential (mV)	-45.10	-2.772	-	-
Standard Deviation	4.19	0.612	-	-
Conductivity (mS/cm)	0.239	12.8	-	-
Standard Deviation	0.004	0.8	-	-

**Table 11 Results average of NM-300K analysed by NRCWE by DLS**

Parameter	NM300K Ag	NM300K Ag
Method	General Purpose (Normal Resolution)	Multi Narrow Modes (High Resolution)
Concentration (mg/ml)	10.71	12.14
Standard Deviation	8.17	9.01
Z-Average (nm)	50.26	38.82
Standard Deviation	15.93	17.58
PDI	0.51	0.43
Standard Deviation	0.07	0.22

Under the conditions where NM-300K was investigated by DLS, a zeta potential of -2.772 was measured close the isoelectric point. Therefore, it is very likely that the silver particles form agglomerates and precipitate. DLS and PTA measure the hydrodynamic diameter of these agglomerates, which are larger than the primary particles measured by TEM and SP-ICP-MS.

It can be concluded that DLS and PTA can be applied to implement the EC definition of NM for near-spherical, near-monomodal NM in colloidal dispersions provided that (i) the size of the particles is in the useful range of the method, and (ii) the dispersions are stable (no agglomeration). Measurement of the zeta-potential can be instrumental to objectify the latter.

## 4.2 Intra-laboratory validation of quantitative TEM analysis of aggregated/agglomerated nanomaterials

These materials are representative test materials obtained from the JRC repository of nanomaterials (IHCP, Ispra, Italy). The intra-laboratory measurement uncertainties were determined according to the guidelines [124, 125].

The traditional technique to measure the size of the PPs inside aggregates and agglomerates relies on tedious manual measurements with extensive operator intervention and interpretation of the EM micrographs [30, 111]. By using these techniques, PPs are successfully characterised in aggregated/agglomerated nanomaterials for  $\text{Al}_2\text{O}_3$  [111], carbon [30],  $\text{Fe}_3\text{O}_4$  [111],  $\text{Fe}_2\text{O}_3$  [111], synthetic amorphous silica [30, 84],  $\text{TiO}_2$  [30, 111],  $\text{ZrO}_2$  [111] and  $\text{ZnO}$  [86] NM. Automation of the detection of PPs in aggregated and agglomerated NMs is achieved by Grishin [112] and Park [113] using the Hough transform based detection and the ultimate erosion points based detection, respectively. However, these automated methods do not allow measuring the median minimal PP size in one dimension of the NM as specified in [22]. The SOPs allow to detect and measure primary particles (PPs) in complex aggregated and agglomerated powdered NMs [20] and allow obtaining a sufficient number of particles to reconstruct a reliable particle size distribution [20].

Below, an overview of the key results for selected parameters is given focussing on the measurands applied to implement the EC definition of nanomaterials. A more elaborate description of the applied methodology, results and discussion is given in the peer-reviewed [24]. Formal validation files with detailed results are included in the quality control system of the EM service of CODA-CERVA. In the context of the EC definition of a nanomaterial [22], the median minimal external dimension of the particles is applied to define nanomaterials. For irregularly shaped particles, Feret min diameter estimation tends to give a biased result overestimating the minimal external dimension of particles [121]. In such cases, MICD gives a better approximation.

In the NANoREG project, selected materials are further analyzed with other complementary techniques (PTA, DLS and SP-ICP-MS) testing the accuracy and precision of the methods and detecting possible bias between method-defined size estimations.

Figure 10 illustrates that the developed SOPs allow measuring the Feret min and MICD of the primary particles and the aggregates of the fractal like JRCNM01000, JRCNM01003, JRCNM02000 and JRCNM02012 with a similar high precision. Since the primary particles have an irregular shape (0) the Feret min values of the examined near-spherical particles are somewhat higher than the MICD values. The shape of the aggregates is more irregular, resulting in larger differences between MICD and Feret min.

An advantage of the Feret min diameter is that its measurements can be verified by manual measurement more easily than MICD measurements. Because of the lack of certified reference materials, many automated image analysis methods are verified based on manual measurement. Hence, Feret min Diameter is often selected as the parameter of choice to implement the EC-definition. To be in line with existing literature data, below, the intra-laboratory measurement uncertainties of the Feret min diameter are represented. The intra-laboratory precision uncertainty is combined with the calibration uncertainty to calculate the combined uncertainty.

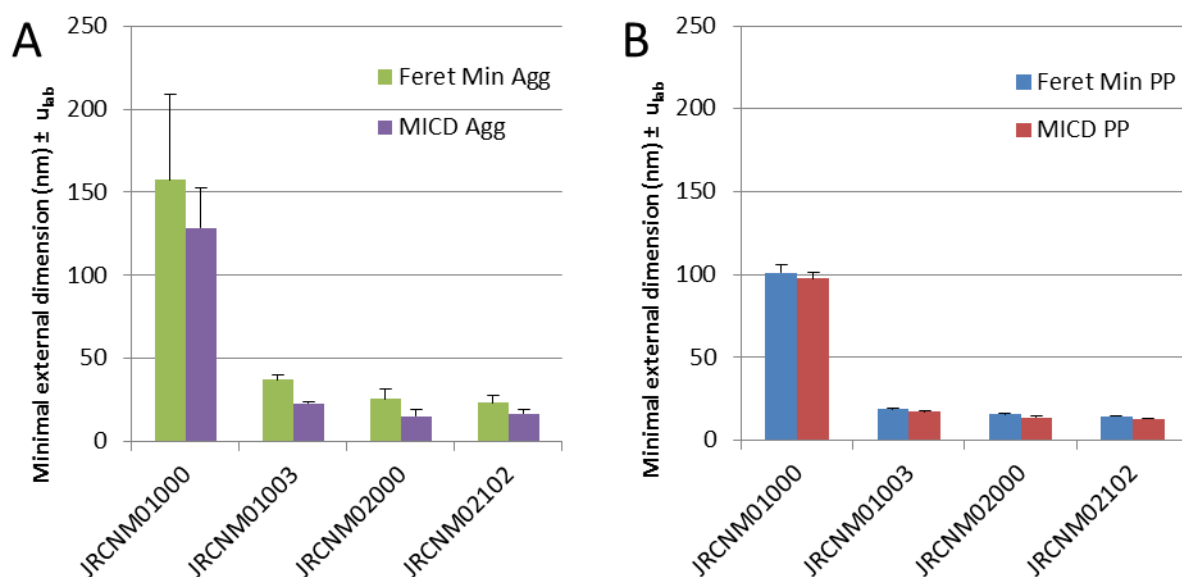


**Figure 10** Histograms showing the minimal external dimension of particles indicating the Feret min and Maximal inscribed circular diameter (MICD measurements of aggregates (A) and primary particles (B) together with the intra-laboratory uncertainty (95%).

The Nanogenotox protocol allowed bringing fractal like nanomaterials in a stable dispersion. The ethanol pre-wetting and BSA were omitted from sample preparation since the materials were prepared for characterization in dispersed form and did not have a hydrophobic coating. The SOPs allow to accurately measuring the Feret min and maximal inscribed circular diameter of titanium dioxide (JRCNM01000 and JRCNM01003), synthetic amorphous silica (JRCNM02000) and cerium oxide (JRCNM02102) core materials of NANoREG. By adapting the image analysis SOP, primary particles in the fractal like aggregates were accurately measured. Even though 23 measurands are recoded for the aggregates here only the MICD measurements are presented here.

**Table 12** Overview table of Maximal inscribed circular diameter measured by TEM showing the median size, repeatability uncertainty, intermediate precision uncertainty and itralab uncertainty.

Name	Median ± U(x)	u(r)	u(ip)	u(lab)
JRCNM01000	97.53 ± 8.24 nm	3.75%	1.94%	4.23%
JRCNM01003	17.07 ± 0.91 nm	1.94%	1.83%	2.66%
JRCNM02000	15.88 ± 1.3 nm	3.74%	1.66%	4.09%
JRCNM02102	12.88 ± 1.23 nm	4.45%	1.76%	4.79%

Table 12 shows that the SOPs in CODA-CERVA resulted in precise measurements of median maximal inscribed circular diameter measurements. The 68% uncertainties lie between 2.6 % and 4.8 %.

### 4.3 Between-laboratory validation (ILC) of the method developed for quantitative TEM analysis

#### 4.3.1 Aim of the ILC study in D2.10

This ILC study aims to validate the developed method for quantitative TEM analysis of the size and shape of the primary particles of colloidal (4.3.5) and aggregated, fractal-like MNM (4.3.7).

#### 4.3.2 Instructions for quantitative TEM analysis

A quantitative TEM analysis of colloidal MNM combines the “Preparation of EM-specimens containing a representative sample of the particles in dispersion” (3.2), “Transmission electron microscopic imaging of nanomaterials” (3.3), a descriptive analysis according to the Guidelines for qualitative characterization of nanomaterials in dispersion in a regulatory framework (3.4), and the “Electron microscopic image analysis of colloidal nanomaterials”(3.5).

A quantitative TEM analysis of aggregated MNM combines the Modified “Final protocol for producing suitable manufactured nanomaterial exposure media” [21] (3.1), the “Preparation of EM-specimens containing a representative sample of the particles in dispersion” (3.2), “Transmission electron microscopic imaging of nanomaterials” (3.3), a descriptive analysis according to the Guidelines for qualitative characterization of nanomaterials in dispersion in a regulatory framework (3.4), and the “Electron microscopic image analysis of primary particles in aggregated nanomaterials”(3.6).

#### 4.3.3 Design of the ILC study in D2.10

The proposed experimental design estimates the variation between competent laboratories applying the procedures that were envisaged to be laboratory- and platform-independent. Basis of this ILC approach is the estimation of the laboratory biases. The intention is that the measurements within each laboratory are performed under reproducibility conditions such that the collected results are independent.

To validate the SOPs applicable to measure the size and shape properties of near-spherical, near-monomodal colloidal MNM, the certified reference material ERM-FD100 [95] and the representative test material NM-300K were examined by all participating laboratories(**Error! Reference source not found.**). The experimental design was elaborated such that each of the participants could estimate also its intra-lab uncertainties, as a basis for intra-laboratory validation of the SOPs.

The competence of the participating laboratories is evaluated based on the measurement of the ECD of ERM-FD100 certified reference material. Although the sample preparation was not done separately, the analyses results of INMETRO obtained using two different microscope configurations were treated as if they came from independent laboratories, since the instruments were calibrated in an independent way and imaging and image analyses were done by different operators. For colloidal MNM the effects of specimen preparation on measurands and their uncertainties are assumed to be minimal.

To validate the SOPs applicable to measure the minimal external size of the primary particles in aggregated, fractal-like MNM, as foreseen in the EC-definition of NM [126], four NANoREG core materials with fractal-like aggregates were included in this study. For comparison, the size and shape properties of the aggregates and their measurement uncertainties were estimated. SOPs were evaluated for JRCNM02000 and JRCNM01003 by 3 labs (INL, CODA-CERVA and NRCWE) or for JRCNM01000 and JRCNM02102 by 4 (INMETRO, CODA-CERVA, INL and NRCWE) partners (**Error! eference source not found.**).

For each EM test sample, at least a 500 discrete particles were imaged and analysed. Foreign artefacts like dust particles, residues from drying, etc., and agglomerates and touching particles measured as one particle, were excluded from the image analysis process. The imaged group of particles, originated from at least 5 different systematically random (widely separated) selected view fields (images) as specified in the SOPs. Each partner sent a detailed and signed analysis report to the ILC coordinator. This analysis report contained the information, listed in Table 21 required to assure traceability of analyses. In addition to the analysis report, the participant provided the measurement results in an electronic reporting template (MS Excel) that provides key information regarding the sample, sample preparation, method and instrument information, imaging and image



analysis. Table 23, Table 25, and Table 27 and Table 24, Table 26 and Table 28 in annex summarize, respectively, the sample preparation conditions, imaging conditions and the image processing conditions for the participating laboratories for ERM-FD100 and NM-300K respectively.

To avoid imprecisions and variability in data analysis, CODA-CERVA technically evaluated and analysed the received raw datasets of colloidal and aggregated MNM using appropriate statistical techniques and represented them according to the relevant ISO-norms (3.7).

#### 4.3.4 Competence of the participants

Each of the participants estimated its intra-lab uncertainties, as a basis for his intra-laboratory validation of these SOPs. **Error! Reference source not found.** gives an overview of the datasets collected for the ILC by the different partners of D2.10, indicating the number of days and repetitions per day (days x repetitions/day). Most labs followed the 5 days and 3 repetitions per day scheme to validate their results. One laboratory only measured for 2 days and 2 repetitions per day which may result in an underestimation of the intra-laboratory uncertainty. Intra-laboratory measurement uncertainties were calculated as described in 4.1.3.1. Table 13 shows that for all labs the measured mean value of ECD is not significantly different from the certified value of 19.4 nm since the difference  $\Delta m$  between the certified and the measured value is larger than the expanded combined uncertainty of result and certified value  $U_{\Delta}$  [120].

**Table 13 Validation results of ERM-FD100 with the mean modal ECD,  $U(X)$ , the expanded intra-laboratory uncertainty (95%) and  $\Delta m$ , the absolute difference with the certified EM value of 19.4 nm and Expanded combined uncertainty of result and certified value  $U_{\Delta}$ .**

Lab	Mode	$U(x)^a$	$\Delta m$	$U_{\Delta}^b$
A	19.1 nm	5.1 %	0.3 nm	1.6 nm
B	18.1 nm	10.4 %	1.3 nm	2.3 nm
C	18.1 nm	3.4 %	1.3 nm	1.4 nm
D	18.2 nm	10.8 %	1.2 nm	2.4 nm
D*	18.4 nm	5.9 %	1 nm	1.7 nm
E	16.5 nm	26.4 %	2.9 nm	4.5 nm
F	19.8 nm	12.0 %	0.4 nm	2.7 nm
G	19.7 nm	12.2 %	0.3 nm	2.7 nm
H	18.6 nm	5.0 %	0.8 nm	1.6 nm

<sup>a</sup> Repeatability, intermediate precision and calibration uncertainties.

<sup>b</sup> 95% expanded combined uncertainty of result and certified value ( $u_{CRM} = 0.65$  nm)

#### 4.3.5 Inter-laboratory validation of the SOPs for near-monomodal, near-mondisperse, colloidal MNM with focus on the application of the EC definition of MNM

Using the SOPs, the participating laboratories could determine the number-based size distribution of the (minimal external) sizes in line with the EC definition, as illustrated in Figure 11.



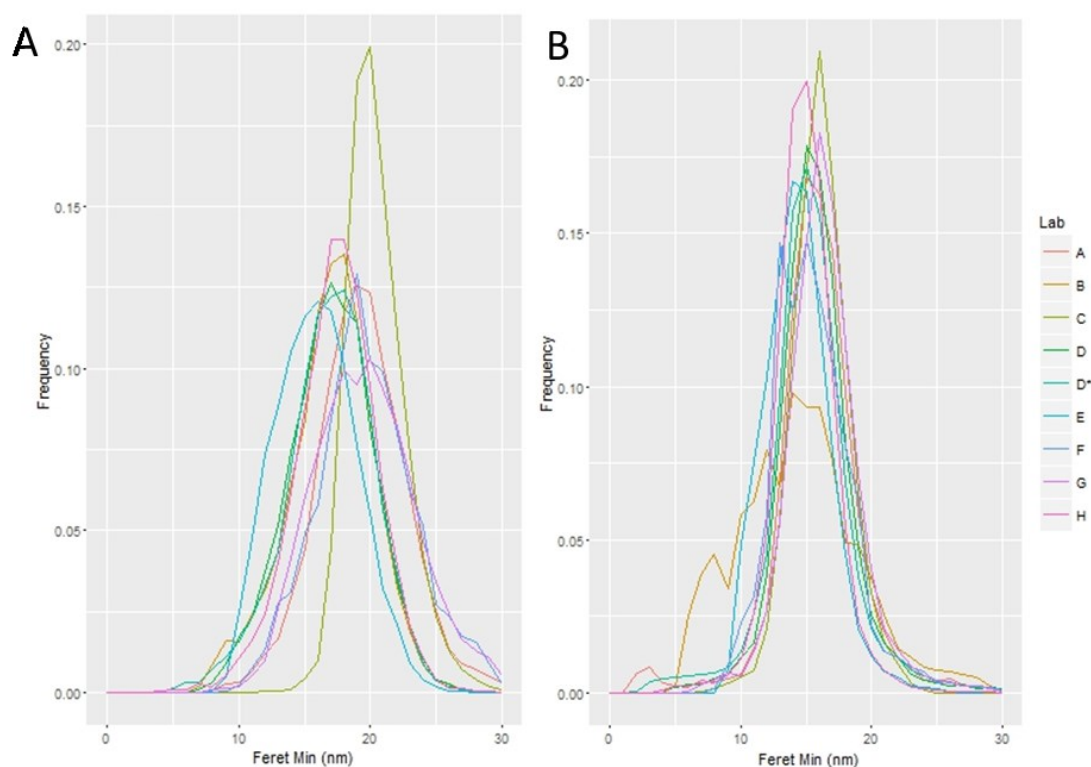


**Figure 11 MinFeret distributions of ERM-FD100 (Left) and NM-300K (Right) for the 9 obtained datasets.**

In this report, the intra-laboratory precision is given for the median values in accordance to the EC definition which is based on the true median size value of the particle size distribution of the minimal external dimension of the particles [22]. The intra-laboratory precision uncertainty is combined with the calibration uncertainty to calculate the combined uncertainty (as described in 4.1.3).

The SOPs allow a precise measurement of the size and shape of the colloidal silver nanomaterial NM-300K and of the near-monodisperse near-spherical synthetic amorphous silica certified reference material ERM-FD100 (Figure 12). Even though 9 measurands are recorded, the focus of this report lies on the minimal external dimension of the particles as applied in the EC definition of the term nanomaterial. This minimal external dimension can be estimated by the MICD and by the Feret min. Both these measurands were measured. The Feret min (Table 14) has the advantage that it can be manually measured.

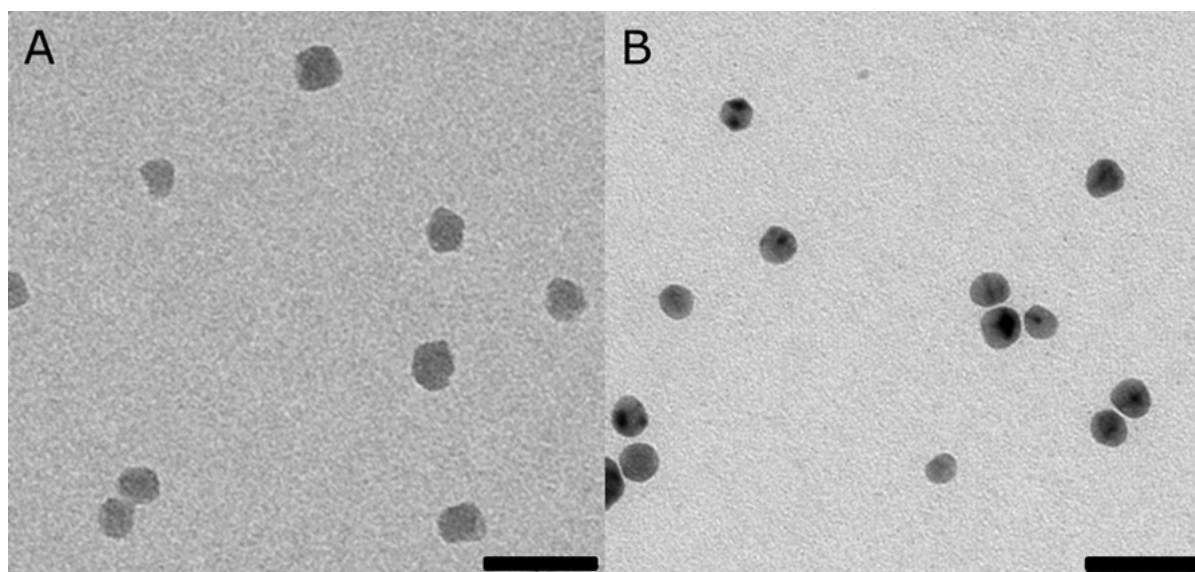


**Figure 12** Selected TEM micrographs of the materials tested during the Inter-Laboratory validation of the SOPs for near-monomodal, near-mondisperse, colloidal MNM ERM-FD100 (A) and NM-300K (B). Bar 50 nm.

The inter-laboratory is calculated as 2 times the standard deviation of the mean median Feret min measurements of the 9 datasets. The intra-laboratory measurement uncertainty of the Feret min measurement is for both examined MNM in the same order as the inter-laboratory measurement uncertainty.

**Table 14** Inter-laboratory comparison of the mean median Feret min measurements for ERM-FD100 and NM-300K with measurement uncertainties.

Lab	ERM-FD100 (mean $\pm$ $u_{lab}$ )	NM-300K (mean $\pm$ $u_{lab}$ )
A	19.3 $\pm$ 1.2 nm	15.8 $\pm$ 0.4 nm
B	17.2 $\pm$ 1.4 nm	14.2 $\pm$ 1.8 nm
C	20.1 $\pm$ 0.3 nm	16.1 $\pm$ 0.4 nm
D	17.1 $\pm$ 1.7 nm	15.5 $\pm$ 0.4 nm
D*	17.1 $\pm$ 1.0 nm	15.2 $\pm$ 0.6 nm
E	15.8 $\pm$ 4.1 nm	14.1 $\pm$ 2.0 nm
F	20.3 $\pm$ 4.3 nm	15.7 $\pm$ 2.3 nm
G	19.6 $\pm$ 2.4 nm	16.2 $\pm$ 0.8 nm
H	17.5 $\pm$ 0.8 nm	14.9 $\pm$ 0.3 nm
Mean $\pm$ inter-laboratory uncertainty (95%)	18.2 $\pm$ 3.2 nm	15.3 $\pm$ 1.5 nm

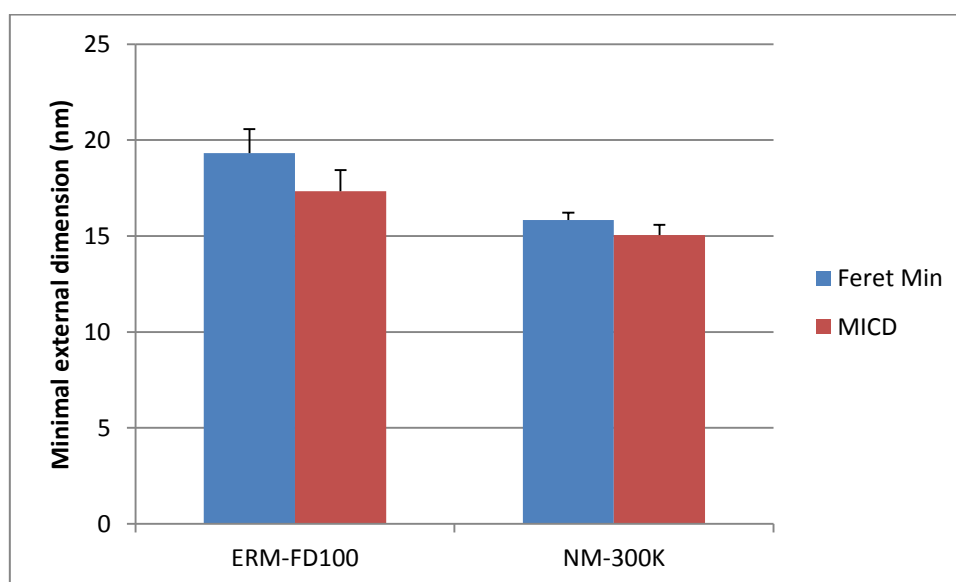


**Figure 13** Minimal external dimension of particles in ERM-FD100 and NM-300K showing the Feret min and MICD measurements together with the intra-laboratory uncertainty (95%).

When the shape of the examined particles is not regular (asymmetric particles), then the Feret min value overestimates the minimal external diameter. In such case, the maximal inscribed circular diameter gives a better estimation. Figure 6 shows that the SOPs allow to precisely measure the Feret min and Maximal inscribed circular diameter for ERM-FD100 and NM-300K. Since the particles of NM-300K are crystalline, they have a smoother surface and therefore, the MICD and Feret min

measurements are closer to each other than for ERM-FD100, an amorphous material where the borders of the particles are more irregular.

#### *4.3.6 Inter-laboratory validation of the SOPs for near-monomodal, near-monodisperse, colloidal MNM with focus on the shape characteristics*

Nanomaterials can be classified based on their shape. The SOPs were evaluated to measure shape characteristics such as the aspect ratio, the circularity, solidity and the roundness of near-monodisperse, near-spherical silver MNM NM-300K and synthetic amorphous silica certified reference material (ERM-FD100).

Table 29 and Figure 15 in annex, show that the SOPs resulted in reproducible measurement of the median aspect ratio since the differences between the laboratories are small, although the AR in ImageJ and in the iTEM software are calculated differently.

For roundness, the SOPs resulted in reproducible results provided that the labs used the same software package. In Table 29, laboratory A reanalyzed the set of images that were originally analyzed in iTEM, in Image J. The latter results was in line with the results of the other laboratories, illustrating the importance of the (calculation defined by the) software. For this reason, the low value for roundness of laboratory F, that also applied the iTEM software, was omitted in the data analysis. These results are visualized in Figure 22.

The SOPs did not result in reproducible results for the circularity measurements where variability between labs was relatively large. Estimation of the circularity depends on a combination of factors including the applied terminology and the calculation method. Even when, supporting on the information in Table 30 in annex, the measurands were renamed and recalculated in an effort to obtain comparable results, large variations in measurement were observed. Circularity is strongly determined by the estimation of the perimeter that depends among others on the calculation method, the pixel size (magnification) and the applied image processing filters. These effects could not be corrected for, supporting on the available data, as summarized in Table 27 and Table 28 in annex,

Although the SOPs were developed to be platform-independent, and although specific guidance and hands-on support were provided, it appeared not easy for the participants of the ILC to select the imaging conditions and the settings and measurands in their software. Continued efforts for standardization are important.

Table 30 illustrates for example the possible influence of the applied software package, For size (ECD, Feret min) and aspect ratio measurements the differences between iTEM and ImageJ were not significant. For Convexity/Solidity measurements the results were biased, although the differences between the software packages were small. For shape factor/circularity and roundness, the differences between the software packages were relatively large.

#### *4.3.7 Inter-laboratory validation of the SOPs for fractal-like, aggregated MNM with focus on the application of the EC definition of MNM*

The Modified “Final protocol for producing suitable manufactured nanomaterial exposure media” [21] (3.1) allowed bringing fractal like nanomaterials in a stable dispersion. The ethanol pre-wetting and BSA treatment were omitted from sample preparation since the examined materials could be prepared in their most dispersed state without BSA and did not have a hydrophobic coating, necessitating ethanol pre-wetting.

The SOP “Preparation of EM-specimens containing a representative sample of the particles in dispersion” (3.2), resulted in an evenly distributions of the material over the EM-grid (Figure 14).

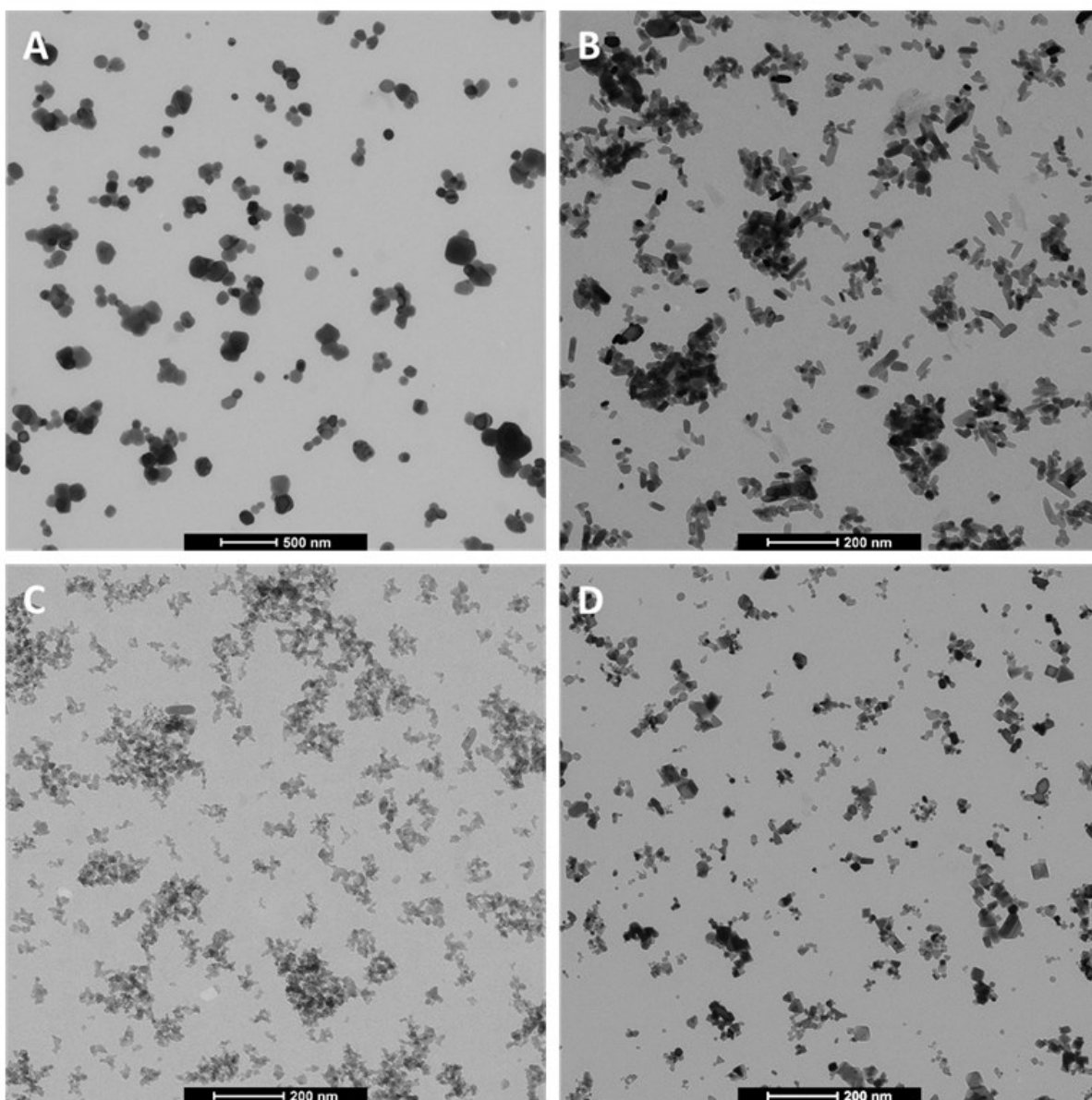
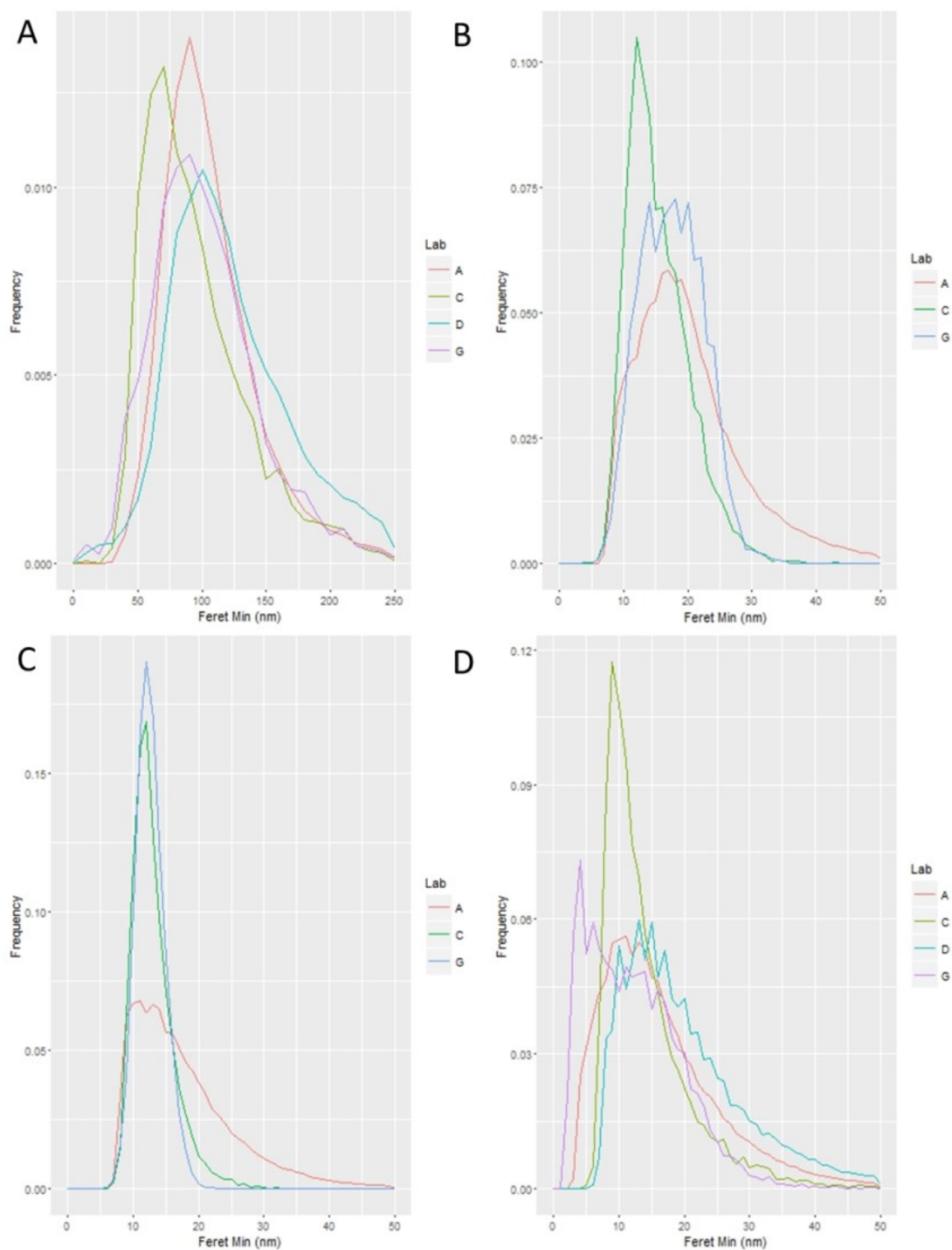


Figure 14 Selected TEM micrographs of the materials tested during the Inter-Laboratory validation of the SOPs for fractal-like, aggregated MNMs JRCNM01000 (A), JRCNM01003 (B), JRCNM02000 (C) and JRC02102 (D). Bar 500 nm (A) and 200 nm (B,C,D).



**Figure 15** Feret min distributions of the primary particles in fractal like aggregated and agglomerated materials JRCNM01000 (A), JRCNM01003 (B), JRCNM02000 (C) and JRCNM02102 (D) for the obtained datasets.

Application of “Transmission electron microscopic imaging of nanomaterials” (3.3), descriptive analysis according to the Guidelines for qualitative characterization of nanomaterials in dispersion in a regulatory framework (3.4), and the “Electron microscopic image analysis of primary particles in aggregated nanomaterials”(3.6) allowed measuring the Feret min, the ECD and the Maximal inscribed



circular diameter of titanium dioxide (JRCNM01000 and JRCNM01003), synthetic amorphous silica (JRCNM02000) and cerium oxide (JRCNM02102) from the cross-cutting suit of materials of NANoREG (Figure 14).

Table 15, Table 16, Table 17 and Table 18 illustrate that the SOPs allow to measure of the minimal external dimension of JRCNM01000, JRCNM01003, JRCNM02000 and JRCNM2102, respectively. Each of the laboratories could estimate its measurement uncertainties. Even though 9 measurands are recoded, the minimal external dimension of the particles is the most appropriate in the framework of the EC definition of the term nanomaterial. Since it can be manually measured and was reported by more laboratories than the MICD, the median Feret min is presented (Figure 15).

The inter-laboratory is calculated as 2 times the standard deviation of the mean median Feret min measurements of the datasets. The intra-laboratory measurement uncertainty of the Feret min measurement is for both examined MNM in the same order as the inter-laboratory measurement uncertainty.

The maximal inscribed circle diameter is proposed as an alternative to the Feret min for materials that deviate from the near-spherical shape. The ECD is proposed as the TEM size measurand that is the best related, in comparison to the MICD and Feret min, to the hydrodynamic diameter measured by PTA and DLS.

When the shape of the examined particles is not regular (asymmetric particles), the Feret min value tends to overestimate the minimal external diameter (Figure 16). In such case, the maximal inscribed circular diameter gives a better estimation.

**Table 15 Overview table of selected TEM minimal size in one dimension (Feret min) of the primary particles showing the median size, repeatability uncertainty, intermediate precision uncertainty and itralab uncertainty for JRCNM01000.**

JRCNM01000	Median $\pm$ U(x)	u(r)	u(ip)	u(lab)
A	101 $\pm$ 10 nm	4.33%	1.31%	4.53%
C	85 $\pm$ 11 nm	5.81%	2.03%	6.15%
D	116 $\pm$ 17 nm	6.83%	2.45%	7.25%
G	98 $\pm$ 8 nm	3.43%	1.75%	3.85%
Mean $\pm$ inter-laboratory uncertainty (95%)	100 $\pm$ 25 nm			

**Table 16 Overview table of selected TEM minimal size in one dimension (Feret min) of the primary particles showing the median size, repeatability uncertainty, intermediate precision uncertainty and itralab uncertainty for JRCNM01003.**

JRCNM01003	Median $\pm$ U(x)	u(r)	u(ip)	u(lab)	Table 17 Overview table of selected TEM minimal size in one dimension (Feret min) of the primary particles showing the median size, repeatability uncertainty, intermediate precision uncertainty and itralab uncertainty for JRCNM02000.
A	18.81 $\pm$ 1.01 nm	1.55%	2.20%	2.70%	
C	14.48 $\pm$ 2.48 nm	6.55%	5.51%	8.56%	
G	17.44 $\pm$ 1.86 nm	4.70%	2.51%	5.32%	
Mean $\pm$ inter-laboratory uncertainty (95%)	16.91 $\pm$ 4.43 nm				

JRCNM02000	Median $\pm$ U(x)	u(r)	u(ip)	u(lab)	Table 18 Overview table of selected TEM minimal size in one dimension (Feret min) of the primary particles showing the median size, repeatability uncertainty, intermediate precision uncertainty and itralab uncertainty for the cerium oxide representative test material JRCNM02012.
A	15.88 $\pm$ 1.30 nm	3.74%	1.66%	4.09%	
C	12.36 $\pm$ 1.33 nm	3.87%	3.73%	5.37%	
G	12.26 $\pm$ 1.74 nm	6.19%	3.48%	7.10%	
Mean $\pm$ inter-laboratory uncertainty (95%)	13.50 $\pm$ 4.12 nm				

JRCNM02012	Median $\pm$ U(x)	u(r)	u(ip)	u(lab)
A	14.44 $\pm$ 1.14 nm	3.90%	0.61%	3.95%
C	12.15 $\pm$ 1.01 nm	3.84%	1.66%	4.18%
D	17.97 $\pm$ 0.43 nm	1.15%	0.35%	1.20%
G	11.26 $\pm$ 3.28 nm	11.12%	9.42%	14.57%
Mean $\pm$ inter-laboratory uncertainty (95%)	13.96 $\pm$ 6.00 nm			



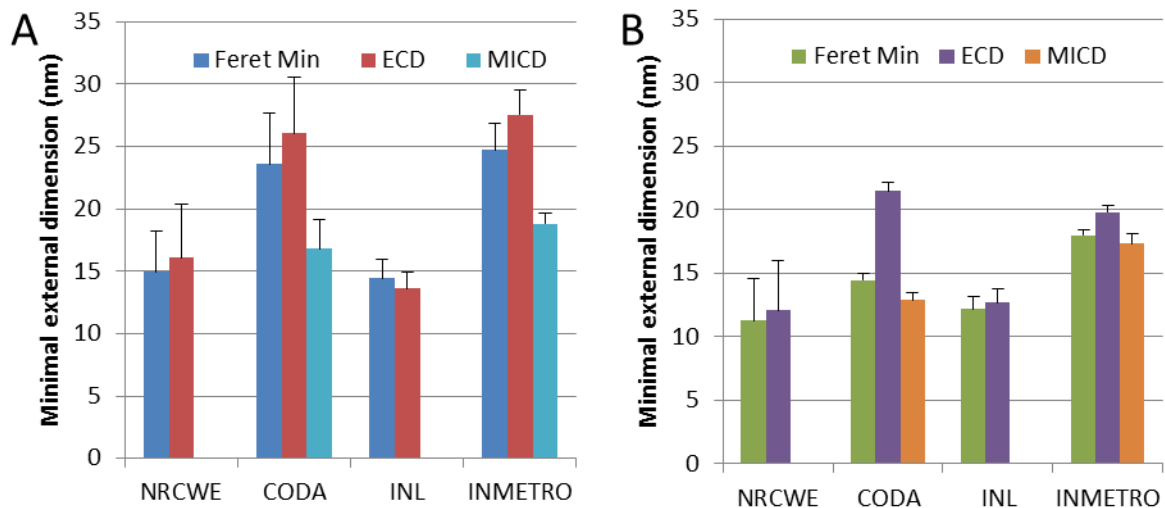


**Figure 16** Minimal external dimension of particles in JRCNM02102 showing the Maximal inscribed circular diameter (MICD), Feret min and ECD measurements of aggregates (A) and primary particles (B) together with the intra-laboratory uncertainty (95%) for JRCNM02102.

Figure 10 illustrates the different possibilities to measure the minimal external dimension of aggregated and agglomerated materials. The Feret min and ECD are close to each other for measurements on the primary particles and aggregates. For NRCWE the uncertainties of size measurements on aggregates are as large as the uncertainties on the size measurements on the primary particles.

In the above-described experiments, the size and shape characteristics of the aggregates were measured as described in Cross reference intra-lab by the ILC partners on the same images. These will be compared with the results of the complementary methods and reported in a peer-reviewed publication (in preparation).

## 5 Size characterisation with on-line technique of spherical or near-spherical airborne nanoparticles generated from colloidal suspension

### 5.1 Comparison of different on-line aerosol instrument for airborne nano particles. (from Levin et al [26])

Three different types of nanoparticle sizing instruments (Fast Mobility Particle Sizer (FMPS), Electrical Low Pressure Impactor (ELPI) and Scanning Mobility Particle Sizer (SMPS)) and one only measuring number concentration Condensation Particle Counter (CPC) was compared in terms of size distributions and number concentration. The particle size range studied was 50 to 800 nm. The comparison was done using spherical oil droplets for 39 different sizes, with geometric mean diameter (GMD) ranging from 50 to 820 nm.

The results show that all three sizing-instruments agree well for particles sizes below 200nm, both in terms of determination of particle size and number concentration. Regarding particle sizing, the regression coefficient of SMPS versus ELPI was close to one ( $R^2=0.98$ ) and no size-dependent shift in the comparison could be observed. The FMPS versus SMPS or ELPI the data correlates well ( $R^2=0.94$ ) when particles sizes is below 200 nm, but for larger particle sizes it is clear that both FMPSs underestimate the particle sizes as compared to both SMPS and ELPI.

Comparison of measuring number concentration showed that there is a good correlation between SMPS and CPC (Ratio= $1.03\pm0.04$ ) and SMPS-ELPI (Ratio= $0.98\pm0.14$ ) in the whole particle size range studied. For the SMPS-FMPS number concentration comparison there is a similar scenario to that of particle size comparison. There is a good correlation up until 200nm (Ratio= $0.99\pm0.12$ ), but for larger particle sizes the FMPS number concentration starts to exceed the other instruments (SMPS and ELPI). The study concludes that particle distributions with a GMD above 200 nm cannot be measured reliably with the FMPS.

### 5.2 Determination of the primary particle size and surface area for airborne aggregates using on-line aerosol measurement technique. (from Svensson et al [27])

Aggregates, clusters of primary particles, is a common particle type in the air. Data regarding their size dependent and morphological properties are important for both health related research and innovation.

The overall aim of this work was to determine the primary particle size/distribution of airborne aggregates using on-line aerosol measurement techniques. The approach used a combination of a differential mobility analyzer (DMA), an aerosol particle mass analyzer (APM) and diffusion limited cluster aggregation theory (later called DMA-APM-DLCA). For comparison, a TEM based primary particle analysis was also performed.

Experiments were performed and for generation of the gold aggregates two spark discharge generators were used – a commercially available (SDG<sub>P</sub>) and a custom built (SDG<sub>C</sub>) – as well as a high temperature-condensation furnace (HT). The generated particles were log-normal distributed in the size range 5 to 300 nm and the bridges between the primaries were 60-70% of the diameter of the primary particles. Downstream the generators a DMA was used to select monodisperse particles. Five aerosols of gold-aggregates with CMD in the range of 28 to 78 nm were with regards to primary particle size and specific surface area (SSA), Table 19.

**Table 19 Characteristics of generated gold aggregates. SDG = spark charge generator, HT = heat temperature furnace. (CMD =count median diameter, GSTD = geometric standard deviation)**

	CMD (nm)	GSTD
SDG-1	28.1	1.64
SDG-2	28.3	1.65
SDG-3	78.4	1.92

HT-1	53.9	1.79
HT-2	74.8	1.80

For determination of the aggregate mass, a DMA was coupled in series with an APM. From the measurements different properties could be estimated as mass-mobility coefficient, effective density and shape factor. For TEM-analysis the particles were collected on grids for pre-sequent analysis of primary particle. Using DMA-APM-measurement, TEM-analysis and DCLA-theory five different methods were used to calculate the specific surface area. A gold density of  $19.6 \text{ g/cm}^3$  was used.

## Results

Figure 17 shows a comparison of the primary particle diameter (calculated as Sauters diameter) for the TEM-analysis versus on-line particle measurement method using the DMA-APM-DLCA method based on Eggesdorfer et al (2012) [127, 128] (later used in approach I for determination of total surface area). Using a linear model, the slope (regression coefficient) is 0.33 between the determined primary particle size using TEM-analysis versus using DMA-APM-DLCA-theory ( $R^2=0.75$ ). Regression of the calculated specific surface area is for the slope 0.29 ( $R^2=0.61$ ), see Figure 18.

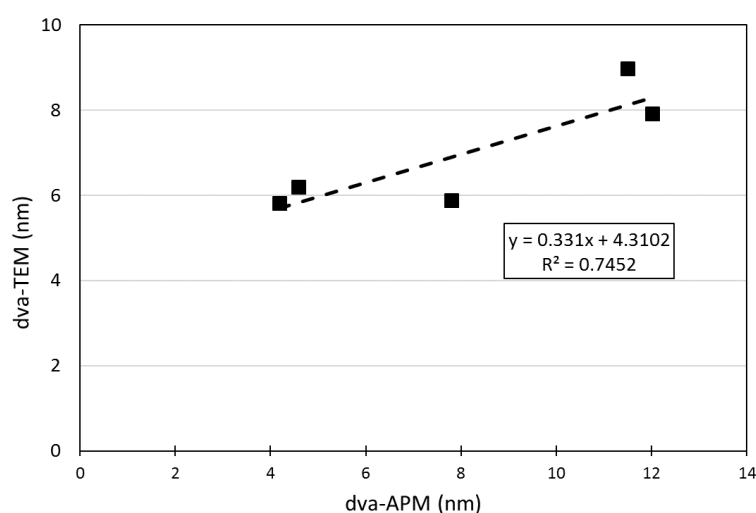


**Figure 17 Comparison of the primary particle diameter (calculated as Sauters diameter) for the TEM-analysis versus on-line particle measurement method using the DMA-APM-DLCA method.**

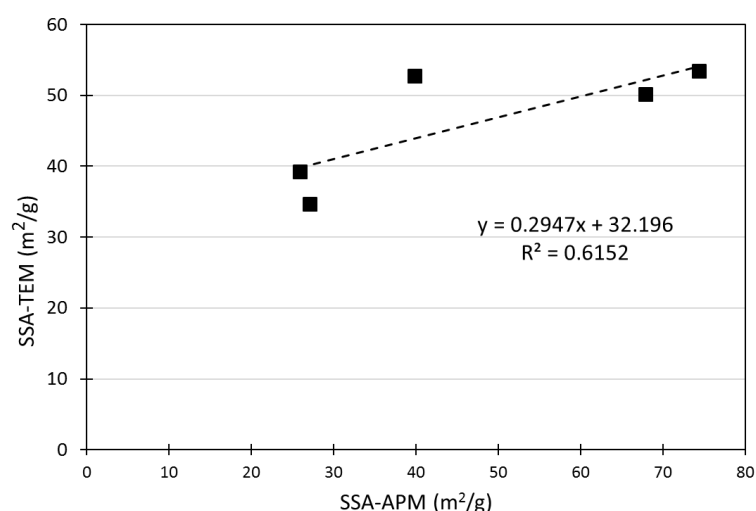


**Figure 18 Comparison of the specific area using TEM-analysis versus on-line particle measurement method using the DMA-APM-DLCA method.**

Table 20 show how the different methods have been combined to estimate the total surface area. The different approaches used different approximations and theories. Approach I is the on-line measurement using DMA-APM, approach V is also on-line measurement, but cannot be used to estimate the primary particle size. All the other approaches require TEM-analysis. Shown in Figure 19 is the result of using different approaches to estimate the total surface area for the five different types of gold-aggregates. Figure 20 shows how the on-line method approach I is related to the other TEM-analysis methods. As seen in the Figure 20, the only approach that fully deviate from the others is approach IV. The other TEM-analysis based methods give a scattered result within  $\pm 30\%$  and the on-line method gives no better or worse result.

**Table 20 Overview of the input needed, empirical (DMA-APM, TEM, SMPS) and theoretical (DLCA), for total surface area estimation using the five different approaches for calculation of aerosol surface area content.**

Approach	I	II	III	IV	V
DMA-APM	X	X			
TEM		X	X	X	
DLCA-theory	X		X	X	
SMPS					X

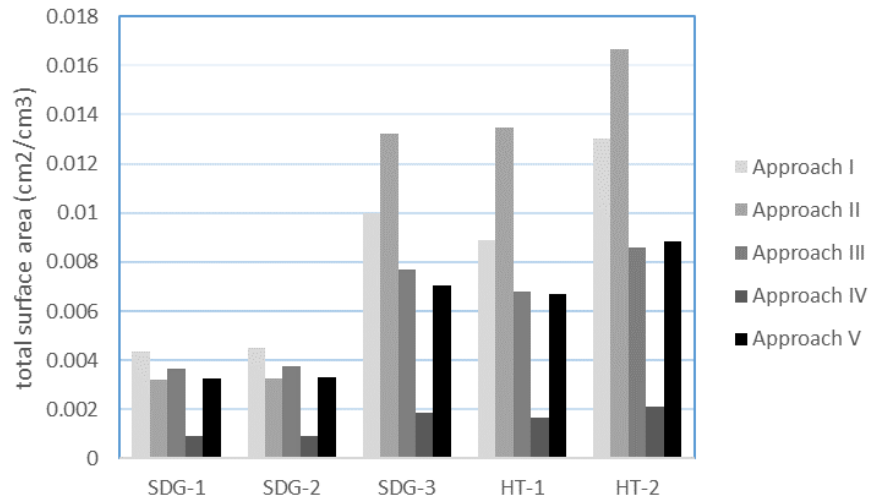


Figure 19 The total surface area estimated using different calculating and approaches used for five aerosols of gold aggregates, generated by SDG or HT.

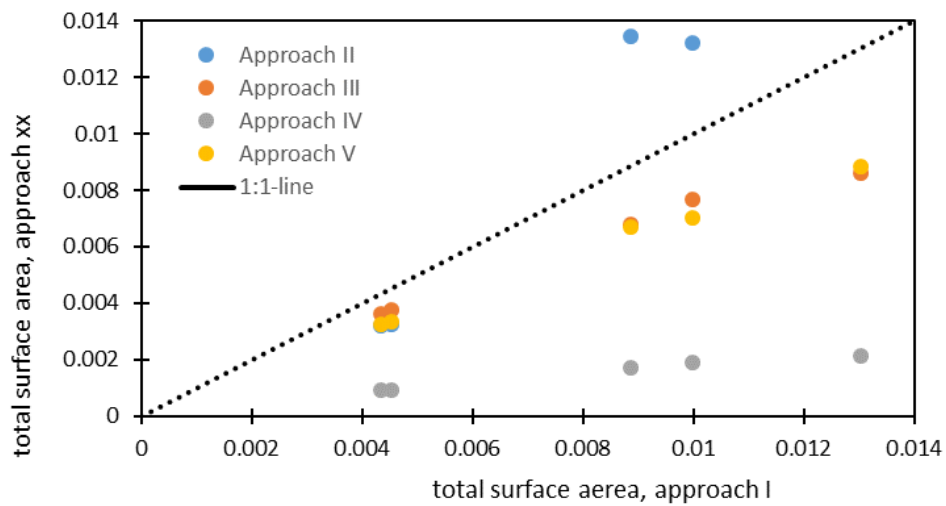


Figure 20 Comparison of estimated total surface: on-line measurement using the DMA-DMA-DCLA-theory (approach I) versus approaches including TEM-analysis, approach II to V.

## 6 Evaluation and conclusions

The objectives presented in the deliverable description aiming to develop and validate SOPs for quantitative TEM analysis of MNM were reached.

SOPs for quantitative TEM analysis of MNM were developed. These SOPs were validated by application on a series of nanomaterials of various types and sizes, by intra-laboratory and inter-laboratory validation based on the estimation of the measurement uncertainties.

These SOPs allow to estimate the minimal external dimension of NM such that the EC definition for NM can be implemented for a wide selection of colloidal and aggregated fractal-like nanomaterials with known measurement uncertainties. Further a large panel of size and shape measurands with measurement uncertainties were determined for these materials, resulting in a detailed characterization required for e.g. risk analyses.

**Figure 21** gives a schematic overview of the steps included in the developed, complete TEM analysis to measure the size and shape of the particles of a MNM in the framework of implementation of the nanomaterial definition and characterisation, for risk analysis.

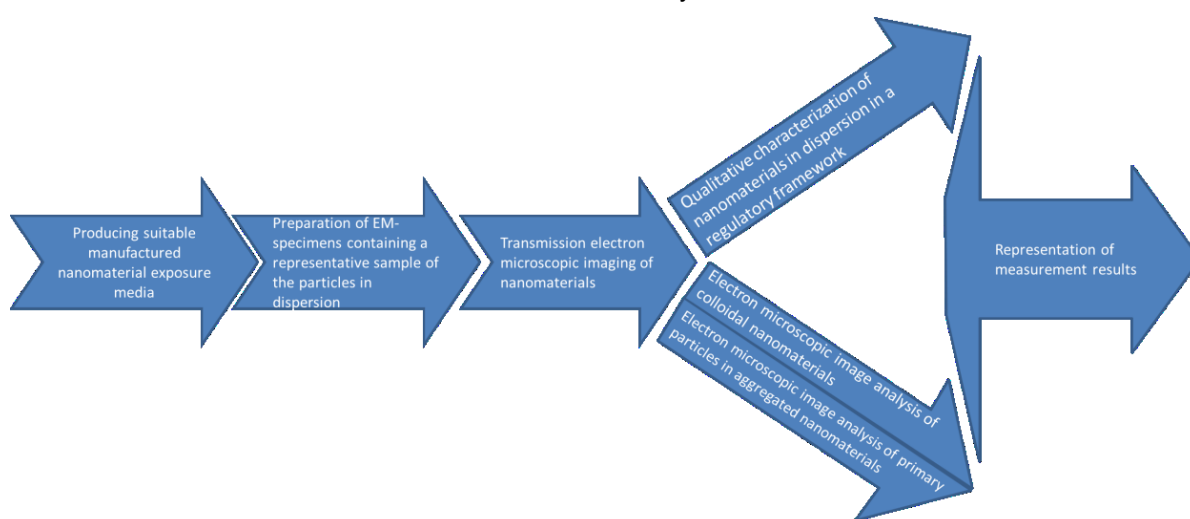


**Figure 21 Schematic overview of the steps included in a complete TEM analysis to measure the size and shape of the particles of a MNM.**

- The SOP to prepare a TEM specimen suitable for qualitative and quantitative analysis from a dispersed NM ensures that the NM samples are suitable for TEM imaging and analysis. The examined materials were evenly distributed over the grids and the fraction of the attached NM represents the dispersed NM optimally.
- The SOP to record a set of calibrated transmission electron micrographs showing NM that are representative for the NM on the EM grid ensures that the number of particles and the magnification of the micrographs are suitable for subsequent descriptive and quantitative image analyses.
- The method for characterizing the primary particles and aggregates of a NM by describing their physical properties based on TEM micrographs provides a step-by-step guide for the descriptive characterization of nanomaterials.
- The SOPs to analyze the 2D properties of the primary and aggregated/agglomerated particles on EM micrographs ensure that the primary particles are detected and that size and shape measurands are determined quantitatively. A modified version allows to measure the size and shape properties of the aggregates/agglomerates.
- Data were analyzed and represented according to relevant ISO-norms.

The EM-based results were related to the results obtained with alternative methods. These include ensemble techniques based on light scattering, such as dynamic light scattering (DLS) and particle

tracking analysis (PTA), and single particle inductively coupled plasma-mass spectrometry (SP-ICP-MS) [1].

Our work illustrates that the size measurands measured with the different techniques are method-defined and cannot be directly compared without prior knowledge. The hydrodynamic radius of near-spherical colloidal NM assessed by DLS and PTA is for example only comparable with the ECD value obtained by TEM when the colloidal suspension is perfectly stable and no aggregation occurs.

The performance of the methods and concepts established in this work was shown in intra- and inter-laboratory validation studies, such that they are ready to be considered for adoption into guidance documents for physico-chemical characterization of nanomaterials applied in various fields.

## 7 Data management

A template for reporting the size distributions of the examined MNM using TEM has been produced. Partners will report their results individually.

## 8 Deviations from the work plan

It is clear that the date of final submission of D2.10 is considerably later than anticipated by the project team.

Reasons for this delay include breakdown and unavailability of equipment, samples arrived late and were not available anymore, alternative test samples had to be fractionated and distributed.

The number of vials of the remaining NANoREG representative test materials (NM-100, NM-103, NM-200 and NM-212) was insufficient to start the 3rd phase of the ILC. To solve this problem, the ILC participants were asked to send their remaining stocks of titanium dioxide (NM-100, NM-103), synthetic amorphous silica (NM-200) and cerium oxide (NM-212) to CODA-CERVA. These materials were fractionated by JRC-Ispra with the following requirements. This resulted in a serious delay regarding the work planned in the D2.10 description.



## 9 References / Selected sources of information (optional)

1. Leshner EK, Poda AR, Bednar AJ, Ranville JF: **Field-Flow Fractionation Coupled to Inductively Coupled Plasma-Mass Spectrometry (FFF-ICP-MS): Methodology and Application to Environmental Nanoparticle Research**: Springer; 2012.
2. SCENIHR: **Opinion on the scientific aspects of the existing and proposed definitions relating to products of nanoscience and nanotechnologies** In: *scenih\_r\_o\_012*. Brussels: Scientific committee on emerging and newly identified health risks; 2007.
3. SCENIHR: **Scientific basis for the definition of the term "Nanomaterial"**. In: *scenih\_r\_o\_030*. Brussels: Scientific Committee on Emerging and Newly Identified Health Risks; 2010.
4. EC: **Commission recommendation of 18 October 2011 on the definition of nanomaterial**. 2011/696/EU. *Off J Eur Union* 2011, **L275**:30-40.
5. EC: **Regulation (EC) No 1223/2009 of the European Parliament and of the Council of 30 November 2009 on cosmetic products**. *Official Journal of the European Union* 2009, **L342**:59-209.
6. EC-1333/2008: **Regulation (EC) No 1333/2008 of the European parliament and of the council of 16 December 2008 on food additives**. *Off J Eur Union* 2008, **L354**:16 - 33.
7. EC-258/97: **Regulation (EC) No 258/97 of the European Parliament and of the Council of 27 January 1997 concerning novel foods and novel food ingredients**. *Off J Eur Communities* 1997.
8. Bleeker EA, de Jong WH, Geertsma RE, Groenewold M, Heugens EH, Koers-Jacquemijns M, van de Meent D, Popma JR, Rietveld AG, Wijnhoven SW: **Considerations on the EU definition of a nanomaterial: science to support policy making**. *Regul Toxicol Pharmacol* 2013, **65**(1):119-125.
9. De Temmerman P-J, Verleysen E, Lammertyn J, Mast J: **Semi-automatic size measurements of primary particles in aggregated nanomaterials by transmission electron microscopy**. *Powder Technol* 2014, **261**(July):191-200.
10. Verleysen E, De Temmerman P-J, Van Doren E, Abi Daoud Francisco M, Mast J: **Quantitative characterization of aggregated and agglomerated titanium oxide nanomaterials by transmission electron microscopy**. *Powder Technol* 2014, **258**:180-188.
11. De Temmerman P-J, Van Doren E, Verleysen E, Van der Stede Y, Francisco M, Mast J: **Quantitative characterization of agglomerates and aggregates of pyrogenic and precipitated amorphous silica nanomaterials by transmission electron microscopy**. *J Nanobiotechnology* 2012, **10**(24).
12. Rauscher H, Roebben G, Amenta V, Boix Sanfeliu A, Calzolari L, Emons H, Gaillard C, Gibson P, Linsinger T, Mech A et al: **Towards a review of the EC Recommendation for a definition of the term "nanomaterial"; Part 1: Compilation of information concerning the experience with the definition**. In: *EUR 26567 EN - 2014*. Luxembourg: Publications Office of the European Union; 2014.
13. Midgley PA, Weyland M: **3D electron microscopy in the physical sciences: the development of Z-contrast and EFTEM tomography**. *Ultramicroscopy* 2003, **96**(3-4):413-431.
14. Van Aert S, Batenburg KJ, Rossell MD, Erni R, Van Tendeloo G: **Three-dimensional atomic imaging of crystalline nanoparticles**. *Nature* 2011, **470**(7334):374-377.
15. Sueda S, Yoshida K, Tanaka N: **Quantification of metallic nanoparticle morphology on TiO<sub>2</sub> using HAADF-STEM tomography**. *Ultramicroscopy* 2010, **110**(9):1120-1127.
16. Pouget EM, Bomans PH, Goos JA, Frederik PM, Sommerdijk NA: **The initial stages of template-controlled CaCO<sub>3</sub> formation revealed by cryo-TEM**. *Science* 2009, **323**(5920):1455-1458.
17. Van Doren E, De Temmerman P-J, Francisco M, Mast J: **Determination of the volume-specific surface area by using transmission electron tomography for characterization and definition of nanomaterials**. *J Nanobiotechnology* 2011, **9**(1):17.
18. Mast J, Verleysen E, De Temmerman P-J: **Physical characterization of nanomaterials in dispersion by transmission electron microscopy in a regulatory framework**. In: *Electron*

- Microscopy of Materials*. Edited by Francis LD, Mayoral A, Arenal R. Cham, Switzerland: Springer International Publishing AG; 2014.
19. Stamm H, Gibson N, Anklam E: **Detection of nanomaterials in food and consumer products: bridging the gap from legislation to enforcement**. *Food Addit Contam Part A-Chem* 2012, **29**(8):1175-1182.
  20. Linsinger TPJ, Roebben G, Gilliland D, Calzolari L, Rossi F, Gibson N, Klein C: **Requirements on measurements for the implementation of the European Commission definition of the term 'nanomaterial'**. In: *EUR 25404 EN*. Luxembourg: Publications Office of the European Union; 2012.
  21. Jensen K, Kembouche Y, Christiansen E, Jacobsen N, Wallin H: **The generic NANOGENOTOX dispersion protocol**. In: *Standard Operation Procedures (SOP) and background documentation: Final Protocol for producing suitable manufactured nanomaterial exposure media* Edited by Jensen K, Thieret N; 2011.
  22. EC: **Commission recommendation of 18 October 2011 on the definition of nanomaterial**. *Official Journal of the European Union* 2011(275):38-40.
  23. De Temmerman P-J, Lammertyn J, Ketelaere B, Kestens V, Roebben G, Verleysen E, Mast J: **Measurement uncertainties of size, shape, and surface measurements using transmission electron microscopy of near-monodisperse, near-spherical nanoparticles**. *Journal of Nanoparticle Research* 2013, **16**(1):1-22.
  24. De Temmerman P-J, Verleysen E, Lammertyn J, Mast J: **Semi-automatic size measurement of primary particles in aggregated nanomaterials by transmission electron microscopy**. *Powder Technology* 2014, **206**:191-200.
  25. De Temmerman P-J, Verleysen E, Lammertyn J, Mast J: **Size measurement uncertainties of near-monodisperse, near-spherical nanoparticles using transmission electron microscopy and particle-tracking analysis**. *Journal of Nanoparticle Research* 2014, **16**(10):1-17.
  26. Levin M, Gudmundsson A, Pagels JH, Fierz M, Mølhave K, Löndahl J, Jensen KA, Koponen IK: **Limitations in the Use of Unipolar Charging for Electrical Mobility Sizing Instruments: A Study of the Fast Mobility Particle Sizer**. *Aerosol Science and Technology* 2015, **49**(8):556-565.
  27. Svensson CR, Ludvigsson L, Meuller BO, Eggersdorfer ML, Deppert K, Bohgard M, Pagels JH, Messing ME, Rissler J: **Characteristics of airborne gold aggregates generated by spark discharge and high temperature evaporation furnace: Mass-mobility relationship and surface area**. *Journal of Aerosol Science* 2015, **87**:38-52.
  28. EFSA: **Scientific Opinion: Guidance on the risk assessment of the application of nanoscience and nanotechnologies in the food and feed chain**. *EFSA Journal* 2011, **9**(5):2140.
  29. OECD: **Guidance on Sample Preparation and Dosimetry for the Safety Testing of Manufactured Nanomaterials**. In: *ENV/JM/MONO(2012)40*. Paris: Organisation for economic co-operation and development; 2012.
  30. **The final NANOGENOTOX publishable report**  
[\[http://www.nanogenotox.eu/files/PDF/nanogenotox\\_web.pdf\]](http://www.nanogenotox.eu/files/PDF/nanogenotox_web.pdf)
  31. Mysels KJ: **Textbook errors: II. Brownian motion and the stability of colloids**. *J Chem Educ* 1955, **32**(6):319.
  32. Kaiser DL, Watters RL: **Reference Material 8011: Gold Nanoparticles, Nominal 10 nm Diameter**. In: *Report of Investigation*. Gaithersburg, MD: National Institute of Standards & Technology; 2007.
  33. Kaiser DL, Watters RL: **Reference Material 8012: Gold Nanoparticles, Nominal 30 nm Diameter**. In: *Report of Investigation*. Gaithersburg, MD: National Institute of Standards & Technology; 2007.
  34. Kaiser DL, Watters RL: **Reference Material 8013: Gold Nanoparticles, Nominal 60 nm Diameter**. In: *Report of Investigation*. Gaithersburg, MD: National Institute of Standards & Technology; 2007.
  35. IRMM: **Certificate of analysis ERM®-FD100**. Institute for Reference Materials and Measurements. In. Geel; 2011.
  36. IRMM: **Certificate of analysis ERM®-FD304**. Institute for Reference Materials and Measurements. In. Geel; 2012.

37. **3000 Series Nanosphere™ Size Standards**  
[<http://www.thermoscientific.com/en/product/3000-series-nanosphere-size-standards.html>]
38. Guiot C, Spalla O: **Stabilization of TiO<sub>2</sub> Nanoparticles in Complex Medium through a pH Adjustment Protocol**. *Environ Sci Technol* 2013, **47**(2):1057-1064.
39. Bihari P, Vippola M, Schultes S, Praetner M, Khandoga A, Reichel C, Coester C, Tuomi T, Rehberg M, Krombach F: **Optimized dispersion of nanoparticles for biological in vitro and in vivo studies**. *Part Fibre Toxicol* 2008, **5**(1):14.
40. Jensen K, Kembouche Y, Christiansen E, Jacobsen N, Wallin H, Guiot C, Spalla O, Witschger O: **The generic NANOGENOTOX dispersion protocol**. In: *Standard Operation Procedures (SOP) and background documentation: Final Protocol for producing suitable manufactured nanomaterial exposure media* Edited by Jensen K, Thieret N; 2011.
41. PROSPECT: **Protocol for Nanoparticle Dispersion**; 2010.
42. Taurozzi JS, Hackley VA: **Preparation of Nanoparticle Dispersions from Powdered Material Using Ultrasonic Disruption**. *National Institute of Standards and Technology* 2012, **NIST SP 1200-2**:15.
43. Taurozzi JS, Hackley VA, Weisner MR: **Preparation of Nanoscale TiO<sub>2</sub> Dispersions in an Environmental Matrix for Eco-Toxicological Assessment** *National Institute of Standards and Technology* 2012, **NIST SP 1200-5**:12.
44. **Surfactant Stabilized Gold Nanoparticles**  
[<http://www.cytodiagnostics.com/store/pc/Surfactant-Stabilized-Gold-Nanoparticles-c141.htm>]
45. Lienemann C-P, Heissenberger A, Leppard GG, Perret D: **Optimal preparation of water samples for examination of colloidal material by transmission electron microscopy**. *Aquat Microb Ecol* 1998, **14**:205-213.
46. Stirling J, Curry A, Eyden B: **Diagnostic Electron Microscopy: A Practical Guide to Tissue Preparation and Interpretation**: John Wiley & Sons; 2012.
47. **Smart Grids: Functionalized grids for advanced imaging**  
[[http://www.dunesciences.com/files/SMARTGrids\\_Brochure.pdf](http://www.dunesciences.com/files/SMARTGrids_Brochure.pdf)]
48. **Powder TEM Sample preparation for Powder sample**  
[<http://mcc.lsu.edu/TEM%20sample%20preparation.html>]
49. De Graef M: **Introduction to conventional transmission electron microscopy**: Cambridge University Press; 2003.
50. Williams D, Carter C: **Transmission Electron Microscopy, vol. II**. ISBN: 0-306-45324-X 1996.
51. De Temmerman P-J, Lammertyn J, De Ketelaere B, Kestens V, Roebben G, Verleysen E, Mast J: **Measurement uncertainties of size, shape, and surface measurements using transmission electron microscopy of near-monodisperse, near-spherical nanoparticles**. *J Nanopart Res* 2013, **16**(1):1-22.
52. Masuda H, Gotoh K: **Study on the sample size required for the estimation of mean particle diameter**. *Adv Powder Technol* 1999, **10**(2):159-173.
53. Merkus HG: **Particle size measurements: fundamentals, practice, quality**. Pijnacker: Springer; 2009.
54. ISO 13322-1: **Particle size analysis - Image analysis methods**. In: *Part 1: Static image analysis methods*. Geneva: International Organization for Standardization; 2014.
55. **iTEM is the image analysis platform for transmission-electron microscopy**.  
[[http://www.soft-imaging.net/en/eu/eng/2343\\_5832.htm](http://www.soft-imaging.net/en/eu/eng/2343_5832.htm)]
56. Visilog: **Visilog is the reference environment for creating image processing applications**. Accessed 2014.
57. **OMERO is client-server software for visualization, management and analysis of biological microscope images**. [<http://www.openmicroscopy.org/site>]
58. Fiji: **Fiji is an image processing package based on ImageJ**. Accessed 2014.
59. ImageJ: **Image Processing and Analysis in Java**. Accessed 2014.
60. Carlson C, Hussain S, Schrand A, K. Braydich-Stolle L, Hess K, Jones R, Schlager J: **Unique cellular interaction of silver nanoparticles: size-dependent generation of reactive oxygen species**. *J Phys Chem B* 2008, **112**(43):13608-13619.
61. Choi JE, Kim S, Ahn JH, Youn P, Kang JS, Park K, Yi J, Ryu D-Y: **Induction of oxidative stress and apoptosis by silver nanoparticles in the liver of adult zebrafish**. *Aquat Toxicol* 2010, **100**(2):151-159.

62. Park E-J, Yi J, Kim Y, Choi K, Park K: **Silver nanoparticles induce cytotoxicity by a Trojan-horse type mechanism**. *Toxicol In Vitro* 2010, **24**(3):872-878.
63. OECD: **"The Price of Prejudice: Labour Market Discrimination on the Grounds of Gender and Ethnicity. Technical Annex"**. *Organisation for Economic Co-operation and Development* 2008.
64. SCENIHR: **Risk Assessment of Products of Nanotechnologies**. *Scientific Committee on Emerging and Newly Identified Health Risks* 2009.
65. Pan Y, Neuss S, Leifert A, Fischler M, Wen F, Simon U, Schmid G, Brandau W, Jahnchen-Dechent W: **Size-Dependent Cytotoxicity of Gold Nanoparticles**. *Small* 2007, **3**(11):1941-1949.
66. Goodman CM, McCusker CD, Yilmaz T, Rotello VM: **Toxicity of gold nanoparticles functionalized with cationic and anionic side chains**. *Bioconjugate Chem* 2004, **15**(4):897-900.
67. Chithrani BD, Ghazani AA, Chan WC: **Determining the size and shape dependence of gold nanoparticle uptake into mammalian cells**. *Nano Lett* 2006, **6**(4):662-668.
68. Walkey CD, Olsen JB, Guo H, Emili A, Chan WC: **Nanoparticle size and surface chemistry determine serum protein adsorption and macrophage uptake**. *J Am Chem Soc* 2012, **134**(4):2139-2147.
69. Suresh AK, Pelletier DA, Wang W, Morrell-Falvey JL, Gu B, Doktycz MJ: **Cytotoxicity induced by engineered silver nanocrystallites is dependent on surface coatings and cell types**. *Langmuir* 2012, **28**(5):2727-2735.
70. ISO 9276-6: **Representation of results of particle size analysis Part 6: Descriptive and quantitative representation of particle shape and morphology**. Geneva: International Organization for Standardization; 2008.
71. Roduner E: **Size matters: why nanomaterials are different**. *Chem Soc Rev* 2006, **35**(7):583-592.
72. Nichols G, Byard S, Bloxham MJ, Botterill J, Dawson NJ, Dennis A, Diart V, North NC, Sherwood JD: **A review of the terms agglomerate and aggregate with a recommendation for nomenclature used in powder and particle characterization**. *J Pharm Sci* 2002, **91**(10):2103-2109.
73. Brittain HG: **Representations of particle shape, size, and distribution**. *Pharm Technol* 2001.
74. USP: **Optical Microscopy, General Test 776, USP 24**. In: *The United States Pharmacopeial Convention, : 2000; Rockville,MD; 2000: 1965-1967*.
75. ASTM: **F1877-05 Standard Practice for Characterization of Particles**. 2010.
76. NIST: **Glossary of Morphology Terms**. Gaithersburg, USA: Center for analytical chemistry, National Institute of Standards and Technology; 2005.
77. Barrett PJ: **The shape of rock particles, a critical review**. *Sedimentology* 1980, **27**(3):291-303.
78. Krumbein WC, Sloss LL: **Stratigraphy and Sedimentation**. San Francisco; 1963.
79. ISO/TS 27687: **Nanotechnologies -Terminology and definitions for nano-objects - Nanoparticle, nanofibre and nanoplate**. Geneva: International Organization for Standardization; 2008.
80. NIST 960-1: **Particle Size Characterization**. In.; 2001.
81. SCENIHR: **Scientific Committee on Emerging and Newly Identified Health Risks**. 2009.
82. Barlow S, Chesson A, Collins JD, Flynn A, Hardy A, Jany K-D, Knaap A, Kuiper H, Larsen JC, Le Neindre P *et al*: **Scientific Opinion of the Scientific Committee: The Potential Risks Arising from Nanoscience and Nanotechnologies on Food and Feed Safety, Question No EFSA-Q-2007-124a**. *The EFSA Journal* 2009, **958**:1-39.
83. Lopez-de-Uralde J, Ruiz I, Santos I, Zubillaga A, Bringas PG, Okariz A, Guraya T: **Automatic morphological categorisation of carbon black nano-aggregates**. In: *Proceedings of the 21st international conference on Database and expert systems applications: Part II*. Bilbao, Spain: Springer-Verlag; 2010: 185-193.
84. Rasmussen K, Mech A, De Temmerman P-J, Mast J, Jensen KA, Levin M, Nielsen SH, Koponen I, Clausen P, Birkedal R *et al*: **Synthetic Amorphous Silicon Dioxide (SAS; NM-200, NM-201, NM-202, NM-203 and NM-204) Characterization, Stability and Homogeneity**. In: *EUR 26046*. Luxembourg: Publications Office of the European Union; 2013.

85. De Temmerman P-J, Van Doren E, Francisco M, Mast J: **Quantitative analysis of the physical characteristics of manufactured silica NP used in food by advanced transmission electron microscopy**. In: *International Symposium on nanotechnology in the food chain (Poster)*. Brussels, Belgium; 2010.
86. Singh C, Friedrichs S, Levin M, Birkedal R, Jensen KA, Pojana G, Wohlleben W, Schulte S, Wiench K, Turney T *et al*: **NM-Series of Representative Manufactured Nanomaterials: Zinc Oxide NM-110, NM-111, NM-112, NM-113 Characterisation and Test Item Preparation**. In: *EUR 25066 EN - 2011*. Luxembourg: Luxembourg; 2011.
87. Verleysen E, De Temmerman P-J, Van Doren E, Abi Daoud Francisco M, Mast J: **Quantitative characterization of aggregated and agglomerated titanium oxide nanomaterials by transmission electron microscopy**. *Powder Technol* 2014, **258**:180-188.
88. De Temmerman P-J, Verleysen E, Lammertyn J, Mast J: **Semi-automatic size measurements of primary particles in aggregated nanomaterials by transmission electron microscopy**. *Powder Technol* 2014, **261**(July):191-200.
89. Klein C, Comero S, Stahlmecke B, Romazanov J, Kuhlbusch T, Van Doren E, De Temmerman P-J, Mast J, Wick P, Krug H *et al*: **NM-Series of Representative Manufactured Nanomaterials: NM-300 Silver Characterisation, Stability, Homogeneity**. In: *EUR 24693 EN - 2011*. Luxembourg: Publications Office of the European Union; 2011.
90. Verleysen E, Van Doren E, Waegeneers N, De Temmerman PJ, Abi Daoud Francisco M, Mast J: **TEM and SP-ICP-MS analysis of the release of silver nanoparticles from decoration of pastry**. *J Agric Food Chem* 2015, **63**(13):3570-3578.
91. **Tools for document assembly and document automation in MS Word!** [<http://www.theformtool.com/>]
92. ISO 9276-2: **Representation of results of particle size analysis**. In: *Part 2: Calculation of average particle sizes/diameters and moments from particle size distributions*. Geneva: International Organization for Standardization; 2001.
93. ISO 9276-1: **Representation of results of particle size analysis**. In: *Part 1: Graphical representation*. Geneva: International Organization for Standardization; 1998.
94. Franks K, Braun A, Charoud-Got J, Couteau O, Kestens V, Lamberty A, Linsinger TPJ, Roebben G: **Certified Reference Material ERM®-FD304: Certification of the Equivalent Spherical Diameters of Silica Nanoparticles in Aqueous Solution**. Luxembourg: European Union; 2012.
95. Braun A, Franks K, Kestens V, Roebben G, Lamberty A, Linsinger TPJ: **Certified Reference Material ERM®- FD100: Certification of Equivalent Spherical Diameters of Silica Nanoparticles in Water**. Luxembourg: European Union; 2011.
96. Rasmussen K, Mast J, De Temmerman P-J, Verleysen E, Waegeneers N, Van Steen F, Pizzolon JC, De Temmerman L, Van Doren E, Jensen K *et al*: **Titanium Dioxide, NM-100, NM-101, NM-102, NM-103, NM-104, NM-105: Characterisation and Physico-Chemical Properties** *Publ Office Eur Union* 2014:210.
97. Leong FW, Brady M, McGee JOD: **Correction of uneven illumination (vignetting) in digital microscopy images**. *J Clin Pathol* 2003, **56**(8):619-621.
98. Chen T, Yin W, Zhou XS, Comaniciu D, Huang TS: **Illumination normalization for face recognition and uneven background correction using total variation based image models**. In: *Computer Vision and Pattern Recognition, 2005 CVPR 2005 IEEE Computer Society Conference on: 2005*: IEEE; 2005: 532-539.
99. **Olympus Stream** [<http://www.olympus-ims.com/en/microscope/stream/>]
100. Grishin I, Thomson K, Migliorini F, Sloan JJ: **Application of the Hough transform for the automatic determination of soot aggregate morphology**. *Appl Opt* 2012, **51**(5):610-620.
101. Zhao J, Brubaker MA, Rubinstein JL: **TMaCS: A hybrid template matching and classification system for partially-automated particle selection**. *J Struct Biol* 2013, **181**(3):234-242.
102. OECD: **Guidance manual for the testing of manufactured nanomaterials: OECD sponsorship programme: first revision** In: *ENV/JM/MONO(2009)20/REV*. Paris: Organisation for economic co-operation and development 2010.
103. EFSA: **Scientific Opinion: The potential risks arising from nanoscience and nanotechnologies on food and feed safety**. *EFSA Journal* 2009, **958**:1-39.
104. Chu Z, Huang Y, Tao Q, Li Q: **Cellular uptake, evolution, and excretion of silica nanoparticles in human cells**. *Nanoscale* 2011, **3**(8):3291-3299.



105. Russ JC: **The image processing handbook**: CRC Press; 2011.
106. Pons MN, Vivier H, Belaroui K, Bernard-Michel B, Cordier F, Oulhana D, Dodds JA: **Particle morphology: from visualisation to measurement**. *Powder Technol* 1999, **103**(1):44-57.
107. ISO 9276-3: **Representation of results of particle size analysis**. In: *Part 3: Adjustment of an experimental curve to a reference model*. Geneva: International Organization for Standardization; 2008.
108. Freedman D, Diaconis P: **On the histogram as a density estimator:L 2 theory**. *Z Wahrscheinlichkeit* 1981, **57**(4):453-476.
109. Scott DW: **Scott's rule**. *Wiley Interdiscip Rev Comput Stat* 2010, **2**(4):497-502.
110. Scott DW: **Sturges' rule**. *Wiley Interdiscip Rev Comput Stat* 2009, **1**(3):303-306.
111. Bau S, Witschger O, Gensdarmes F, Rastoix O, Thomas D: **A TEM-based method as an alternative to the BET method for measuring off-line the specific surface area of nanoaerosols**. *Powder Technol* 2010, **200**(3):190-201.
112. Grishin I, Thomson K, Migliorini F, Sloan JJ: **Application of the Hough transform for the automatic determination of soot aggregate morphology**. *Appl Opt* 2012, **51**(5):610-620.
113. Park C, Huang CC, Ji JX, Ding Y: **Segmentation, Inference and Classification of Partially Overlapping Nanoparticles**. *IEEE Transactions on Pattern Analysis and Machine Intelligence* 2013, **35**(3):1-1.
114. Brasil AM, Farias TL, Carvalho MG: **A recipe for image characterization of fractal-like aggregates**. *Journal of Aerosol Science* 1999, **30**(10):1379-1389.
115. De Temmerman P-J, Lammertyn J, De Ketelaere B, Kestens V, Roebben G, Mast J: **Measurement uncertainties of size, shape and surface measurements using transmission electron microscopy of near-monodisperse, near-spherical nanoparticles**. *Journal of Nanoparticle Research* 2013, (Submitted).
116. Linsinger TPJ: **Application Note 1: Comparison of a measurement result with the certified value**. In: *European Reference Materials' application note* Geel, Belgium; 2010.
117. Braun A, Couteau O, Franks K, Kestens V, Roebben G, Lamberty A, Linsinger TPJ: **Validation of dynamic light scattering and centrifugal liquid sedimentation methods for nanoparticle characterisation**. *Advanced Powder Technology* 2011, **22**(6):766-770.
118. ASTM: **Standard Practice for Calibrating the Magnification of a Scanning Electron Microscope**. *ASTM INTERNATIONAL* 2014:6.
119. ISO/IEC GUIDE 98-3: **Uncertainty of measurement**. In: *Part 3: Guide to the expression of uncertainty in measurement (GUM:1995)*. Geneva: International Organization for Standardization; 2008.
120. Linsinger TPJ: **ERM Application Note 1**. In: *Comparison of a measurement result with the certified value*. Geel, Belgium: European Commission - Joint Research Centre Institution for Reference Materials and Measurements (IRMM); 2010.
121. Linsinger T, Roebben G, Gilliland D, Calzolai L, Rossi F, Gibson P, Klein C: **Requirements on measurements for the implementation of the European Commission definition of the term 'nanomaterial'**. In.: Publications Office of the European Union; 2012.
122. ISO: **Nanotechnologies - Terminology and definitions for nano-objects - Nanoparticle, nanofibre and nanoplate**. In: *ISO/TS 27687:2008*. Geneva: International Organization for Standardization; 2008.
123. Klein CL, Comero S, Stahlmecke B, Romazanov J, Kuhlbusch TAJ, Van Doren E, De Temmerman PJ, Mast J, Wick P, Krug HF et al: **NM-Series of representative manufactured nanomaterials: NM-300 silver - Characterisation, stability, homogeneity - 2011**. In.: JRC Scientific and Technical Reports; 2011: 86.
124. ISO: **Uncertainty of measurement - Part 3: Guide to the expression of uncertainty in measurement (GUM:1995)**. In: *ISO/IEC GUIDE 98-3:2008*. Geneva: International Organization for Standardization; 2008.
125. Koeber R: **Guideline for in-house validation: Development of an integrated approach based on validated and standardized methods to support the implementation of the EC recommendation for a definition of nanomaterial**. In., vol. FP7-NMP-2013-LARGE-7: Nanodefine; 2015.
126. The European Commission: **Commission Recommendation of 18 October 2011 on the definition of nanomaterial**. In. Official Journal of the European Union; 2011.

127. Eggersdorfer ML, Gröhn AJ, Sorensen CM, McMurphy PH, Pratsinis SE: **Mass-mobility characterization of flame-made ZrO<sub>2</sub> aerosols: Primary particle diameter and extent of aggregation.** *Journal of Colloid and Interface Science* 2012, **387**(1):12-23.
128. Eggersdorfer ML, Kadau D, Herrmann HJ, Pratsinis SE: **Aggregate morphology evolution by sintering: Number and diameter of primary particles.** *Journal of Aerosol Science* 2012, **46**:7-19.

## 10 List of abbreviations (optional)



# 11 Attachments

**Table 21 Electronic reporting template (MS Excel) that is distributed together with the samples and provides key information regarding the ILC.**

<b>Generic information</b> (according to ISO/IEC 17025 )
Name and address of the participant, and location where tests were carried out, if different from the address of the participant.
Name and address of the ILC coordinator (CODA-CERVA)
Unique identification of the test report, repeated on each page of the report
Page numbering indicated as e.g., "Page 1 of 15"
Operator's name
Name, function and signature of persons authorising the test report
<b>Sample information</b> (according to ISO 13322-1 [54])
Date of receipt of each sample
Identification of the samples and, if relevant, identification assigned to the samples by the participant
Date when the recipient were opened and EM test samples were prepared
Identification of the EM test samples (e.g., recipient #, replicate#)
Complete description of the method used for sub-sample, if required, and EM test sample preparation, with full quantitative details of the nominal mass, volumes and compositions of products, in case dilution was applied
Type of the used sample holder/substrate
Sample preparation
Sample volume intake
Sample preparation/drying
Sample grid/sample holder (mesh size, coating, Copper/gold/mica)
Method and instrument information
Make and type of the electron microscope
Frame size camera (pixels)
Date of the last instrument performance check/maintenance
Description of the image magnification calibration procedure.
Calibration uncertainty
Description of the method used (magnifications, CCD camera, nominal camera length, acceleration voltage, tilt angle, spot size, aperture, etc.)
Image analysis and results
Date of performance of the tests
Micrographs used for analysis and identification number of the view fields
Pixel size (nm)
Micrograph size ( $\mu\text{m}$ )
Total area sampled per sample ( $\mu\text{m}^2$ )
Counting procedure: Treatment of particles cut by the measurement frame [54] (Exclude border particles, include border particles, include 50%, other)
Estimation of the measurement uncertainty associated to the number-based modal and median particle diameter values.
Number of counted (measured) particles
All particle size results shall be reported in nanometres (nm)
Description of the image software package used
Description regarding adjustment of contrast, brightness, greyscale threshold, etc.
Description regarding the usage of image filters (smoothing, NxN, mean, median)
Description regarding dealing with touching particles (manually/automatically discard all touching particles, Manual or automatic particle separation filters, morphology threshold based separation)

**Table 22 Terminology in iTEM and ImageJ, ISO terminology and Equation.**

iTEM	ImageJ	ISO 13322-1	ISO 9276-6	Equation
Area	Area	Area	Projection Area	
Feret max	N/A	Maximum Feret diameter	Maximum diameter	Feret

Feret min	MinFeret	Minimum Feret diameter	Minimum Feret diameter	Feret	
ECD	N/A	Area-equivalent diameter	Equivalent circle diameter		$2\sqrt{Area/\pi}$
Elongation		Shape factor	(Aspect ratio) <sup>-1</sup>		$Feret\ max/Feret\ min$
	AR				$Major/Minor^b$
Aspect Ratio					$Width/Height^a$
Shape factor	Circularity		Form factor		$4\pi Area/Perimeter^2$
	Round				$4 Area/\pi Major^2$
			Roundness		$4 Area/\pi Feret\ max^2$
Convexity	Solidity		Solidity		$Area/Convex\ area$

<sup>a</sup> Width and height of the smallest bounding rectangle Feret diameter (ISO9276-6).

<sup>b</sup> Major and minor axis of the fitted ellips

1 **Table 23 Summary of the sample preparation conditions reported by the labs for the analysis of ERM-FD100**

Organization	A	B	C	D	D*	E	F	G	H
Dilution	1000	1000	10	4	4		10000	1000	81
Homogenization	Vortex for 5 sec	Gently inverted						Vortex for 5-10 sec	Hand shaken for 4 minutes
Sample volume intake	10 µl	10 µl	15 µl	20 µl	20 µl		10 µl	10 µl	20 µl
Grids	Carbon and pioloform-coated mesh, home-made	Carbon-coated, 400 mesh carbon grids (Agar Scientific, Essex, England)	Continuous carbon coated copper grids, 400mesh. Ted Pella	Holey carbon coated, 300 mesh copper grids (EMS)	Holey carbon coated, 300 mesh copper grids (EMS)		400 mesh, pioloform coating, copper	Continuous carbon coated copper grids, 400mesh. (www.grid-tech.com) Cu-400CN	copper, mesh 400, carbon and formvar coated
Grid pre-treatment	1% Alcian blue-treated	1% Alcian blue-treated		1% of Alcian blue	1% of Alcian blue				
Specimen preparation	Grid on drop + Blotting	grid on drop + blotted	Grid on drop + blotting				drop-on-grid + air dried for 2 hours	Grid on drop + blotting	Grid on drop+ blotting
Incubation	10 min	10 min in chemical hood					2h		1 min
Rinsing				30 second on a drop of water	30 second on a drop of water				5 times washed for 1 min each

2

3 **Table 24 Summary of the sample preparation conditions reported by the labs for the analysis of NM-300K**

Organization	A	B	C	D	D*	E	F	G	H
Dilution	10	To 5 mg/mL		To 1% w/w	To 1% w/w		5000	10	161
Homogenization	Vortex for 5 sec							Vortex for 5-10 sec	Hand shaken for 4 minutes
Sample volume intake	10 µl	10 µl	15 µl	20 µl	20 µl		10 µl	10µl	20 µl
Grids	Carbon pioloform-coated mesh, Cu, and 400	400 mesh carbon grids (Agar Scientific, Essex, England)	Continuous carbon coated copper grids, 400mesh. Ted Pella	Holey carbon coated, 300 mesh copper grids (EMS)	Holey carbon coated, 300 mesh copper grids (EMS)		400 mesh, pioloform coating, copper	Continuous carbon coated copper grids, 400mesh. (www.grid-tech.com) Cu-400CN	copper, mesh 400, carbon and formvar coated
Grid pre-treatment	1% Alcian blue-treated	1% Alcian blue		1% of Alcian blue	1% of Alcian blue				
Specimen preparation	Drop on grid + Blotting	grid drop on	Grid drop on + blotting				drop-on-grid + air dried for 2 hours	Grid on drop + blotting	Grid on drop+ blotting
Incubation	10 min	10 min					2h		1 min
Rinsing			washed two times in drops of distilled water	30 second on a drop of water	30 second on a drop of water				

4

5 **Table 25 Summary of the instrument conditions reported by the labs for analysis of ERM-FD100**

Organization	A	B	C	D	D*	E	F	G	H
# days	5	5	5	5	3	3	3	5	2
# repetitions	3	3	3	3	3	3	3	3	2
# particles analysed	8271	7882	12047	9020	8290	4915	3622	20036	5797
Instrument	FEI tecna G2 Spirit	Jeol JEM 1011	FEI Titan ChemiSTEM	FEI- Tecnai G2 Spirit	FEI Titan 80-300 (FEI Company)	FEI F30	FEI Morgagni 268	Tecna T20 G2	FEI Tecnai 12 G2 Spirit, Twin lens config
Acceleration voltage	120 kV	100 kV	80 kv-200 kV	120 kV	300 kV	300 kV	80 kV	200 kV	120 kV
Electron source type	LaB6		S-FEG	LaB6	FEG			LaB6	W
Magnification	68 kX	20 kX	32 kX	220 kX	56 kX	39 kX	56 / 89 kX	19.5 / 38 kX	135 kX
Calibration and traceability	Cross-grating (2160 lines/mm) <sup>a</sup>	Cross-grating (2160 lines/mm) <sup>a</sup>	Optical diffraction cross-grating (S106) with 2160 lines/mm and 463 nm line spacing (Agar Scientific)	Cross-grating (2160 lines/mm) <sup>a</sup>	Cross-grating (2160 lines/mm) <sup>a</sup> + Mag*1*Cal Reference Standard for TEM (Narrow Scientific Ltd.)	Calibrated by using the lattice parameter of silicon.		Optical diffraction cross-grating (S106) with 2160 lines/mm and 463 nm line spacing (Agar Scientific)	Negatively stained catalase crystals (TAAB C074) with assumed lattice plane spacing of 8.75 nm
Calibration uncertainty	1.3%		< 1%	0.5%	0.5%			1%	1.4%
Frame size (pixels)	4096 x 4096	2.7 k x 2.7 k	2 k x 2 k	1376 x 1032	2 k x 2 k	2 k x 2 k	2048 x 2048	2 k x 2 k	2656 x 2656
Pixel dimension (nm/pixel)	0.16	0.33	0.5	0.34	0.1929	0.25641	0.84/0.53	0.56	0.27
Area sampled (µm <sup>2</sup> )	52.63	~ 7.9	~ 25	24.645	6.09		247	~ 40	~ 54
Image analysis software	iTEM	ImageJ	ImageJ	ImageJ	ImageJ	ImageJ	iTEM, 5.2 (Build 3554)	ImageJ	ImageJ

6 <sup>a</sup> Calibration software which is integrated in the Tecnai user interface software (FEI company)

7 **Table 26 Summary of the instrument conditions reported by the labs for analysis of NM-300K**

Organization	A	B	C	D	D*	E	F	G	H
# days	5	3	3	3	3	3	3	3	2
# repetitions	3	3	3	3	3	3	3	3	2
# particles analysed	10582	9352	29506	7470	16543	5007	12352	17029	10865
Instrument	FEI tecnai G2 Spirit	Jeol JEM 1011	FEI Titan ChemiSTEM	FEI- Tecnai G2 Spirit	FEI Titan 80-300 (FEI Company)	FEI F30	FEI Morgagni 268	Tecnai T20 G2	FEI Tecnai 12 G2 Spirit, Twin lens config
Acceleration voltage	120 kV	100 kV	80 kv-200 kV	120 kV	300 kV	300 kV	80 kV	200 kV	120 kV
Electron source type	LaB6		S-FEG	LaB6	FEG			LaB6	W
Magnification	68 kX	12 kX	32 kX	220 kX	56 kX	39 kX	56 kX	19.5 kX and 38 kX	135 kX
Calibration and traceability	Cross-grating (2160 lines/mm) <sup>a</sup>	Cross-grating (2160 lines/mm) <sup>a</sup>	Optical diffraction cross-grating (S106) with 2160 lines/mm and 463 nm line spacing (Agar Scientific)	Cross-grating (2160 lines/mm) <sup>a</sup>	Cross-grating (2160 lines/mm) <sup>a</sup> + Mag*1*Cal Reference Standard for TEM (Narrow Scientific Ltd.)	Calibrated by using the lattice parameter of silicon.		Optical diffraction cross-grating (S106) with 2160 lines/mm and 463 nm line spacing (Agar Scientific)	Negatively stained catalase crystals (TAAB C074) with assumed lattice plane spacing of 8.75 nm
Calibration uncertainty	1.3%		< 1%	0.5%	0.5%			1%	1.4%
Frame size (pixels)	4096 x 4096	2.7 k x 2.7 k	2 k x 2 k	1376 x 1032	2 k x 2 k	2 k x 2 k	2048 x 2048	2 k x 2 k	2656 x 2656
Pixel dimension (nm/pixel)	0.16	0.56	0.32	0.34	0.1929	0.25641	0.84	0.56	0.27
Area sampled (µm <sup>2</sup> )	52.63	~ 22.6	~ 25	24.645	18.73		147	~ 30	~ 54
Image analysis software	iTEM	ImageJ	ImageJ	ImageJ	ImageJ	ImageJ	iTEM, 5.2 (Build 3554)	ImageJ	ImageJ

8 <sup>a</sup> Calibration software which is integrated in the Tecnai user interface software (FEI company)

9 **Table 27 Summary of the image processing conditions reported by the labs for analysis of ERM-FD100**

Organization	A	B	C	D	D*	E	F	G	H
Frame dimensions	Measurement frame set at 10% from top and left size of micrograph		10% of the image borders are cut by the measurement frame.		Measurement frame set at 5% from the sides of micrograph		area 0-86 nm from micrograph margins	10% of the image borders are cut by the measurement frame.	Measurement frame set at 10% from top and left size of micrograph
Treatment of particles cut by the edge of the measurement frame	Exclusion of particles touching the bottom and right image border	Particles touching the bottom and right and left sides of the image were manually rejected			All particles with an X or Y coordinate outside of the measurement frame, were excluded from the dataset.		Exclude border particles		Exclusion of particles touching the bottom and right image border
Particle removal	Size below 100 pixels	Circularity below 0.5	Size below 15 nm and above 30 nm	Remove outliers of 10 pixels			Shape factor below 0.8 and above 1.1	Size below 15 nm and above 30 nm	Area below 100 pixels and size larger than 10% of image width
Background removal			Inverted Gaussian	Subtract background function (50 pixels)	Gaussian blur (sigma of 2 pixels) filter	Rolling ball radius = 100-200 pixels	Square Polynomial fit (0.1 % Overflow), Multiplicative Assumed deterioration, Source 1	Inverted Gaussian option	Band pass filtering (below 5 pixels and above 500 pixels)
Smoothing filter	10 x 10 filter		Median r =1	median filter 2 pixels		median: radius = 4.0 pixels		Median r =1	5x5 median filter
Thresholding	Manual thresholding	manual grey-scale thresholding	Manual thresholding	Manual		Auto threshold: Mean	Visually	Auto threshold (triangle)	Manual
Particle treatment		Separate particles	Watershed filter used for separation	Watershed and fill holes				Watershed filter	
Touching particles			Discarded all touching particles	Superposing particles were discarded	Superposing particles were discarded			Automatically discarded all touching particles	Manual removal of bad particles (touching, aggregated, wrong local threshold level)



Table 28 Summary of the image processing conditions reported by the labs for analysis of NM-300K

Organization	A	B	C	D	D*	E	F	G	H
Frame dimensions	Measurement frame set at 5% from the sides of micrograph		10% of the image borders are cut by the measurement frame.		Measurement frame set at 5% from the sides of micrograph		area 0-86 nm from micrograph margins	10% of the image borders are cut by the measurement frame.	Measurement frame set at 10% from top and left size of micrograph
Treatment of particles cut by the edge of the measurement frame	All particles with an X or Y coordinate outside of the measurement frame, were excluded from the dataset.	Particles touching the bottom and right and left sides of the image were manually rejected			All particles with an X or Y coordinate outside of the measurement frame, were excluded from the dataset.		Exclude border particles		Exclusion of particles touching the bottom and right image border
Particle removal	Size below 100 pixels, Convexity below 0.85 and sphericity below 0.6	Circularity below 0.5	Size below 10 nm and above 25 nm	Remove outliers of 10 pixels	remove outliers (radius of 10 pixels)	Size below 75nm <sup>2</sup> and above 1200nm <sup>2</sup>	Shape factor below 0.9 and above 1.1	Size below 15 nm and above 30 nm	Area below 100 pixels and size larger than 10% of image width
Background removal			Inverted Gaussian	Subtract background function (50 pixels)	Gaussian blur (sigma of 2 pixels) filter	Rolling ball radius = 100-200 pixels	Square Polynomial fit (0.1 % Overflow), Multiplicative Assumed deterioration, Source 1	Inverted Gaussian option	Band pass filtering (below 5 pixels and above 500 pixels)
Smoothing filter	3 x 3 filter		Median r =1	median filter 2 pixels		median: radius = 4.0 pixels		Median r =1	5x5 median filter
Thresholding	Manual thresholding	manual grey-scale thresholding	Manual interactive	Manual		Auto threshold: Mean	Visually	Auto threshold (triangle)	Manual
Particle treatment	Watershed (EDM + separator)	Separate particles	Watershed filter used for separation	Watershed and fill holes	dilate and watershed.			Watershed filter	
Touching particles			Discarded all touching particles	Superposing particles were discarded	Superposing particles were discarded			Automatically discarded all touching particles	Manual removal of bad particles (touching, aggregated, wrong local threshold level)

**Table 29 Inter-laboratory comparison of the mean median circularity, aspect ratio, Roundness and solidity for ERM-FD100 and NM-300K.**

Code	ERM-FD100				NM-300K			
	Circ.	AR	Round	Solidity	Circ.	AR	Round	Solidity
A	0.71	0.84	0.74	0.93	0.82 <sup>a</sup> (0.78 <sup>b</sup> )	0.89 <sup>a</sup> (0.86 <sup>b</sup> )	0.81 <sup>a</sup> (0.86 <sup>b</sup> )	0.96 <sup>a</sup> (0.94 <sup>b</sup> )
B	0.75	- <sup>c</sup>	0.86	0.75	0.88	-	0.86	0.94
C	0.43	0.83	0.83	0.76	0.4	0.88	0.88	0.86
D	0.88	0.9	0.9	0.97	0.91	0.91	0.91	0.97
D*	0.78	0.86	0.86	0.96	0.87	0.91	0.91	0.97
E	0.82	0.87	0.87	0.95	0.88	0.91	0.91	0.97
F	0.25	0.88	0.72	0.88	0.96	0.89	1.00 <sup>d</sup>	0.97
G	0.69	0.86	0.86	0.9	0.86	0.89	0.89	0.94
H	0.88	0.88	0.88	0.97	0.89	0.9	0.91	0.97
Mean	0.69	0.86	0.83	0.9	0.83	0.9	0.88	0.95
Stdev	0.21	0.02	0.06	0.09	0.17	0.01	0.03	0.04

<sup>a</sup> analysis in iTEM

<sup>b</sup> analysis in ImageJ

<sup>c</sup> missing measurement

<sup>d</sup> all particles had a roundness of 1

**Table 30 Comparison between measurands measured in iTEM and ImageJ including the average difference between paired measurements (Bias) and the standard error on the difference.**

iTEM	ImageJ	Bias (%)	Standard error (%)
Area (nm <sup>2</sup> )	Area	0.00 <sup>a</sup>	0.00
Feret min (nm)	MinFeret	0.08	0.01
ECD (nm)	ECD <sup>B</sup>	0.00 <sup>a</sup>	0.00
Perimeter (nm)	Perim.	-22.74	2.50
Elongation	AR	0.00 <sup>a</sup>	0.00
Aspect ratio	AR	-0.60 <sup>a</sup>	0.52
Shape factor	Circ.	22.10	2.04
Roundness <sup>b</sup>	Round	25.64	1.69
Convexity	Solidity	-0.66	0.03

<sup>a</sup> Bias is not significantly different from zero (T-test for paired measurements at 5% level).

<sup>b</sup> Calculated parameters

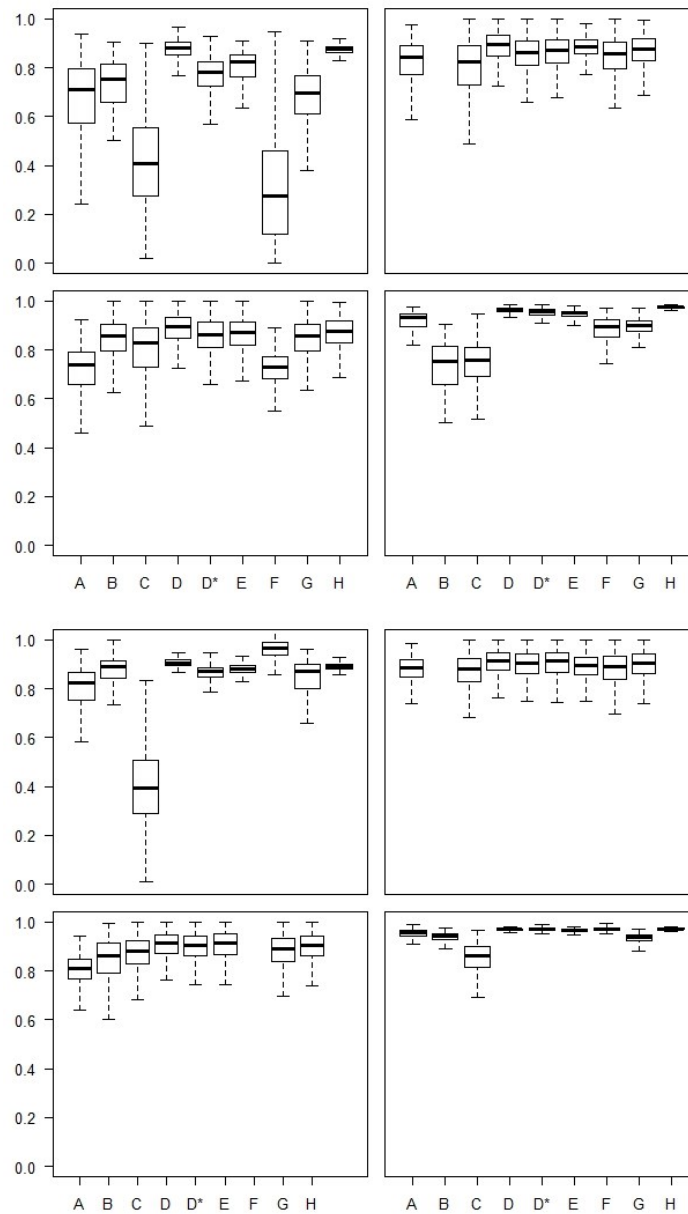


Figure 22 Boxplots showing the distribution of circularity, aspect ratio, roundness and solidity for ERM-FD100 (Top) and NM-300K (Bottom).